THE CALIBRATION OF SHALLOW WATER MULTIBEAM ECHO-SOUNDING SYSTEMS

A. GODIN

March 1998

PREFACE

In order to make our extensive series of technical reports more readily available, we have scanned the old master copies and produced electronic versions in Portable Document Format. The quality of the images varies depending on the quality of the originals. The images have not been converted to searchable text.

THE CALIBRATION OF SHALLOW WATER MULTIBEAM ECHO-SOUNDING SYSTEMS

André Godin

Department of Geodesy and Geomatics Engineering
University of New Brunswick
P.O. Box 4400
Fredericton, N.B.
Canada
E3B 5A3

March 1998

PREFACE

This technical report is a reproduction of a report submitted in partial fulfillment of the requirements for the degree of Master of Engineering in the Department of Geodesy and Geomatics Engineering, December 1996. The research was jointly supervised by Dr. David Wells and Dr. Larry A. Mayer, and it was supported by Fisheries and Oceans Canada and the Natural Sciences and Engineering Research Council of Canada.

As with any copyrighted material, permission to reprint or quote extensively from this report must be received from the author. The citation to this work should appear as follows:

Abstract

Multibeam echo-sounders have been developed to gather bathymetric and acoustic data for more efficient and more exact mapping of the oceans. This gain in efficiency does not come without drawbacks. Indeed, the finer the resolution of remote sensing instruments, the harder they are to calibrate. This is the case for multibeam echo-sounding systems (MBES). We are no longer dealing with sounding lines where the bathymetry must be interpolated between them to engender consistent representations of the seafloor. We now need to match together strips (swaths) of totally ensonified seabed. As a consequence, misalignment and time lag problems emerge as artifacts in the bathymetry from adjacent or overlapping swaths, particularly when operating in shallow water. More importantly, one must still verify that bathymetric data meet the accuracy requirements.

This Master of Engineering report summarizes the system integration involved with MBES and identifies the various sources of errors pertaining to shallow water surveys (100 m and less). A systematic method for the calibration of shallow water MBES is proposed and presented as a set of field procedures. The procedures aim at detecting, quantifying and correcting systematic instrumental and installation errors. Hence, calibrating for variations of the speed of sound in the water column, which is natural in origin, is not addressed in this document.

Calibration data, acquired by the Canadian Hydrographic Service using Simrad EM1000 and EM100 multibeam echo-sounders, have been used to demonstrate the proposed techniques. The method uses a post-processing system that allows the visualization of swaths in plan views and cross-sections, and requires the ability to perform digital manipulation of datasets and statistical analysis. To this end, the HIPS post-processing package (Universal System Ltd) has been used.

Hydrographers using MBES must still certify the acquired bathymetric data comply with their national accuracy standards or with the ones defined by the International Hydrographic Organisation (IHO). With an adequate calibration, hydrographers will ensure the sounding system operates without the loss of accuracy that results from systematic biases. When the sound speed profile of the water column is well known, accurate and consistent depth measurements will be obtained. A post-calibration quality assessment procedure, herein called the "performance check", is presented. The procedure employs the existing "Reference Surface Methodology", developed by the Ocean Mapping Group of the University of New Brunswick, along with other statistical tools to assess the overall accuracy of the calibrated system. The output of the performance check can be used to certify that the data meet accuracy requirements.

Acknowledgements

I would first thank my supervisor Dr. D.E. Wells and co-supervisor Dr. Larry Mayer for their support in making this report a decent one. Thanks also to Dr. John Hughes Clarke, for his solicitude and patience with regard to my numerous inquiries.

I should not forget to acknowledge the encouragement and financial support of the Canadian Department of Fisheries and Oceans and more specifically from the regional director of the Canadian Hydrographic Service, Mr. Denis Hains.

Finally, I thank my family for their patience and support throughout my studies at UNB. I thank also my mother and father in law who demonstrated unequaled generosity and readiness to help us get through this strenuous episode of our life.

Table of Contents

---

3. Sources of Error for Shallow Water MBES   **36**

List of Figures

---

1. Introduction

A **multibeam echo-sounder** is a device that simultaneously acquires a multitude of depth measurements, regularly spread athwart-ship, in a fan-shape pattern (Figure 1.1). The reason for using these sonars is to sweep a swath-like corridor of the bottom so as to ensure a complete coverage of the seafloor.
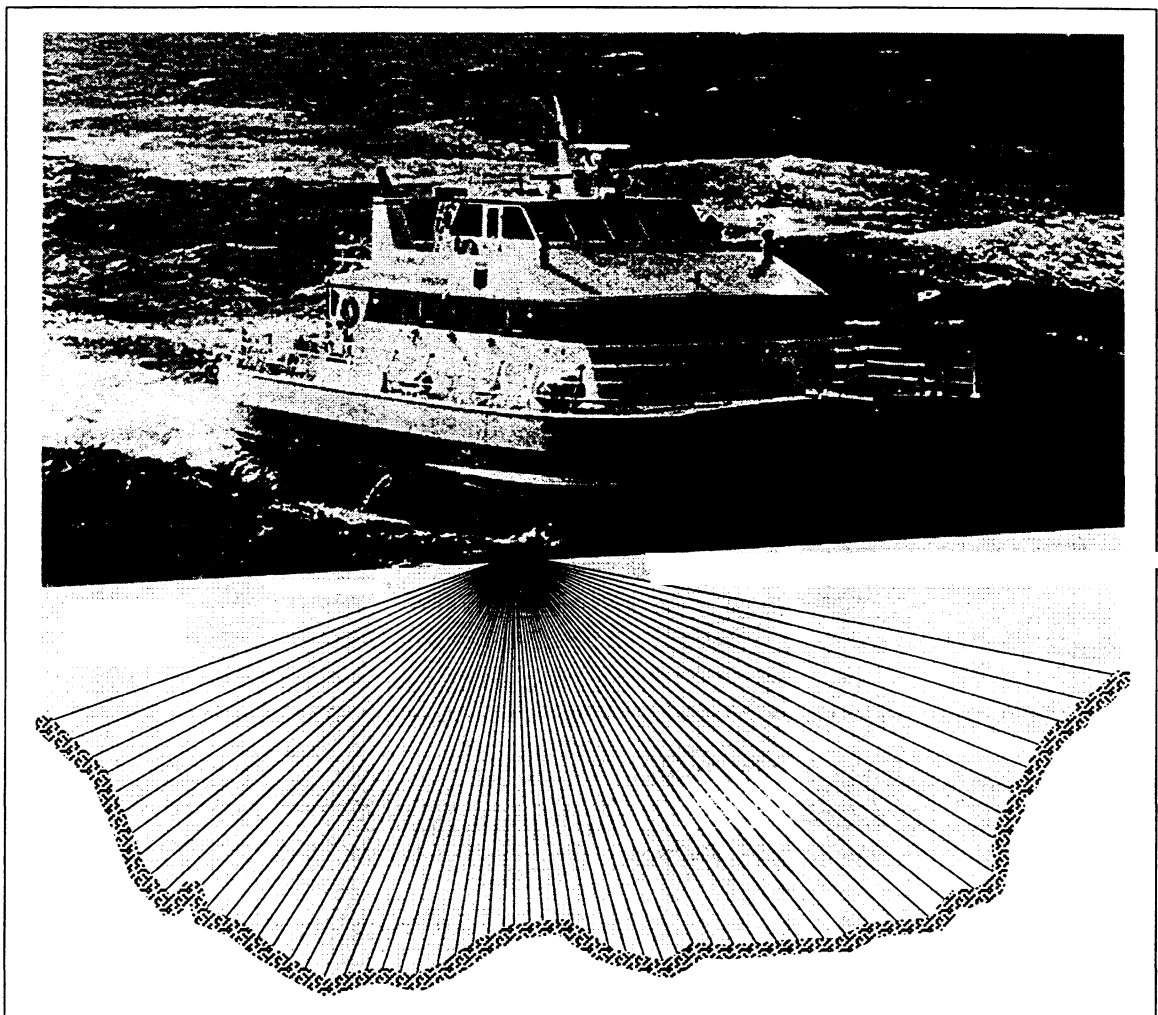
Figure 1.1   Typical beam arrangement and ensonified area on the seafloor for a multibeam echo-sounder (photograph of the NSC Frederick G. Creed).

The goal of this project is to identify and describe the sources of systematic error that affect shallow water multibeam echo-sounding data as well as to come up with field procedures for (a) their calibration and for (b) post-calibration quality assessment.

Many surveying companies and organisations are now using multibeam echo-sounders for their operations, either offshore or in coastal and inland waters. The applications are numerous. Multibeam Echo-sounding Systems (MBES), also known as swath systems, can be used for technical surveys for oil and ore prospecting, for cable route assessment, for environmental monitoring or for hydrographic surveys supporting marine cartography or dredging operations.

The required levels of accuracy for these various applications are not identical. The most demanding application in terms of accuracy is probably the bathymetric monitoring of navigation channels and the related dredging operations, where payments are determined according to computed volume of sediment to be removed. The hydrographic offices, which use MBES for the establishment of nautical charts, have their own set of accuracy standards for hydrographic surveys, which generally comply with the standards defined by the IHO [International Hydrographic Organisation, 1987]. In most

countries, nautical charts are legal documents and the level of accuracy associated with the source data is quite high.

1.1 The Needs

Unlike single beam echo-sounders, multibeam sonars are complex and hard to calibrate. They include many sub-systems that possess their own configuration and calibration routines. There are several sources of error associated with MBES depth measurements, and they must be detected and quantified by systematic testing procedures before being corrected or eliminated. Deep water MBES surveys (> 1000 m) involve much larger sonar footprints and thus, corresponding lower accuracy both in the positioning and in the depth measurements are usually acceptable. The accuracy requirements are much harder to meet in shallow waters (< 100 m) where the calibration of the sounding systems becomes a critical issue. Indeed, as one gets closer to shore, one must deal with:

- A reduction of the footprint size, and consequently an increase of the horizontal resolution, which requires better positioning to keep consistency in the data.

- An increase in spatial and/or temporal variations of the speed of sound in the water column, which will result in different ray bending

---

patterns, affecting the position of the acoustic footprint on the seabed and the slant range measurements.

- An increase in spatial and/or temporal tidal variations and the difficulty in getting the right water level at the survey location.

- The presence of turbid waters or biological activity (fish, micro-organisms, weeds) that will affect acoustic bottom detection.

- The use of smaller survey platforms which are prone to larger and faster motions (roll, pitch, and yaw) and draught changes (larger percentage of depth compared to deep water surveys), requiring more accurate motion sensors with higher sampling rates.

Some calibration procedures have been implemented in the past and are still in use [Wheaton, 1988; Simrad, 1994], but they do not overcome the difficulties posed by shallow water operations. At the present time, no standardized calibration procedures exist among the IHO recommendations for correcting multibeam echo-soundings and there is a **need for:**

1) A set of calibration procedures specifically developed for shallow water MBES which will take into account the source of errors that are not addressed by any existing calibration techniques.

2) Effective routines for testing MBES repeatability.

3) A way to calibrate for spatial and temporal variations of the speed of sound in the surveyed water mass.

---

4) New accuracy standards for depth measurements and hydrographic surveys that would take into account the total bottom coverage that can be obtained with MBES.

1.2 The Motivation

The Canadian Hydrographic Service (CHS), for whom the author is currently employed, operates several Simrad multibeam echo-sounders in the Canadian coastal and inland waters. A Simrad EM1000 ultra wide multibeam echo-sounder is installed on the 20 m long NSC "Frederick G. Creed" while an EM100 is operated on the 30 m long CSS "Matthew". Since 1989, the CHS has been using existing calibration procedures [Herlihy, 1989; Simrad Subsea, 1994] as well as developing new approaches for detecting certain system biases. Nonetheless, no specific instructions have been added to the CHS Standing Orders for the calibration of MBES. This task remains to be done.

Furthermore, the CHS has recently purchased three new shallow water multibeam echo-sounders (Simrad EM3000). These are operating on even smaller vessels (10 m) and in shallower waters (< 25 m), and will therefore be even more critically affected by calibration problems. Thus, the elaboration of

systematic calibration procedures for shallow water MBES will also serve the operation of these new systems for hydrographic surveys.

1.3 What will this Report Satisfy?

This Master of Engineering report will provide a good understanding of the concepts and parameters involved in the integration of multibeam echo-sounding systems. It also emphasizes the important aspects of the calibration of MBES and outlines the major sources of error. Altogether, this Master of Engineering report will provide:

- A short review of MBES terms and concepts.

- A list and detailed description of sources of error pertaining to the operations of shallow water MBES

- Field Calibration Procedures for shallow water MBES and a demonstration of the calibration of a Simrad EM1000 multibeam echo-sounding system.

- A post-calibration quality assessment procedure for certifying the effectiveness of the calibration and that the bathymetric data meet accuracy requirements.

1.4 What is not Covered by the Report

Because of the unpredictable nature of the sound velocity profile of the water column and given the extent of this subject, the calibration for beam refraction and for temporal and/or spatial changes in the harmonic mean of the speed of sound is not addressed in this report.

The elaboration of accuracy standards for depth measurements is a process usually undertaken by national hydrographic authorities, by means of IHO working groups, or revising committees. Accuracy standards have not yet been specifically developed for bathymetric data obtained with MBES. So far, the hydrographic offices use the existing accuracy requirements for their multibeam echo-sounding data. The goal of this report is not to propose new standards for the accuracy of MBES data. One approach which could be taken would be to establish the required accuracy level, independently for each component of the echo-sounding system, in order to comply with the IHO performance standard for depth measurements [International Hydrographic Organisation (1987)]. However, in that case one faces numerous combinations of sensors, some of which are constantly undergoing technological enhancements. One is still subjected to errors coming from variations of the speed of sound in the water column, that render the assessment of depth measurement accuracy impractical, if not impossible. This is all to say that this report will neither propose new standards for MBES

data nor will it indicate the required level of accuracy each sensor must possess in order to meet the overall accuracy requirements.

1.5 Outline of the Report

This Master of Engineering report is divided into five chapters. Chapter 1 introduced the subject and outlined the goal, the needs, and the motivation for the work involved. Chapter 2 provides theoretical concepts as background material to support the subsequent chapters. A brief review of the general arrangement and working principles of a MBES is made. The integration of sensor outputs to come up with geo-referenced depth measurements is explained. The IHO and CHS accuracy requirements for depth measurements and soundings to be incorporated in nautical documents are also stated.

The remainder of the report is devoted to error sources for MBES and methods to resolve them. Hence, Chapter 3 outlines the major sources of error for MBES bathymetric data and lists the sources of systematic errors pertaining to shallow water surveys. Graphics and mathematical expressions are used to depict and describe these sources of error in a meaningful and practical fashion. Chapter 4 contains the field procedures for the calibration of a shallow water MBES. These procedures address the sources of error introduced in the previous chapter. Guidelines are provided for the

assessment of the calibration, and of the overall performance of the sounding system. Examples are provided, which use Simrad EM1000 data collected by the NSC "Frederick G. Creed". The post-processing of calibration data was made with the CARIS Hydrographic Information Processing System [Universal Systems Ltd., 1994]. Chapter 5 presents conclusions and recommendations for future research work for improving the calibration of multibeam echo-sounding systems.

2. Multibeam Echo-sounding Systems and Accuracy Requirements: General Concepts

The understanding of sources of error for MBES requires a good knowledge of the associated spatial references and of system integration leading to the computation of soundings' coordinates. This chapter outlines the various components that constitute the multibeam echo-sounding system and introduces the theoretical concepts of system integration (non-steered beams systems only). Spatial conventions adopted herein and used to develop the mathematical expressions are also presented. It is assumed that the reader possesses a basic knowledge of echo-sounders, so the theory associated with echo-sounding will not be developed. In-depth treatment of the engineering aspects of MBES, which is not the scope of this study, is also excluded.

The calibration of MBES is performed in order to acquire accurate and correct water depths (to mean water surface) at the moment of measurement. The soundings are further reduced to chart datum. This action introduces an external component to the measurement: the tide corrections. The sections relating to system integration and ship's elevation deal only with depth measurements that refer to the mean instantaneous water plane. Thus, tide gauges and water level corrections are not considered in this Chapter.

2.1 The Multibeam Echo-sounding System

Multibeam echo-sounding systems represent a group of sensors, installed on a survey platform, that are used together to collect instantaneous depth measurements. In this study, the term "system" in MBES refers to the set of all these sensors, including the survey platform. The basic instrumentation that characterizes multibeam echo-sounding systems is as follows:

- Transducer

- Transceiver

- Integration and control unit

- Vertical Reference Unit (roll, pitch, yaw and heave sensors)

- Sound velocimeters

- Positioning system

- Heading sensor

Peripherals such as monitors and plotters are commonly used for real time monitoring and quality assessment. A logging unit is also integrated with the system. The transducer, which can be flat or cylindrical, is an array

of small hydro-acoustic elements. The transceiver controls the transmission, reception and amplification of acoustic signals and performs the signal processing and beam forming. The basic measurements made by the multibeam echo-sounder are the beam pointing angle (β) with respect to the transducer's normal and the two-way travel time of the acoustic signals.

Some multibeam echo-sounders form discrete beams at transmission while others transmit one broad (transversally) fan-shaped acoustic pulse at a time. In all cases, the transmitted beams are narrow in the longitudinal direction. A multitude of discrete narrow beams are formed at reception. As shown in Figure 2.1, the intersection of the transmitted and received signals
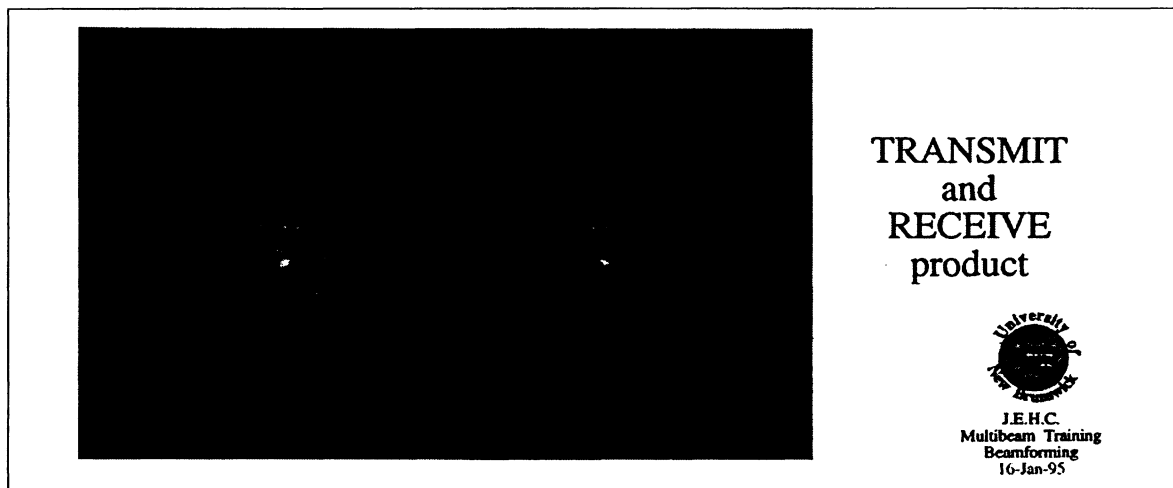
Figure 2.1   Intersection of the transmit beam and two formed beam 45° on each side of nadir (from Hughes Clarke et al. [1995]) shown in intensity level. Black is less than -40 dB.

on the seafloor forms small footprints, much smaller that those commonly obtained by single beam echo-sounders.

The Vertical Reference Unit (VRU) measures the ship's attitude (roll, pitch and yaw) and heave. Heading is provided by gyro-compass or by some attitude sensors coupled with GPS. To make a distinction between yaw and heading, we will say that yaw is the oscillation of the vessel about its vertical axis (see also § 2.2.1), characterized by a zero mean, while heading is the angle between a line pointing toward the geographic north and the ship's centre line, projected onto the horizontal plane.

A sound velocimeter or a CTD is used to get a sound speed profile of the water column. These data are used to correct for beam refraction. The speed of sound in the water column can vary both in time and space. The greatest variations generally occur at the water surface and often a sound velocimeter is mounted to the hull, to be used in real time for beam steering.

The positioning system provides the XY (or ϕ, λ) coordinates of the vessel and the soundings. As explained in the following sections, the depth measurements obtained at the transducer location are positioned relative to a certain point on the survey platform. The output from the above mentioned sensors are used to transform the ship's relative coordinates of the depth measurements into geographic ones.

2.2 System Integration and Reference Systems

System integration is the transformation of the sonar vector (expressed relative to the transducer), through the use of the external sensor outputs and the static offsets between them, to produce a complete geo-referenced solution: the sounding. The following sub-sections define the reference frames used in this report and describe the general concepts of system integration for MBES that do not perform beam steering. As defined in lecture note No.19 of the *Coastal Multibeam Sonar Training Course* [Hughes Clarke et al., 1996] : "Beam steering is the process of forming a beam in a given direction θ_s. It is achieved by phase-shifting the hydrophone contributions so as to create a virtual array whose face is perpendicular to the desired steering direction." The system integration can differ from one system to another and the information provided in this report highlights only the main factors.

2.2.1 Reference Frames and Ship's Attitude

The "Local-Level" spatial reference frame adopted here is a triaxial coordinate system which has the y-axis Y pointing toward the geographic North, the x-axis X pointing toward East and the z-axis Z pointing downward. The Z axis in the Local-Level coordinate system is pointing downward, to keep the sounding values positive. The survey platform, as shown in Figure

2.2, is a rigid body which has its own coordinate system (x, y, z) referred to as the "Body-Frame". Notice that the Body-Frame is a right-hand coordinate system while the Local-Level one is left-hand. Notice also that both Local-Level and Body-Frame coordinate systems share a common origin (RP). Each time the transmitted acoustic signal is received by the transducer, the Local-Level reference frame is redefined to match the local earth-fixed coordinate system. The origin of the Local-Level reference frame is thus shifted as the vessel moves, for each ping cycle.
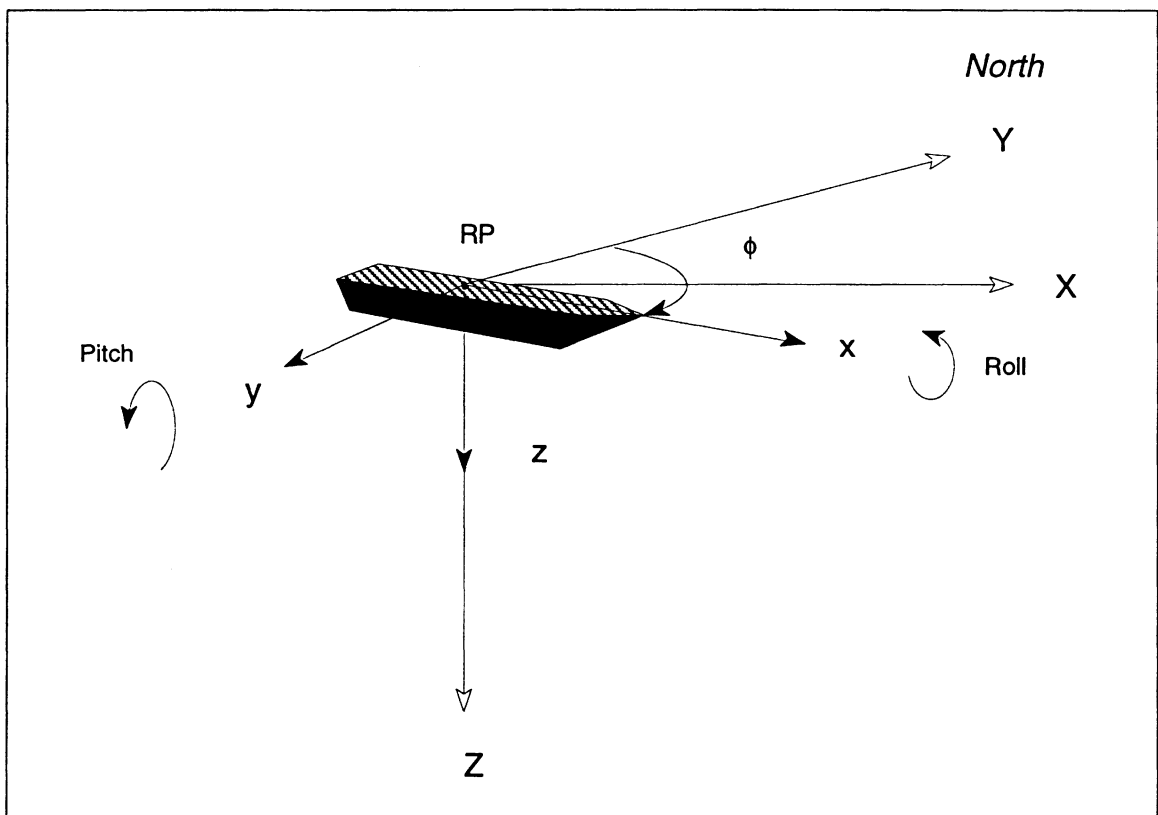
Figure 2.2   Local-Level (XYZ) and Body-Frame (xyz) coordinate systems. The azimuth is represented by the angle φ, on the horizontal plane. RP is the reference point of the vessel.

The ship's attitude is defined about the three axes of the Body-Frame which intersect at a point, sometimes called the Reference Point (RP). The centre of gravity of the survey vessel is commonly adopted as reference point which is an approximation (metre level for large vessel and decimetre level for launches) for the ship's motion axes. The intersection of the ship's centre line and the water plane is a better location for the roll axis while the pitch axis would certainly pass through the centre of floatation [Derrett, 1964]. In the convention adopted here, a survey vessel will thus roll about the x-axis, positively with the starboard side down. It will pitch positively about the y-axis with the bow up and will yaw about the z-axis, positively clockwise. The rotations associated to ship's motions are defined by the two independent Euler angles ψ, θ (representing roll, and pitch) and use the following rotation matrices:

$$R_x(\psi) = \begin{bmatrix} 1 & 0 & 0 \\ 0 & \cos(\psi) & \sin(\psi) \\ 0 & -\sin(\psi) & \cos(\psi) \end{bmatrix} \tag{2.1}$$

$$R_y(\theta) = \begin{bmatrix} \cos(\theta) & 0 & -\sin(\theta) \\ 0 & 1 & 0 \\ \sin(\theta) & 0 & \cos(\theta) \end{bmatrix} \tag{2.2}$$

Where $R_x(\psi)$ and $R_y(\theta)$ are the rotation operators for roll and pitch respectively. The sequence of rotation adopted here is similar to the sequence

used in the Tate-Bryant convention [Mimkler and Mimkler, 1990]: yaw comes first, followed by pitch, then roll. The starting point for these angles is when the ship is leveled with respect to the horizontal plane (i.e. the Body-Frame z-axis is parallel to the local vertical) and when its x-axis is pointing north. Since the ship's z-axis is first perpendicular with the horizontal plane, we will replace yaw by the azimuth angle ϕ. The rotation matrix for azimuth is:

$$R_z\left(\phi - \frac{\pi}{2}\right) = \begin{bmatrix} \sin(\phi) & -\cos(\phi) & 0 \\ \cos(\phi) & \sin(\phi) & 0 \\ 0 & 0 & 1 \end{bmatrix} \tag{2.3}$$

In order to pass from the Local-Level left-hand system to the Body-Frame right-hand one, $\pi/2$ radians are added to the azimuthal rotation ϕ; a reflection about the xz plane is to follow for the y coordinates. The transformation matrix to pass from the Local-Level coordinate system to the Body-Frame one is defined by the **P** operator:

$$P = R_{yy}R_x(\psi)R_y(\theta)R_z(\phi - \pi/2) \tag{2.4}$$

$$P = \begin{bmatrix} \cos(\theta)\sin(\phi) & -\cos(\theta)\cos(\phi) & -\sin(\theta) \\ -\cos(\psi)\cos(\phi) - \sin(\psi)\sin(\theta)\sin(\phi) & \sin(\psi)\sin(\theta)\cos(\phi) - \cos(\psi)\sin(\phi) & -\sin(\psi)\cos(\theta) \\ -\sin(\psi)\cos(\phi) + \cos(\psi)\sin(\theta)\sin(\phi) & -\sin(\psi)\sin(\phi) - \cos(\psi)\sin(\theta)\cos(\phi) & \cos(\psi)\cos(\theta) \end{bmatrix}$$

Where $R_{yy} = \begin{bmatrix} 1 & 0 & 0 \\ 0 & -1 & 0 \\ 0 & 0 & 1 \end{bmatrix}$ is a reflection matrix through the y-axis

In the above described rotations, one should differentiate between the transformed roll angle (β) made by the twice rotated ship's Body-Frame y-axis and the horizontal plane and the independent roll angle ψ. The transformed roll β, as explained in Appendix I, is the angle observed by the attitude sensor. The same consideration will not apply to azimuth and pitch angles: the azimuth is measured on the horizontal plane by the gyro-compass, whose sensitive elements are on gimbals; the pitch angle is the first rotation used in the transformation sequence which departs from the horizontal plane (equal to the angle between the ship's x-axis and the horizontal plane). Although shown on different reference frames, the two successive independent pitch and roll rotations are illustrated in Figure I.1 of Appendix I.

2.2.2 Sensor Static Offsets

The transducer, VRU and positioning system antenna are commonly installed at different locations on the survey platform. The static linear offsets are measured from the reference point and are used in the coordinate transformation of depth measurements. An example of sensors offsets is illustrated in Figure 2.3. The Vertical Reference Unit is not represented in this figure but it is assumed positioned at the reference point. If the VRU

cannot be positioned at the RP, it is recommended that it is installed as close

as possible to it. We will see in the section covering changes in transducer
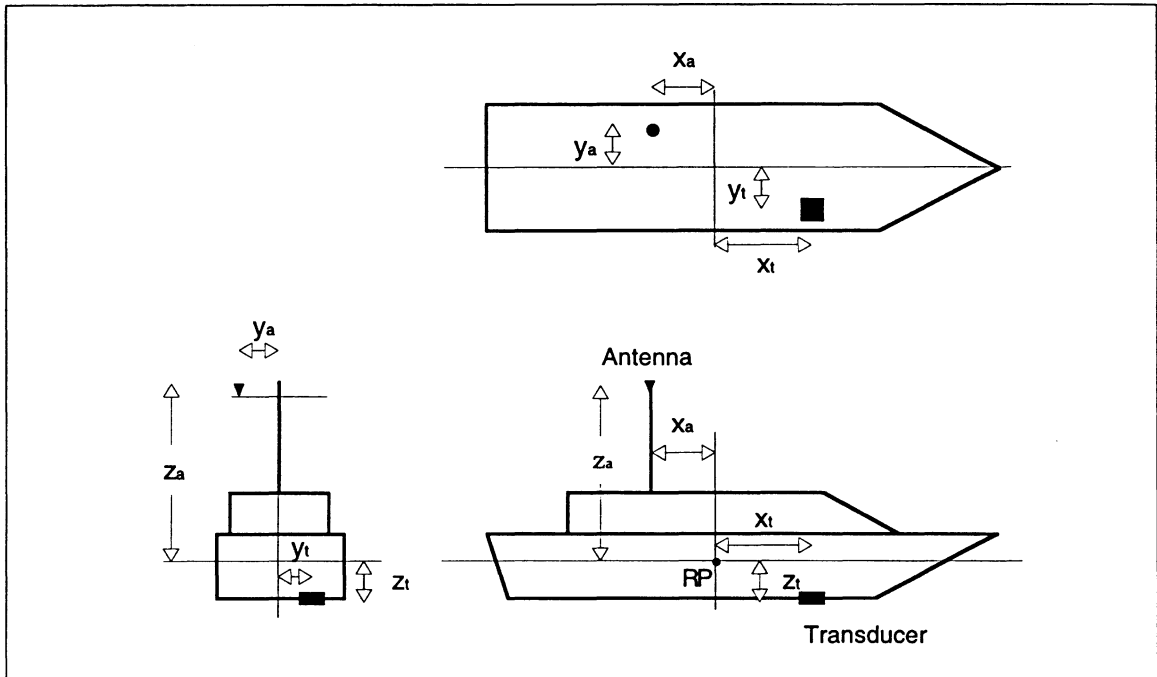
Figure 2.3   Static offsets for the transducer and the positioning system antenna, in the Body-Frame coordinate system and with respect to the reference point. The subscripts t and a refer to the transducer and the antenna respectively. The transducer offsets are represented by the vector [x_t y_t z_t] and the antenna ones by [x_a y_a z_a].

elevation with respect to the reference level why it is important the VRU be

installed at the RP location. The position of each sensor with respect to the

reference point can be represented by vectors, expressed in the Body-Frame

coordinate system:

$$\text{Antenna} = \begin{bmatrix} x_a \\ y_a \\ z_a \end{bmatrix}$$

$$\text{Transducer} = \begin{bmatrix} x_t \\ y_t \\ z_t \end{bmatrix} \tag{2.5}$$

2.2.3 Speed of Sound in the Water Column and Beam Refraction

In most waters, oblique sound rays follow a tortuous path, which is due to the refraction of the rays as they pass through layers of water of different density. The beam refraction at the water interface, illustrated in Figure 2.4, can be computed using the Snell's law:

$$\frac{\sin \Lambda_1}{C_1} = \frac{\sin \Lambda_2}{C_2} \tag{2.6}$$

Where Λ_1 is the incidence (launch) angle

Λ_2 is the angle for the refracted ray

C_1 is the speed of sound in the first layer

C_2 is the speed of sound in the second layer
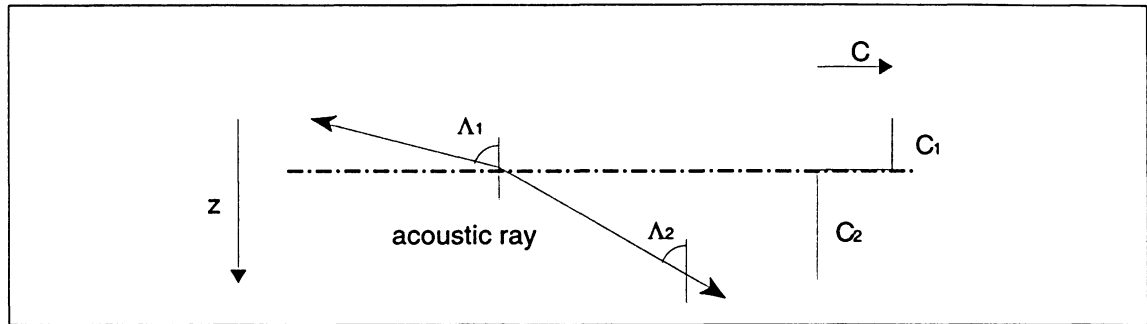
Figure 2.4 Beam refraction at a water interface with speed of sound decreasing from C_1 to C_2.

The launch angle Λ is the combination of the pitch θ, the roll ψ and the beam pointing angle β, depicted in Figure 2.5 and obtained as follows:

$$\cos \Lambda = \cos \theta \cos(\psi + \beta) \tag{2.7}$$

The beam refraction solution is computed in the vertical plane that passes through the centre of the transducer and the intersection of the transmitted signal and received beam (Figure 2.5). When applied in real time, the correction for beam refraction is not computed for each beam but look-up tables for transit time and launch angle are produced from the information obtained by the sound velocity profile [Hughes Clarke et al., 1995]. The look-up tables provide approximated depth and horizontal radial distance (in the plane of the refraction solution), for each beam. This information is further used to derive depth, x and y coordinates relative to the transducer and expressed in an intermediate coordinate system: the Leveled Body-Frame

---

(LBF). The obtained quantities only need transformations for heading,

position and reduction to a vertical datum to produce the final soundings.
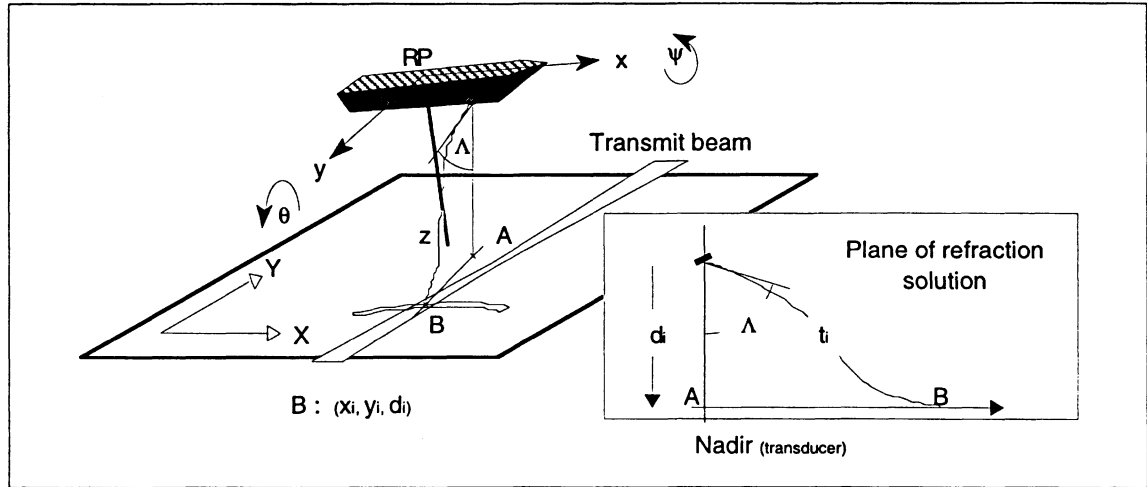
Figure 2.5   Refracted acoustic ray, launched at angle Λ and with t$_i$ 2-way travel time. The plane of the refraction solution passes through point A and B. The look-up tables for these measurements would give, for that beam i, the leveled Body-Frame coordinates x$_i$ and y$_i$ and a depth of d$_i$ under the transducer.

Done in real time or in the post-processing, the refraction solution is

computed for each beam couplet (β$_i$, t$_i$) and a new set of coordinates is

produced, expressed in a leveled Body-Frame system. For the sake of this

study, we will designate this new entity as the Beam Vector:

$$BV_i = \begin{bmatrix} x_i \\ y_i \\ d_i \end{bmatrix}_{LBF} \qquad (2.8)$$

Where   x$_i$ and y$_i$ are the Leveled Body-Frame (LBF) coordinates

d$_i$ is the depth under the transducer for beam i

2.2.4 Coordinate Transformations

The transformation of the beam vectors from the Leveled Body-Frame to the Local-Level coordinate system is made in a time framework. The transformation is two-fold: first the horizontal position (in the Local-Level reference frame) of each beam vector is computed for the time of reception and secondly, the depth values obtained from the refraction solution (still in the Leveled Body-Frame system) are reduced for changes in elevation of the transducer and tied to a vertical datum, also at reception time.

2.2.4.1 Horizontal transformation

In order to transform a Body-Frame vector $\underline{x}$ (e.g. equation 2.3) into the Local-Level coordinate system with the herein adopted spatial conventions, one must multiply this vector $\underline{x}$ by the inverse of $\mathbf{P}$ (2.4) as in the following linear relationship:

$$\underline{x} = \mathbf{P}\underline{x}' \quad \Leftrightarrow \quad \underline{x}' = \mathbf{P}^{-1}\underline{x} \tag{2.9}$$

Where $\underline{x}$ is the Body-Frame vector
$\underline{x}'$ is the Local-Level vector

The position of the RP in the Local-Level coordinate system is obtained at transmission of the acoustic signal by interpolating (with time) two consecutive positions of the antenna (earth-fixed geographic coordinates), corrected for attitude. Since the attitude data is rarely recorded synchronously with the positions, they will be interpolated in time at the moment of the fixes. The horizontal position of each beam vector is then transformed at reception time, using the VRU and Gyro output, the linear offsets between the transducer and the RP and using the Leveled Body-Frame coordinates of the beam vectors. The overall operation can be seen as follows:

$$RP(t_0) = A(t_0) - P^{-1}[x_a \quad y_a \quad z_a]^T$$

$$RP(t_1) = A(t_1) - P^{-1}[x_a \quad y_a \quad z_a]^T$$

$$RP(t) = RP(t_0) + \left(\frac{t - t_0}{t_1 - t_0}\right)[(X_1 - X_0) \quad (Y_1 - Y_0) \quad 0]^T \qquad (2.10)$$

And for each beam vector i:

$$D_i(t) = RP(t) + R_z^T\left(\phi - \frac{\pi}{2}\right)\left[R_y^T(\theta)R_x^T(\psi)\begin{bmatrix}x_t \\ y_t \\ z_t\end{bmatrix}_{BF} + \begin{bmatrix}x_i \\ y_i \\ d_i\end{bmatrix}_{LBF}\right] \qquad (2.11)$$

Where - RP, A and D are the position (LL) for the reference point, the antenna and the sounding respectively

---

- t is time, with subscript 0 and 1 for two successive positions of the antenna, t alone being the time at transmission of the acoustic signals. The values for roll, pitch and heading used in the transformations are the readings at time t, t_0 and t_1

- X_0 and Y_0 are the X and Y coordinates of the RP at time t_0
- X_1 and Y_1 are the X and Y coordinates of the RP at time t_1

2.2.4.2 Vertical transformation

Soundings are always referred to a specific datum. On nautical chart, the sounding datum is a particular tidal datum (in Canada: Lower Low Water Large Tide [Forrester, 1983]) under which depths are reduced. The vertical position of the transducer with respect to the water plane is obtained from the ship's mean draught (from draught marks) but subsequent changes in elevation will occur due to ship's dynamics and eventually changes in water density. The depth measurements, which are made about the transducer, must therefore be corrected for changes in elevation (Z) of the transducer. The changes in transducer's elevation can be separated into short and long period variations:

Short period variations (< 20 sec)

- heave caused by waves and swell

- induced heave (lever arm effects caused by roll and pitch)

Long period variations (> 20 sec)

- draught changes due to changes in ship's displacement

- ship's settlement (defined in § 3.1.6.1)

- long term (> 20 s) list and/or trim induced heave

- changes in draught due to change in water density

- tides in coastal waters and water level changes in lakes and rivers

Because they affect not only a part of the swath but the entire across-track profile, variations in the elevation of the transducer must be considered with care. **Any undetected changes of the transducer draught will contribute in the total depth error of all beams.** The short period changes in the transducer elevation will be constantly monitored by the heave sensor (or VRU) but the long period ones exceed the common bandwidth of most heave sensors and these variations will be undetected. In the case of ship settlement, the sudden change in ship's mean draught will probably be sensed by the VRU but because of the cut-off period of the heave high-pass filter, the long term DC offset taken by the ship settlement will not be recorded by the VRU. Timing again is of importance: time for positions, attitude and heave must be logged

accurately and in synchronization with the logging system or the echo-sounder's clock. Figure 2.6 illustrates the various components used in the vertical transformation of depth measurements obtained after the refraction solution.

Change in transducer draught (squat, loading, ...)

Pitch 0°   Pitch 5°

Induced heave

Heave
+
Induced heave

Water Level

Tide

Sounding Datum

Sounding = Depth meas.
+ Transducer draught
+ Squat
- Heave
- Induced Heave
- Tide
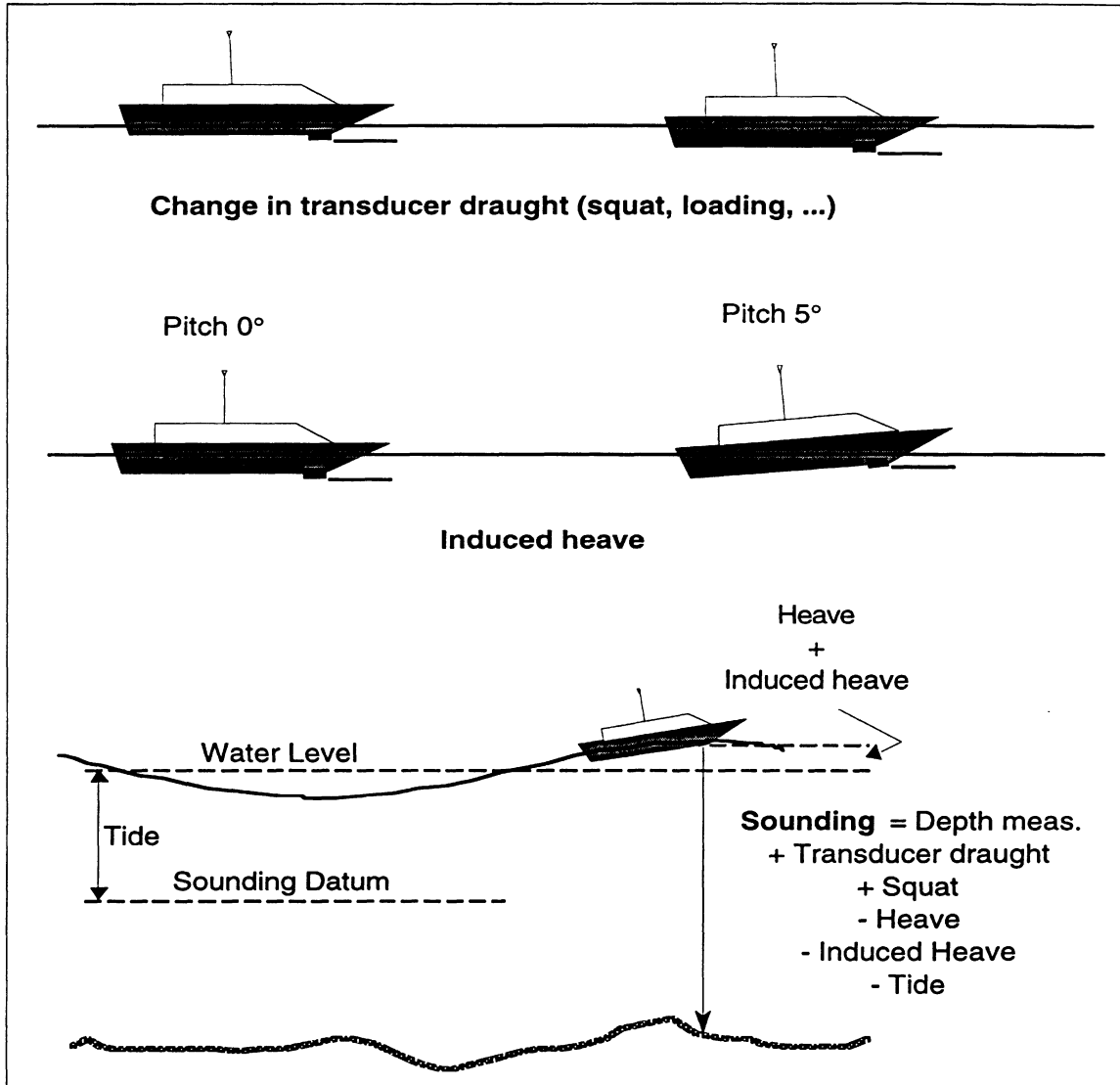
Figure 2.6   Changes in transducer draught and sounding reduction to a vertical datum.

The heave caused by the sea is measured by the VRU or by an independent heave sensor. Roll and pitch induced heave is a change in the transducer draught that can be computed, at time of reception, using the following equation:

$$IH_t(t) = -\sin(\theta)x_t + \cos(\theta)\sin(\psi)y_t + \cos(\theta)\cos(\psi)z_t \qquad (2.12)$$

This equation shows the approach used to compute the induced heave in shallow water (< 100 m). In deep water (> 100 m), where the 2-way travel time of the acoustic signal is longer, it may be necessary to record the heave and induced heave at both transmission and reception time in order to take into account the changes in heave and induced heave experienced by the transducer during the ping cycle. In shallow water, the time delay between transmission and reception is short compared to heave, pitch and roll periods and these changes can be neglected.

The VRU should be positioned at (or close to) the intersection of the roll and pitch axes of the vessel in order to correct appropriately for vertical movements of the transducer caused by roll and pitch induced heave. If the VRU is not located at the intersection of motion axes, induced heave will be sensed by the VRU for short period pitch and roll motions but the measured value for the DC offset taken will decay toward zero when the cut-off period of the heave high-pass filter is reached (also explained in § 3.1.6.5).

Corrections for VRU induced heave would be erroneous for trim and heel settling of the vessel (ballasting, prevailing wind, movement of personnel, etc.) that is beyond the cut-off frequency. If the VRU is located at the RP, it will monitor the ship's attitude and the heave caused by waves and swell but will not undergo any induced heave due to the absence of lever arms.

Hence, the last step in system integration has been to incorporate the vertical transformation into the z component of the beam vectors. These vertical variations must be carefully taken into account to keep consistency in the inter-swath coverage and to keep depth error within the specified limits for shallow water surveys. Error in tide and water level corrections will also contribute in the total depth error budget of soundings and they must be considered when evaluating against accuracy requirements.

2.2.5 A Simplified Approach for System Integration

This section will introduce the system integration in a simplified way. This new approach will make the explanation of sources of errors (chapter 3) simpler by not incorporating sophisticated models for the refraction solution of the acoustic beams. Hence, the remainder of the background material will ignore beam refraction and treat the propagation of the acoustic signals in a simplified form: the sound rays are linear, as if there were a homogeneous

water column with no sound velocity gradient due to increase in pressure (depth). This assumption will simplify the theory of errors produced by system biases but will slightly increase the level of uncertainty associated with the estimation of these errors. The reader must keep in mind that the real case includes non-homogenous watermasses in which beams are refracted and for which uncertainties in the water column parameters can contribute significantly to the total error budget.

2.2.5.1 The Sonar Vector

The Body-Frame "sonar vector" is the beam depth measurement that would occur in the absence of beam refraction. The sonar vector, as shown in Figure 2.7, is represented by a beam pointing angle β from the transducer's normal and by a slant range distance r from the projected centre of the transducer to the seafloor. The slant ranges are obtained from the 2-way travel time of the acoustic signals and a fixed speed of sound (as in shallow and well mixed water). The Sonar Vector (SV) differs from the beam vector (c.f. § 2.2.3) in the sense that it is expressed in a non-leveled Body-Frame coordinate system (i.e. not rotated for pitch and roll) and which is always perpendicular to the z-x plane in the Body-Frame.
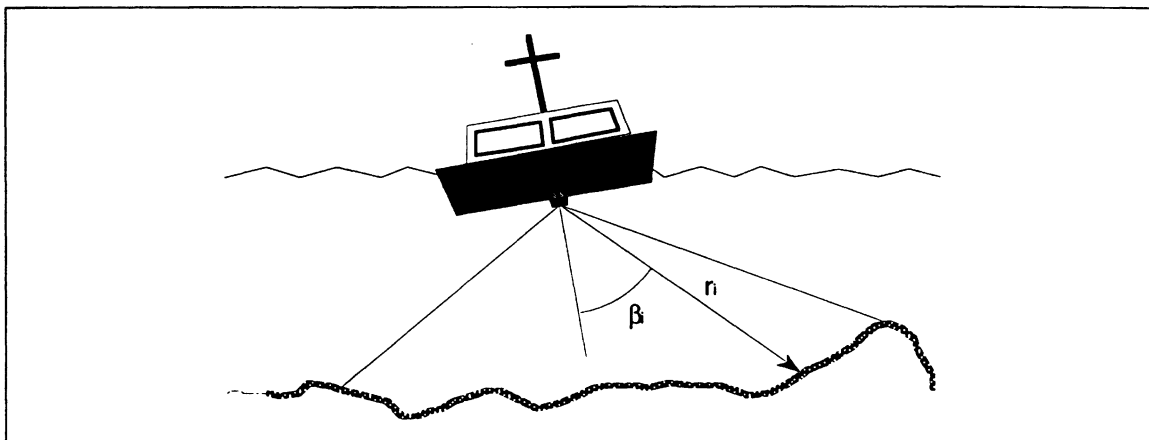
Figure 2.7 The Sonar Vector with beam pointing angle β and slant range r for beam i.

The sonar vectors are observed relative to the location of the transducer, in the Body-Frame coordinate system, through the relation:

$$\begin{bmatrix} x_i \\ y_i \\ z_i \end{bmatrix}_{BF} = \begin{bmatrix} 0 \\ -r\sin\beta_i \\ r\cos\beta_i \end{bmatrix} \qquad (2.13)$$

The subscript BF indicates that the coordinates are expressed in the Body-Frame system and the subscript i is to represents the ith beam.

2.2.5.2 Transformation of the Sonar Vector

The combination of the sonar vectors with the other sensor outputs is also based on temporal and spatial references. The transformation of the

---

sonar vector, from the Body-Frame to the Local-Level coordinate system can be done at once for the three rotations using the following relation:

$$D_i(t) = RP(t) + P^{-1} \left[\begin{bmatrix} x_t \\ y_t \\ z_t \end{bmatrix} + \begin{bmatrix} 0 \\ -r \sin\beta_i \\ r \cos\beta_i \end{bmatrix} \right] \qquad (2.14)$$

We used here the position of the reference point, obtained in Equation 2.8 and we rotated the sonar vectors, referred to the RP using the transducer offsets. In order to refer the soundings to a vertical datum the remaining transformations would consist of correcting for the vertical position of the RP with respect to the mean water plane and for ship settlement, heave and tide. Notice that the induced heave is taken care of during the transformation of the transducer vector (transducer offsets to the RP).

2.3 Accuracy Standards

The accuracy requirements for depth measurements and soundings presently in force at the IHO, and globally adopted by hydrographic offices are the ones established in the publication S44 [International Hydrographic Organisation (1987)]. These standards were originally established for hydrographic surveys using single beam echo-sounders and do not take into

account the use of MBES and other technologies achieving full bottom coverage. The main differences between MBES and single beam echo-sounders reside in the overall accuracy and in the digitizing and post-processing methods, and that single beam sounding lines provide interpo-lated bathymetry while MBES provides full bottom coverage. Up to now, users of multibeam echo-sounders had to comply with the accuracy requirements specified by the IHO or by the national standing orders for hydrographic surveys. The IHO accuracy standards for measuring depths, at the 90% confidence level, are as follow:

- ± 0.3 m for depths less than 30 m

- ± 1% for depths greater than 30 m

Including the tidal reduction, the IHO accuracy standards at 90% confidence level are:

- ± 0.42 m for depths less than 30 m

- ± 1.41% for depths greater than 30 m

The CHS accuracy standards, as prescribed in its Survey Standing Orders, uses the above mentioned IHO tolerance level as a basis. As for water level corrections, the CHS Standing Orders for "Reference of sounding to vertical

datum" state, somewhat vaguely, that "Location and duration of tidal observations are to be such that soundings, referenced to the sounding datum, should not have errors greater than one-half that specified in section 4" [CHS, 1986], which section refer to the IHO standards. Although not specified, this tolerance requirement is probably expressed at the same 90% confidence level. Consequently, the CHS allowable total error of soundings (i.e. referred to sounding datum) at the 90% confidence level (1.67 σ) become :

- ± 0.34 m for depths less than 30 m

- ± 1.12% for depths greater than 30 m

Additionally, the section in the CHS Standing Orders on "Allowable Discrepancies of Check Lines and Lines Crossing" states that differences between regular soundings and those obtained by check lines should be, 90% of the time, within 0.5 m for depth below 30 m and within 1.6% of the water depth for deeper waters. These tolerance levels are less stringent but much more pragmatic, and are the ones mostly achieved in practice for CHS hydrographic surveys.

Depth measurements acquired with multibeam echo-sounding systems will very often meet these accuracy requirements. But the outer beams of ultra-wide MBES (systems for which the swath width exceeds 5 times the

water depth), which are severely affected by roll errors and beam refraction, can depart significantly from these accuracy standards.

3. Sources of Error for Shallow Water MBES

The purpose of this chapter is to identify the sources of error that affect MBES data and list the systematic errors that should be considered for shallow water operations. The identification of these sources of systematic errors will define the system "integration parameters" required to compute correct geo-referenced depth measurements to the mean water surface, when not affected by refraction solution errors.

3.1 Sources of Errors

Sources of errors present in multibeam echo-sounding systems can be separated into two categories:

     (1)   The sources that contribute to "DEPTH ERROR"

     (2)   The sources that contribute to "POSITION ERROR"

Figures 3.1 and 3.2 outline these errors. One can see that each category of error sources is further divided into specific components. Those sources of error do not all generate systematic depth and position errors, and will not all be regarded as causes for biases that can be corrected by calibration.
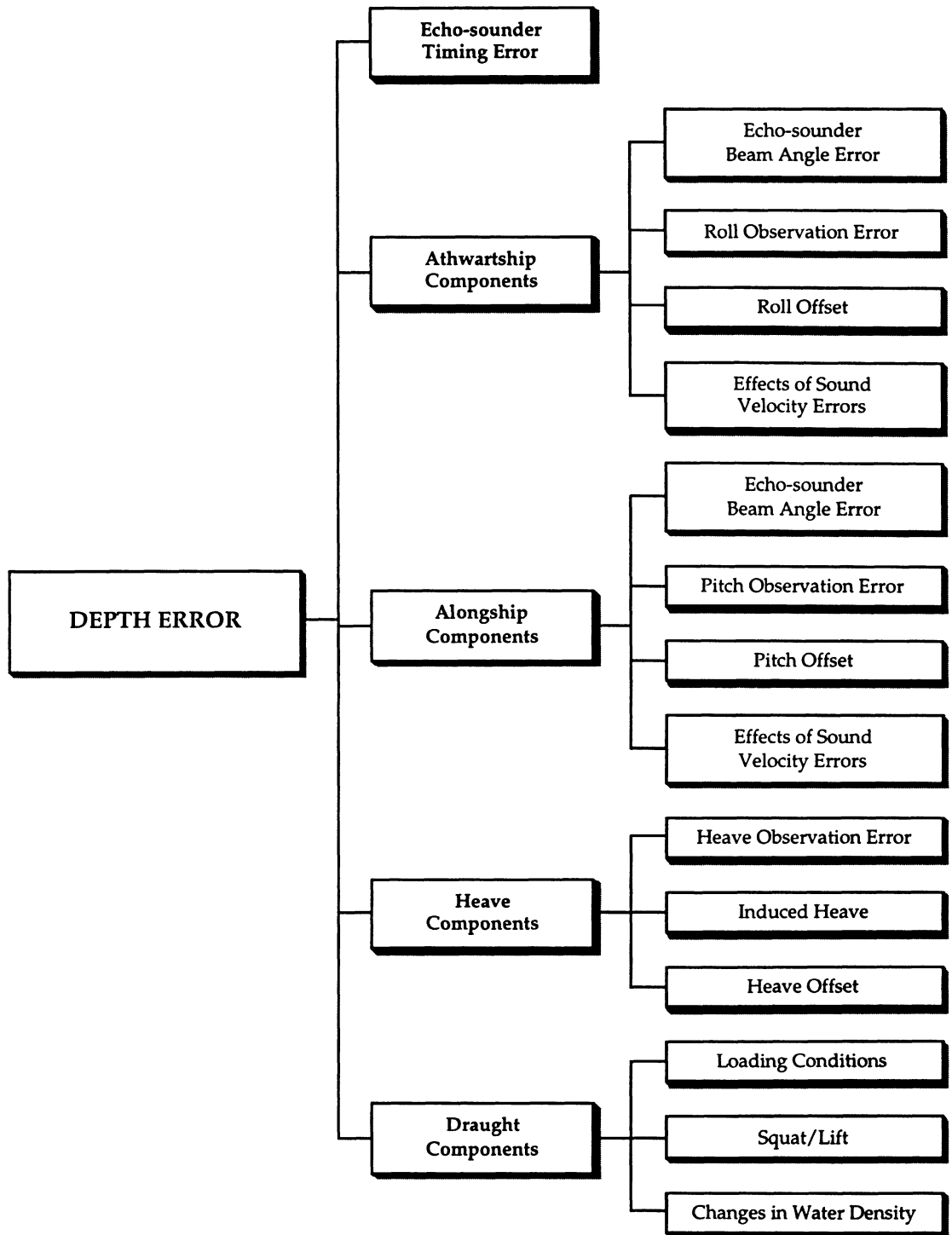
Figure 3.1 Sources of depth error of soundings.
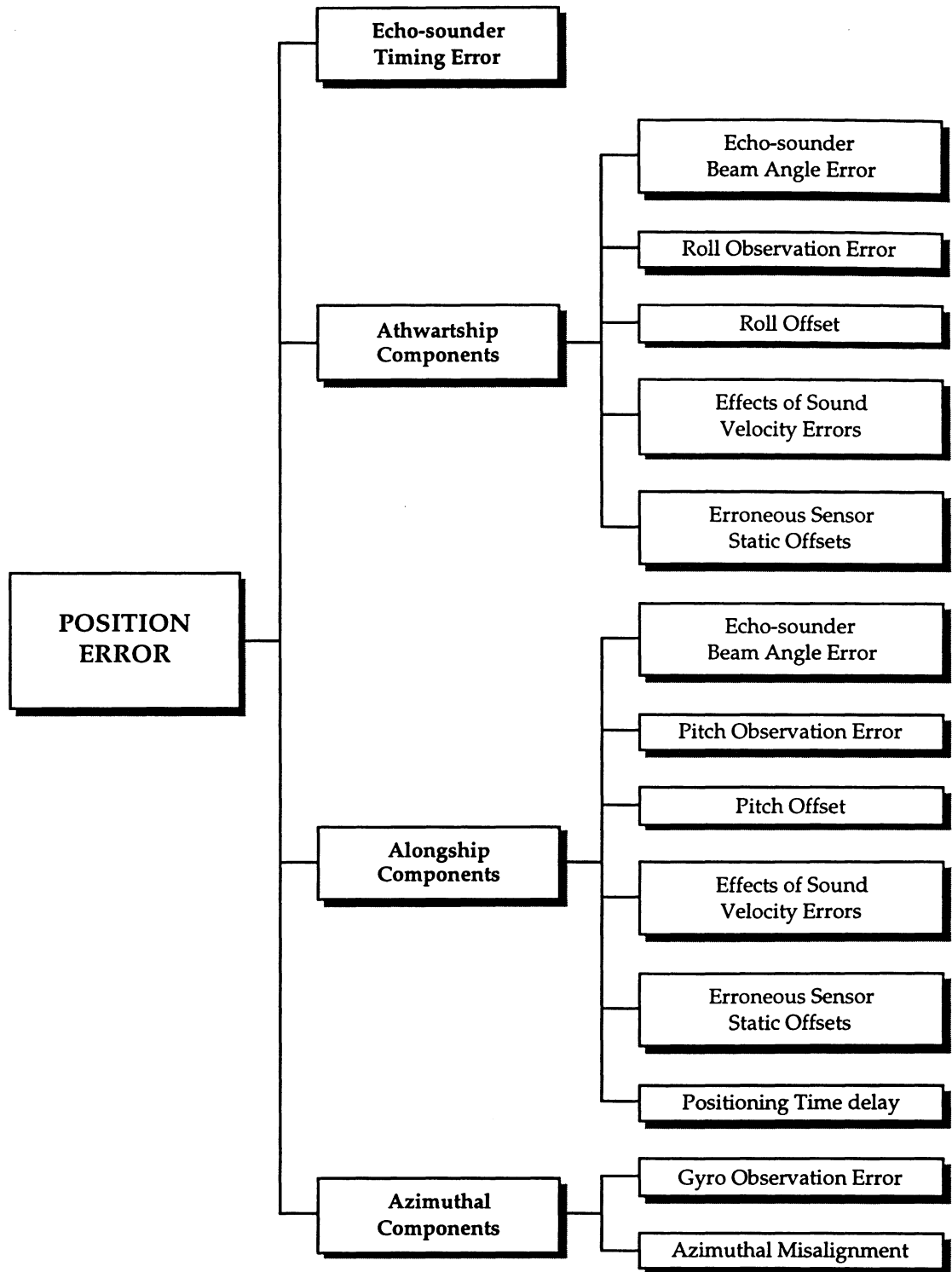
Figure 3.2   Sources of position error of soundings.

In fact, many of these sources generate random errors, some being instrument specific, such as echo-sounder range and beam angle errors, while other are peculiar to a particular installation, such as dynamic draught or Gyro-compass observation errors. Not included in the "depth error" are tide gauge and tide correction errors, which affect the accuracy of soundings with respect to a specific datum.

Amongst all the listed sources of error, the ones that will systematically affect depth and position of soundings of shallow water MBES surveys have been identified as follow:

- Roll offset

- Pitch offset

- Gyro offset

- Azimuthal misalignment of the VRU

- VRU time delay

- Dynamic draught (ship settlement, loading conditions, water density)

- Sensor static offsets (position and induced heave errors)

- Positioning time delay

- Echo-sounder instrumental errors

- Variations of the speed of sound in the water column

There are different types of systematic error that can be generated by these error sources. For instance, angular offsets produce systematic "cyclic errors", which vary regularly in both size and sign [Mikhail and Gracie, 1981], following an oscillatory pattern. Others, such as ship settlement or positioning time delay, will create "constant" systematic errors in either depth or position.

In the following sub-sections, the relative position and depth errors are defined as such: the relative position error is the distance in X or Y, measured on the horizontal plane (Local-Level reference frame for Gyro offset and Leveled Body-Frame for the other error sources), from the observed sonar vector (real hit on the seafloor) to the position where we assume it is located (position affected by the bias); the depth error is the vertical projection of the difference between the observed sonar vector and the biased one. Also, in order to keep the explanations simple, we will derive the errors as if there were no roll and pitch motions of the survey platform. Nevertheless, one should realize that the apparent depth error (apparent depth minus true depth, located at the apparent position) is the one that would eventually be present on the charted sounding.

3.1.1 Roll Offset

Roll offset is one of the most important sources of error. The angular offset ρ lies between the VRU's vertical reference and the Transducer's normal in the y-z plane. In other words, it is the residual angle between the transducer's and the VRU's y axes, in the Body-Frame. The depth error of the soundings, caused by a roll offset, increases with beam obliquity and with increasing depth while the position error remains almost constant with obliquity but increases with increasing depth. For a flat bottom, these errors are proportional to beam angle and depth under the keel. The errors can easily be seen when the multibeam echo-sounder is sweeping a flat seabed. Figure 3.3 illustrates the geometry of a port beam affected by a positive roll offset. The real hit on the seafloor is represented by:

$$y_i = -r_i \sin(\beta_i - \rho) \tag{3.1}$$

$$z_i = d = r_i \cos(\beta_i - \rho) \tag{3.2}$$

Where y_i is the LBF y coordinate relative to the transducer

d is the depth below the transducer

β is the beam pointing angle (w.r.t. transducer's normal)

ρ is the roll offset

The apparent y' and z' relative coordinates for a beam i are retrieved by

applying a rotation of angle ρ to the real sonar vector:

$$\begin{bmatrix} x_i' \\ y_i' \\ z_i' \end{bmatrix}_{LBF} = \begin{bmatrix} 1 & 0 & 0 \\ 0 & \cos(\rho) & -\sin(\rho) \\ 0 & \sin(\rho) & \cos(\rho) \end{bmatrix} \begin{bmatrix} 0 \\ -r_i \sin(\beta_i - \rho) \\ r_i \cos(\beta_i - \rho) \end{bmatrix}$$

$$= \begin{bmatrix} 0 \\ -r_i \cos(\rho) \sin(\beta_i - \rho) - r_i \sin(\rho) \cos(\beta_i - \rho) \\ -r_i \sin(\rho) \sin(\beta_i - \rho) + r_i \cos(\rho) \cos(\beta_i - \rho) \end{bmatrix} \qquad (3.3)$$

$$= \begin{bmatrix} 0 \\ -r_i \sin(\beta_i) \\ r_i \cos(\beta_i) \end{bmatrix}$$
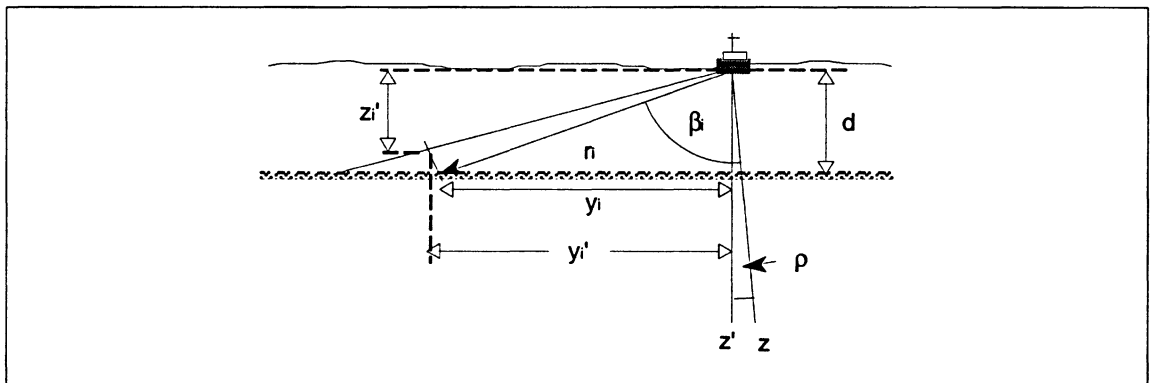
Figure 3.3   Representation of a positive roll offset ρ and the geometry associated with the real hit on the seafloor, having a measured slant range r_i and across-track distance y_i on the LBF reference frame. The z' axis is the VRU's vertical, the distance y_i' represents the assumed relative across-track distance (LBF) for a beam i pointing at angle β from the transducer's normal.

Figure 3.4 illustrates depth and position errors caused by a roll offset and

the associated apparent profile of the seafloor.
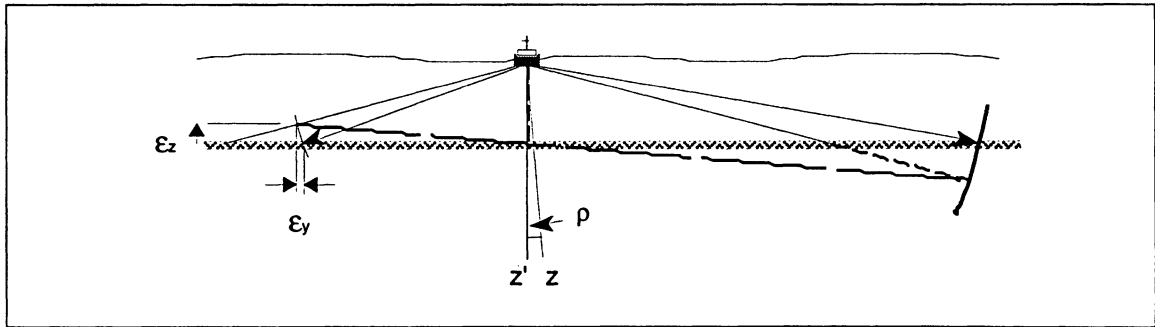
Figure 3.4 Effect of a positive roll offset ρ on bathymetry, over a flat bottom, when seen from astern. The horizontal line is the true location of the bottom while the dashed line represents the apparent seafloor; εz and εy are the depth and position errors respectively for the outer port beam.

Assuming the swept surface is absolutely planar, the relative position

(across-track distance) error εy and depth error εz for a beam i, caused by a roll

offset can be computed as follows:

$$\varepsilon y_i = y_i - y_i' = r_i\left[\sin(\beta_i) - \sin(\beta_i - \rho)\right] \tag{3.4}$$

$$\varepsilon z_i = z_i - z_i' = r_i\left[\cos(\beta_i - \rho) - \cos(\beta_i)\right] \tag{3.5}$$

Expressed as a function of depth **d** under the transducer:

$$r_i = \frac{d}{\cos(\beta_i - \rho)}$$

$$\mathcal{E}y_i = d \left[\frac{\sin(\beta_i)}{\cos(\beta_i - \rho)} - \tan(\beta_i - \rho) \right] \qquad (3.6)$$

$$\mathcal{E}z_i = d \left[1 - \frac{\cos(\beta_i)}{\cos(\beta_i - \rho)} \right] \qquad (3.7)$$

As plotted in Figure 3.5, the depth error increases rapidly with increasing

beam pointing angle β (the cosine increases greatly for angles $15° \leq \beta \leq 75°$.

This explains why a roll offset is of particular concern for wide opening swath

systems. With a roll offset of 1°, the 1% IHO accuracy requirement for depth

measurements is reached at about 30° from nadir. Notice that the relative

position offset remains almost constant throughout the swath.
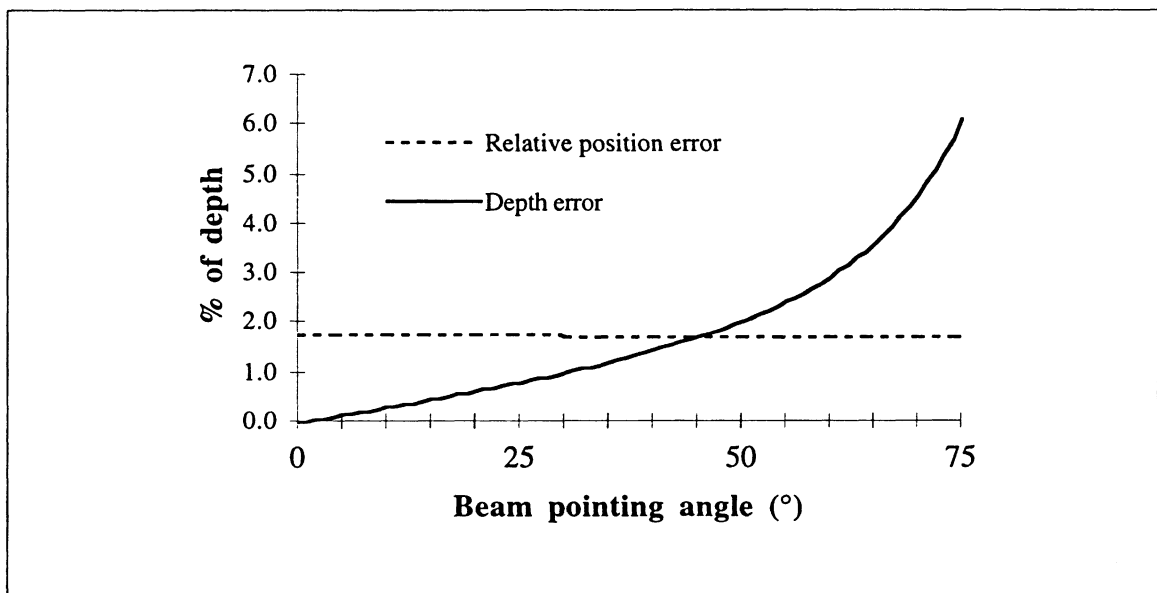
Figure 3.5   Relative position and depth error (absolute value) represented in percentage of depth d under the transducer, as a function of β the beam pointing angle and for a roll offset of 1°.

To correct a roll offset, one can subtract the error to the roll value in the coordinate transformation, which becomes:

$$\begin{bmatrix} x_i \\ y_i \\ z_i \end{bmatrix}_{LL} = R_y \, R_z^t(\phi - 90°) \, R_y^t(\theta) \, R_x^t(\psi - \rho) \begin{bmatrix} 0 \\ -r_i' \, \sin\beta_i \\ r_i' \, \cos\beta_i \end{bmatrix}_{BF} \qquad (3.8)$$

The problem in correcting for a roll bias in the transformation is that it does not physically remove the offset, hence systematically reducing the swath width on one side of the ship. One should try instead to correct the VRU mount angle or its output value for roll.

3.1.2 Pitch Offset

The pitch offset is the angular bias λ lying between the VRU's vertical reference and the transducer's normal in the x-z plane (BF). The contribution of the pitch offset to the depth and position errors of the soundings is relatively small in shallow water or over a flat terrain. The depth and position errors are more pronounced when surveying perpendicularly to slopes and are increasing with increasing depths. Hence, systematic depth and position errors caused by a pitch offset are proportional to the depth under the keel.
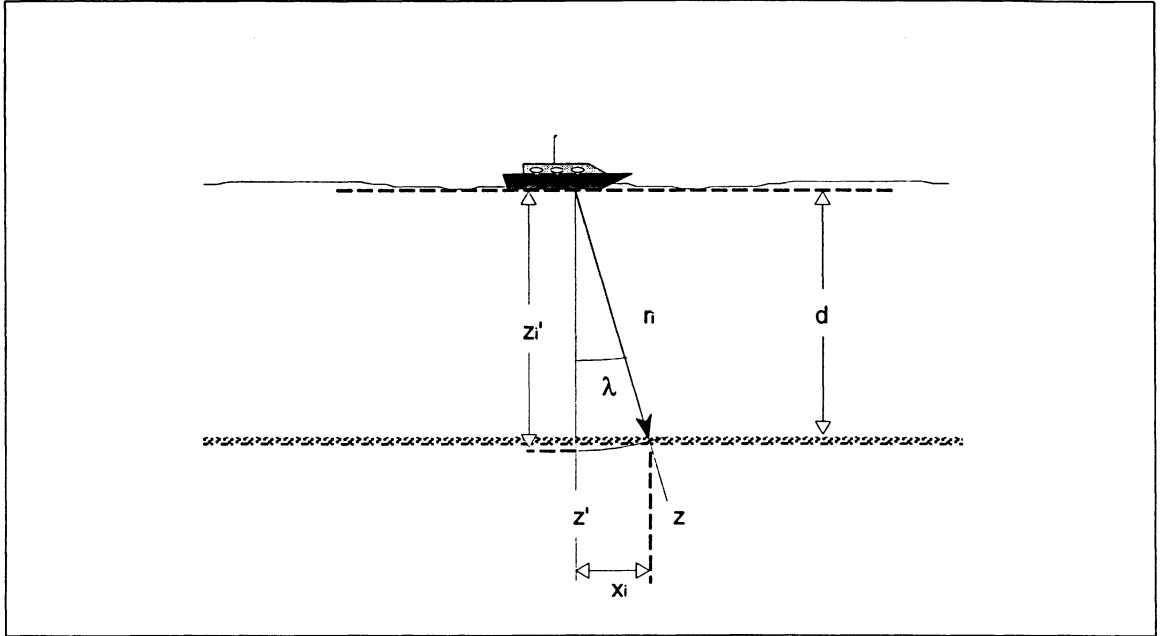
Figure 3.6 Geometry for a beam i with a negative pitch offset λ when sounding over a **flat** bottom or along a contour line. Depth under keel is d but the depth read by the beam is z_i'. The z' axis is the VRU's vertical and z represents the transducer's normal.

Let us examine the effect of a pitch offset on the sonar vector when surveying over a flat terrain or along a contour line (along the strike). Figure 3.6 illustrates the geometry of a beam affected by a negative pitch error. The real hit on the seafloor can be obtained as follows:

$$
\begin{bmatrix} x_i \\ y_i \\ z_i \end{bmatrix}_{BF} = \begin{bmatrix} \cos(\lambda) & 0 & -\sin(\lambda) \\ 0 & 1 & 0 \\ \sin(\lambda) & 0 & \cos(\lambda) \end{bmatrix} \begin{bmatrix} 0 \\ -r_i \sin(\beta_i) \\ r_i \cos(\beta_i) \end{bmatrix}
$$

$$
= \begin{bmatrix} -r_i \sin(\lambda)\cos(\beta_i) \\ -r_i \sin(\beta_i) \\ r_i \cos(\lambda)\cos(\beta_i) \end{bmatrix}
$$

(3.9)

With the apparent sonar vectors being:

$$
\begin{bmatrix} x_i' \\ y_i' \\ z_i' \end{bmatrix} = \begin{bmatrix} 0 \\ -r_i \sin(\beta_i) \\ r_i \cos(\beta_i) \end{bmatrix}
\tag{3.10}
$$

The relative position error $\mathcal{E}x$ and depth error $\mathcal{E}z$, for each beam i, are obtained from the relations:

$$
\mathcal{E}x_i = -r_i \sin(\lambda) \cos(\beta_i)
\tag{3.11}
$$

$$
\mathcal{E}z_i = z_i - z_i' = r_i \cos(\lambda) \cos(\beta_i) - r_i \cos(\beta_i)
$$

$$
= r_i \cos(\beta_i)[\cos(\lambda) - 1]
\tag{3.12}
$$

And as a function of depth (d) under the keel:

$$
r_i = \frac{d}{\cos(\beta_i) \cos(\lambda)}
\tag{3.13}
$$

$$
\mathcal{E}x = -d \tan(\lambda)
\tag{3.14}
$$

$$
\mathcal{E}z = d \left[1 - \frac{1}{\cos(\lambda)} \right]
\tag{3.15}
$$

As shown in Figure 3.7, the relative position error is one order of magnitude larger then the depth error for small pitch biases (< 2°).
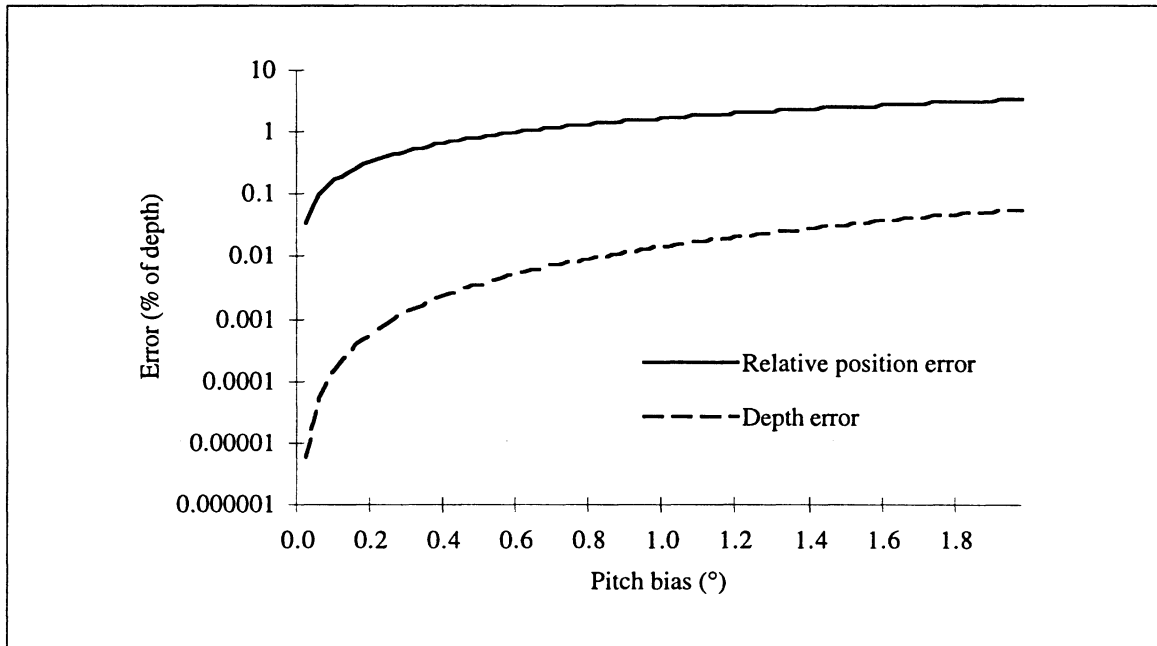
Figure 3.7   Relative position and depth error (absolute value) represented (logarithmic scale) in percentage of depth d under the transducer, as a function of the pitch bias λ.

The relative position and depth errors are different when the ship is surveying across contour lines — not a common practice for MBES but employed to detect pitch offset and positioning time delay — which is illustrated in Figure 3.8.
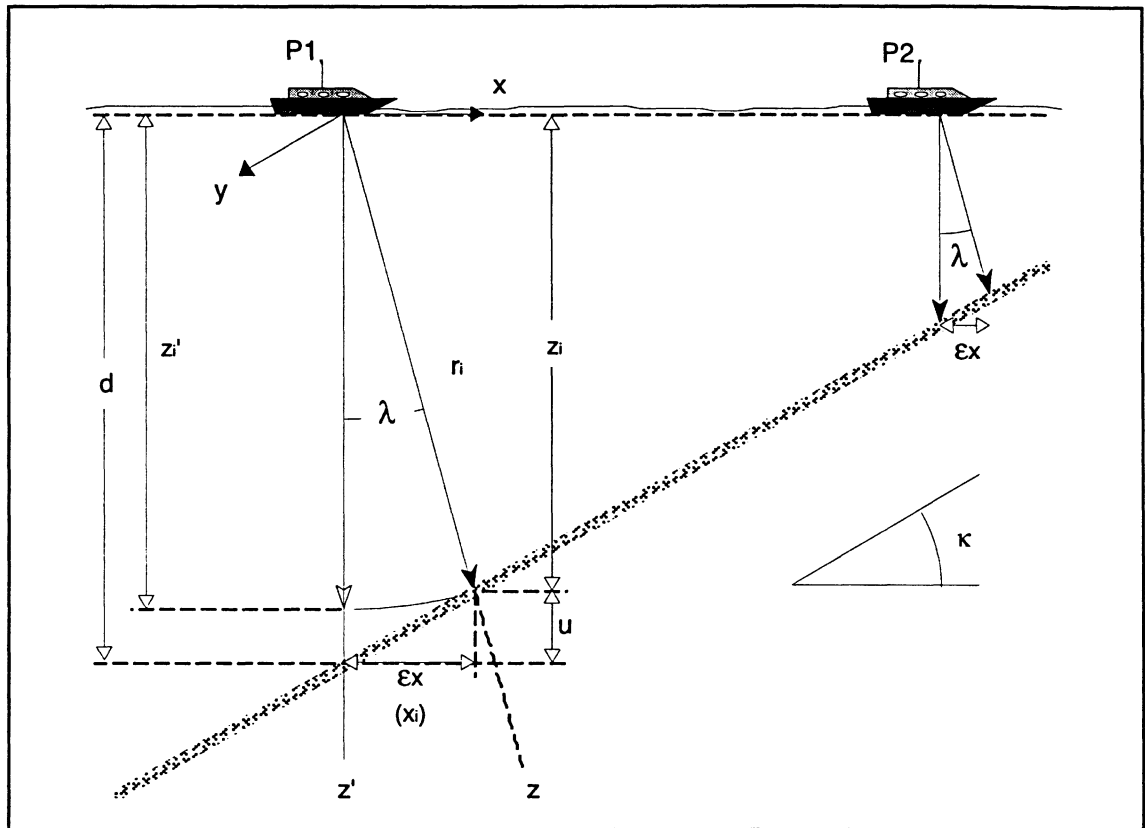
Figure 3.8 Cross section of a survey line going upslope, showing the effect of a negative pitch offset on the sonar vectors. The slope κ and the pitch offset λ have been intentionally exaggerated to emphasize the relative position and depth error εx. Notice how larger the relative position error is in deeper water (P1).

In Figure 3.8 above, the depth **d** under the transducer is equivalent to:

$$u = x_i \tan(\kappa)$$

$$d = z_i + u$$

$$= r_i \cos(\lambda) \cos(\beta_i) + \left[-r_i \sin(\lambda) \cos(\beta_i) \tan(\kappa)\right]$$

$$= r_i \cos(\beta_i)[\cos(\lambda) - \sin(\lambda) \tan(\kappa)]$$

and
$$r_i = \frac{d}{\cos(\beta_i)[\cos(\lambda) - \sin(\lambda)\tan(\kappa)]} \qquad (3.16)$$

With the case of a sloping seafloor, and assuming the swept surface is absolutely planar, the relative position error $\mathcal{E}x$ and depth error $\mathcal{E}z$ caused by a pitch offset, as a function of depth d under the transducer and for each beam i are as follows:

$$\mathcal{E}x_i = -r_i \sin(\lambda)\cos(\beta_i)$$

$$= \frac{-d \, \sin(\lambda)}{\cos(\lambda) - \sin(\lambda)\tan(\kappa)} \qquad (3.17)$$

$$\mathcal{E}z_i = r_i \cos(\beta_i)[\cos(\lambda) - 1]$$

$$= \frac{d\,[\cos(\lambda) - 1]}{\cos(\lambda) - \sin(\lambda)\tan(\kappa)} \qquad (3.18)$$

The same way roll offset was corrected, one can subtract the error of the pitch value in the coordinate transformation to compensate for a pitch offset:

$$\begin{bmatrix} x_i \\ y_i \\ z_i \end{bmatrix}_{LL} = R_y \, R_z^t(\phi - 90°)\, R_y^t(\theta - \lambda)\, R_x^t(\psi) \begin{bmatrix} 0 \\ -r_i{}' \, \sin\beta_i \\ r_i{}' \, \cos\beta_i \end{bmatrix}_{BF} \qquad (3.19)$$

The problem of correcting for a pitch bias in the transformation is that when the beam refraction solution is performed in real time, it uses the instantaneous plane of insonification, which will be erroneous if the pitch values are not corrected in real time as well.

3.1.3 Gyro Offset

The gyro offset is the angular misalignment between the Gyro-compass heading reference and the transducer x-axis. The projected fan, which is supposed to be exactly perpendicular to the transducer x-axis, will make an angle with the perpendicular of the ship's heading. Consequently, the beams that spread out on either side of nadir are subject to position error which will grow as we move away from nadir. The errors associated with a gyro offset are proportional to depth and to the beam pointing angle. Figure 3.9 illustrates the gyro offset.

Even in presence of a gyro offset, there will be no depth error for soundings acquired over a flat seafloor. Indeed, there is no azimuth angle ϕ in the lower term of the inverse of the transformation matrix P (2.4):

$$P^{-1} = \begin{bmatrix} \sin(\phi)\cos(\theta) & \sin(\phi)\sin(\theta)\sin(\psi) + \cos(\phi)\cos(\psi) & \sin(\phi)\sin(\theta)\cos(\psi) - \cos(\phi)\sin(\psi) \\ -\cos(\phi)\cos(\theta) & -\cos(\phi)\sin(\theta)\sin(\psi) + \sin(\phi)\cos(\psi) & -\cos(\phi)\sin(\theta)\cos(\psi) - \sin(\phi)\sin(\psi) \\ -\sin(\theta) & \cos(\theta)\sin(\psi) & \cos(\theta)\cos(\psi) \end{bmatrix}$$

$$(3.20)$$
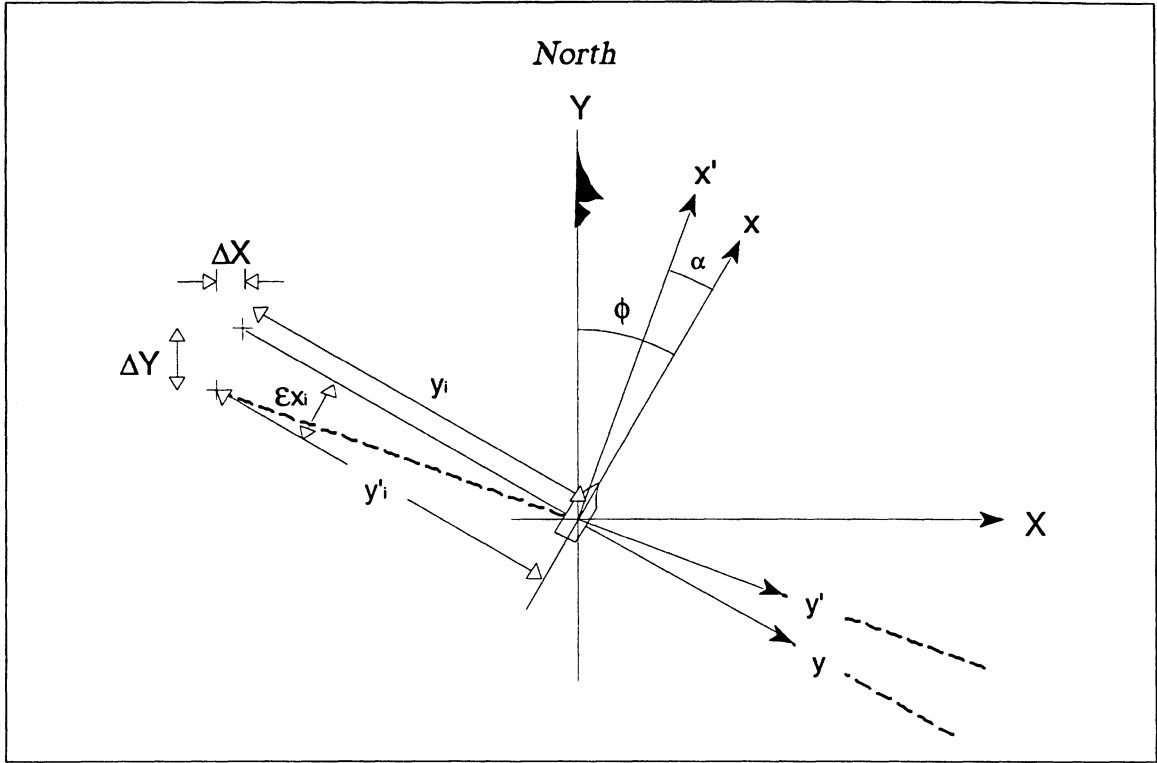
Figure 3.9   Plan view of a negative gyro offset α. Local-Level coordinate system XY is shown, along with the azimuth angle φ. Position discrepancies for an outer port beam are represented by ΔX and ΔY in Local-Level coordinates. LBF y coordinate is shown along with the LBF y' for the assumed location of beam i and its relative position error εx.

For a gyro offset α, the real hit on the seabed made by the sonar vectors

are represented by:

$$
\begin{bmatrix} x_i \\ y_i \\ z_i \end{bmatrix}_{BF} = \begin{bmatrix} \cos(\alpha) & \sin(\alpha) & 0 \\ -\sin(\alpha) & \cos(\alpha) & 0 \\ 0 & 0 & 1 \end{bmatrix} \begin{bmatrix} o \\ -r_i \sin(\beta_i) \\ r_i \cos(\beta_i) \end{bmatrix}
$$

$$
= \begin{bmatrix} -r_i \sin(\alpha) \sin(\beta_i) \\ -r_i \cos(\alpha) \sin(\beta_i) \\ r_i \cos(\beta_i) \end{bmatrix}
$$

(3.21)

Obviously, the assumed sonar vectors remain unchanged:

$$\begin{bmatrix} x_i{}' \\ y_i{}' \\ z_i{}' \end{bmatrix} = \begin{bmatrix} 0 \\ -r_i \sin(\beta_i) \\ r_i \cos(\beta_i) \end{bmatrix}$$

The corresponding relative position and depth errors are obtained as follow:

$$\mathcal{E}x_i = x_i - x_i{}'$$

$$= -r_i \sin(\alpha) \sin(\beta_i) \tag{3.22}$$

$$\mathcal{E}y_i = y_i - y_i{}'$$

$$= -r_i \cos(\alpha) \sin(\beta_i) + r \sin(\beta_i) \tag{3.23}$$

$$= r_i \sin(\beta_i)[1 - \cos(\alpha)]$$

$$\mathcal{E}z_i = z_i - z_i{}' = 0 \tag{3.24}$$

And as a function of depth **d** under the transducer:

$$r_i = \frac{d}{\cos(\beta_i)}$$

$$\mathcal{E}x_i = -d \sin(\alpha) \tan(\beta_i) \tag{3.25}$$

$$\mathcal{E}y_i = d \tan(\beta_i) [1 - \cos(\alpha)] \tag{3.26}$$

The relative position errors (LBF), as shown in Figure 3.10, increase with

increasing beam obliquity. For small gyro offsets (< 2°) the relative position

error in x is one order of magnitude larger then the one in y.
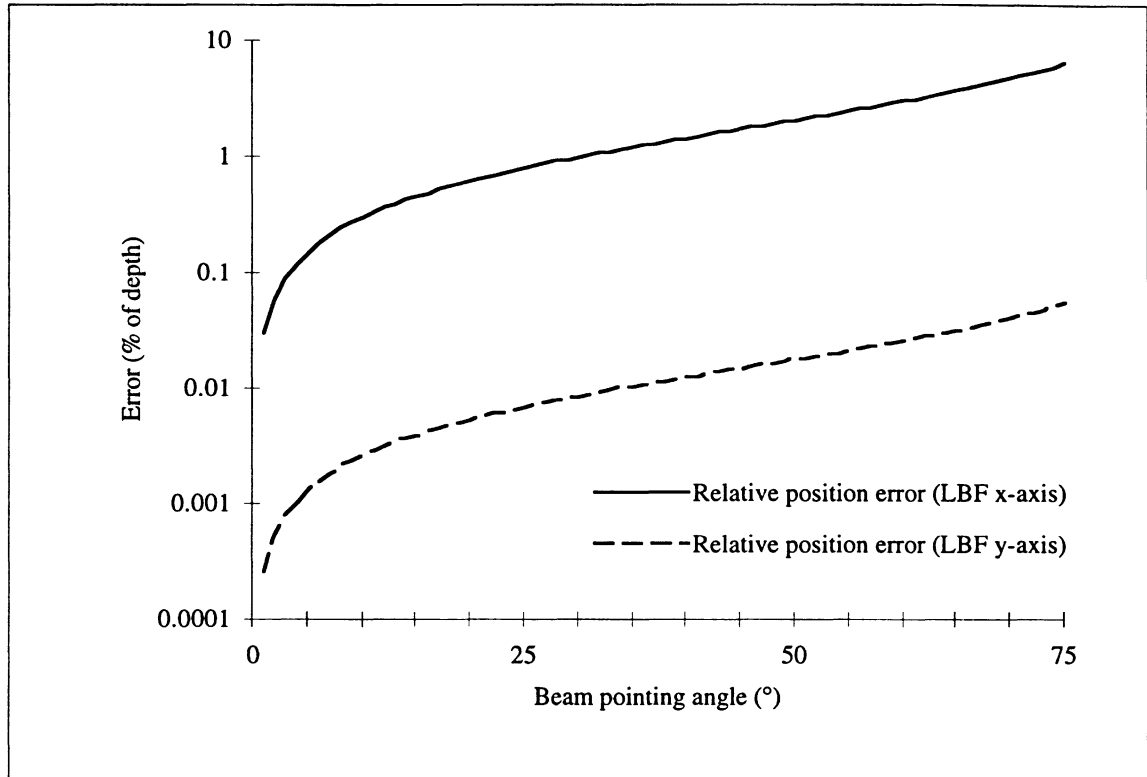
Figure 3.10 Relative position errors (absolute value) represented (logarithmic scale) in
percentage of depth d under the transducer, as a function of the beam pointing
angle β. A 1° gyro offset was used to compute these values.

The same way roll and pitch offsets were corrected, one can subtract the

error to the gyro value in the coordinate transformation to compensate for a

gyro offset:

$$
\begin{bmatrix} x_i \\ y_i \\ z_i \end{bmatrix}_{LL} = R_y \, R_z^t(\phi - 90° - \alpha) \, R_y^t(\theta) \, R_x^t(\psi) \begin{bmatrix} 0 \\ -r_i' \, \sin\beta_i \\ r_i' \, \cos\beta_i \end{bmatrix}_{BF} \tag{3.27}
$$

Doing so would correct the situation but would limit the swath width on both sides of the ship. One should rather rotate mechanically the gyro-compass or correct its output values. If the offset is caused by a misalignment of the transducer (not perpendicular to the ship's longitudinal axis), the transducer itself must be rotated.

3.1.4 Azimuthal Misalignment of the VRU

If the sensitive axes of the Vertical Reference Unit are not well aligned with the ship's x and y axes, there will be "cross talk" between the roll and pitch sensitive axes of the motion sensor. The relations between roll and pitch measurements (Euler angles), in the presence of a misalignment γ are:

$$
\sin(\psi') = \cos(\gamma) \sin(\psi) - \sin(\gamma) \sin(\theta) \tag{3.28}
$$

$$
\sin(\theta') = \cos(\gamma) \sin(\theta) - \sin(\gamma) \sin(\psi) \tag{3.29}
$$

Where ψ' is the erroneous roll

  ψ is the true roll

θ' is the erroneous pitch

θ is the true pitch

The theory behind these two expressions is explained in Appendix I. The next two figures (3.11 & 3.12) are sensitivity plots that show how an azimuthal misalignment of the VRU can affect roll measurements. Fixed pitch values of 5° and 10° (rough survey conditions) have been used to generate these graphs. Pitch error can be demonstrated the same way. Nevertheless, a pitch of more than 15° is not likely to occur in normal survey operations and the associated pitch error is of less importance.
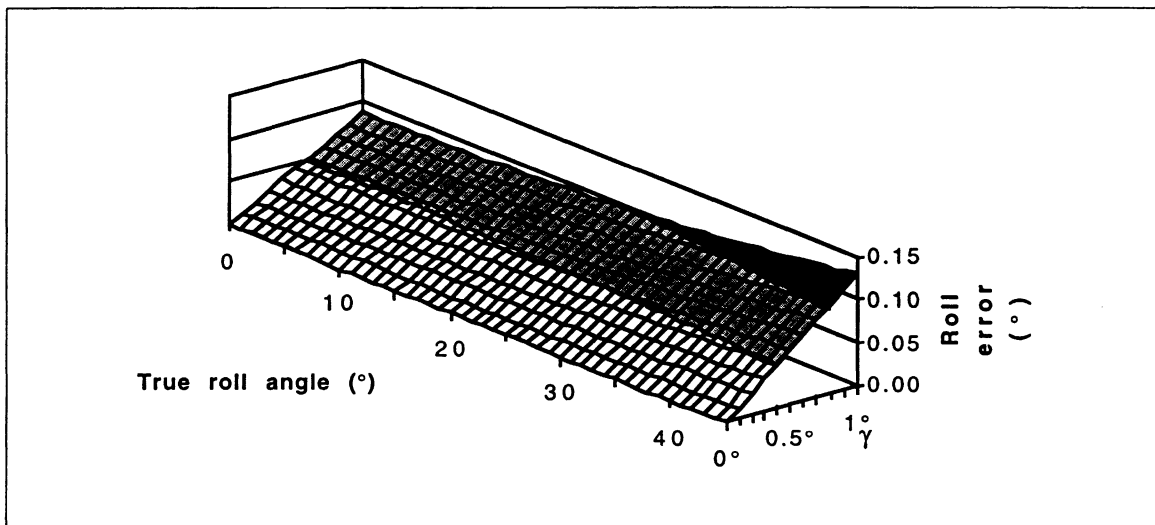
Figure 3.11 Sensitivity plot for roll error caused by VRU misalignment γ with a pitch of 5°.

Pitch and roll errors associated with the azimuthal misalignment of the Vertical Reference Unit are systematic cyclic errors. They are thus dynamic

errors characterized by a zero mean if the vessel is even keel at rest. They will

generate, proportionally to beam angle, bottom slope and water depth,

position and depth errors of soundings (just like roll and pitch offsets would

do).
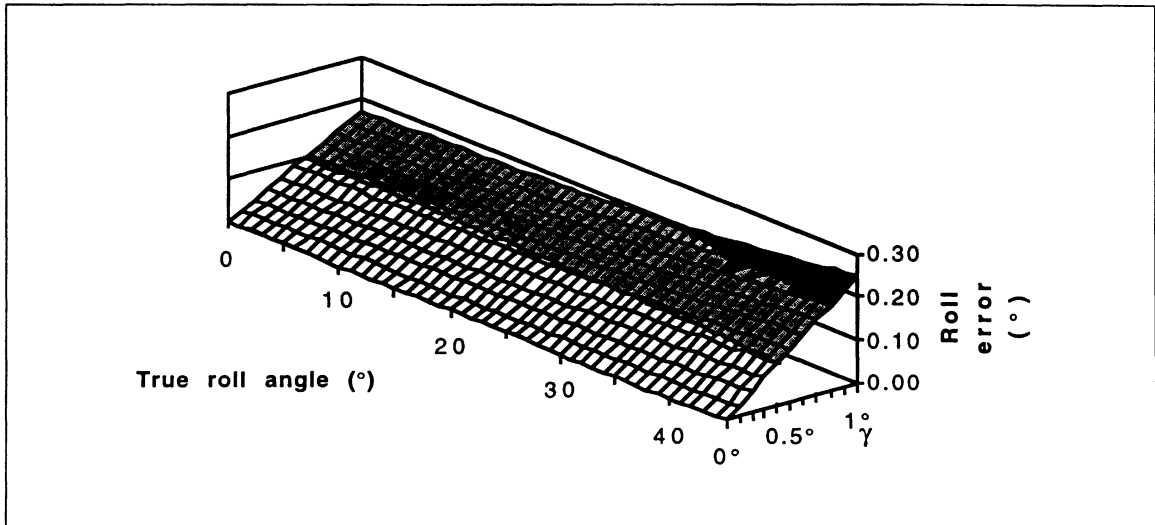
Figure 3.12   Sensitivity plot of Roll error caused by VRU misalignment γ with a pitch of 10°.

3.1.5 VRU time delay

Another source of cyclic error is time delay in the measurement of ship's

motions output by the Vertical Reference Unit. Time delay will generate

pitch and roll errors and errors in heave when values for vertical motion are

also measured by the VRU. The effects of VRU time delay are particularly

noticeable from roll errors where the seafloor slope, as measured by the

multibeam echo-sounder in the across-track sense, oscillates about the mean

value with a period similar to the ship's roll [Hughes Clarke, 1993a]. This effect is illustrated in Figure 3.13.
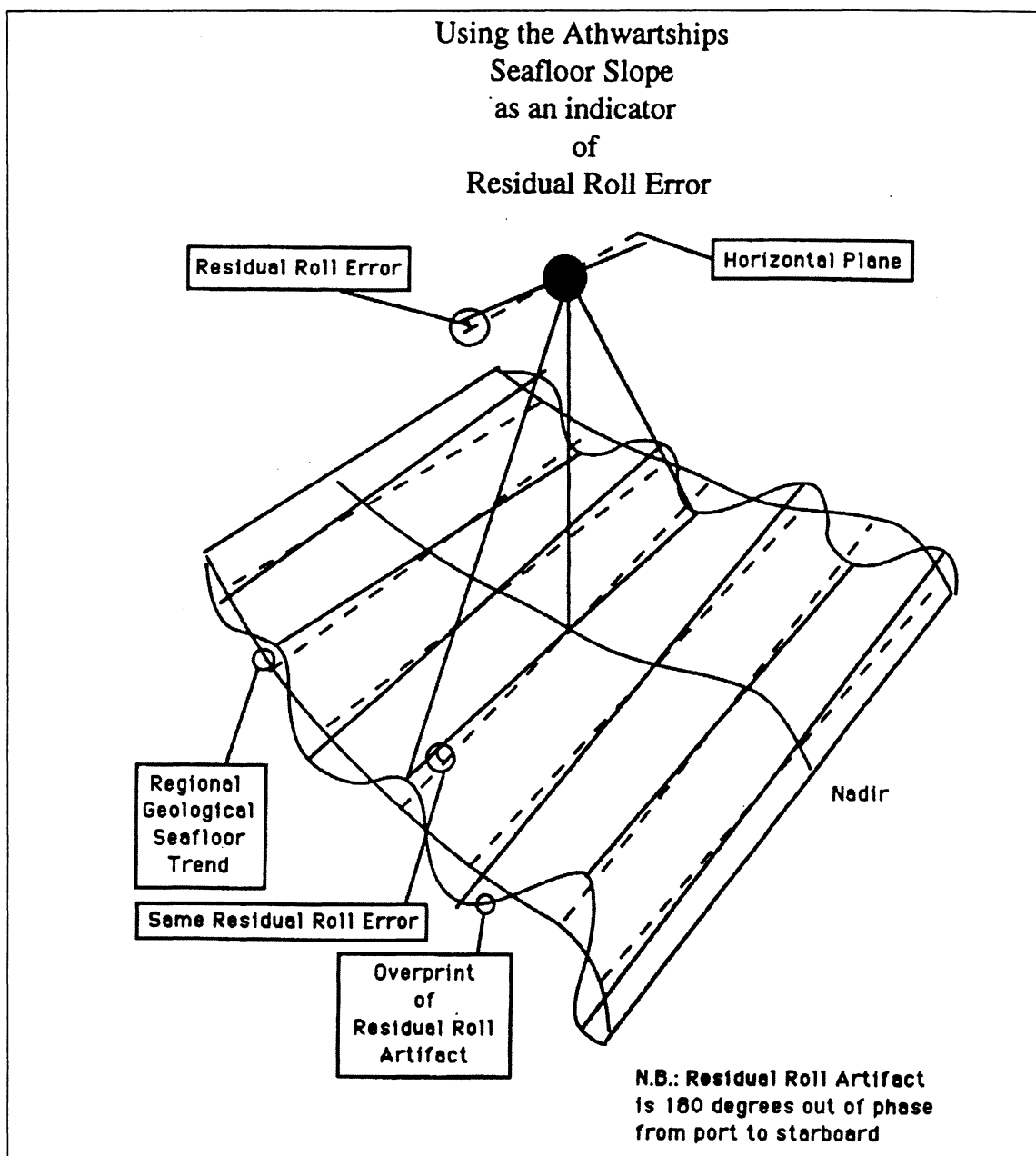
Figure 3.13   Residual Roll Error caused by time delay in the VRU roll output [from Hughes Clarke, J. (1993), Appendix]

The errors caused by a time lag in the VRU output can be seen as a varying roll or pitch offsets, with periods equal to the ship's roll and pitch. The maximum roll or pitch error would occur during the maximum rate of change in the ship's motion. Figure 3.14 represents the cyclic roll errors caused by a VRU time delay and Figure 3.15 is a sensitivity analysis for varying time delay and roll frequency. Roll has been chosen here as an example, but the effect can be applied as well to pitch or heave (where amplitude is elevation about mean).
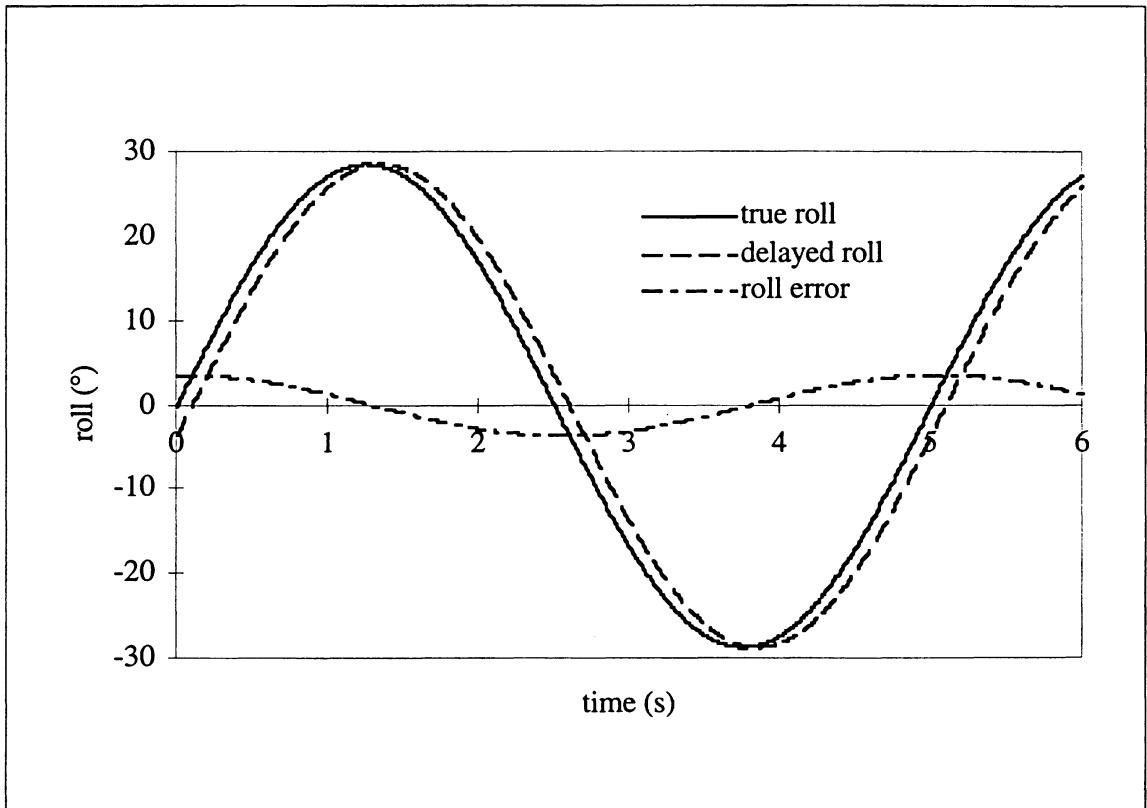
Figure 3.14 Simulated roll, delayed roll and roll error with a roll frequency of 0.2 Hz and a 0.1 sec time delay.

The roll error of Figure 3.14 has been computed as follow:

$$\text{roll} = a \sin(2\pi f t) \tag{3.30}$$

$$\text{delayed roll} = a \sin(2\pi f(t - \Delta t)) \tag{3.31}$$

$$\varepsilon_{roll} = \text{roll - delayed roll}$$

$$\tag{3.32}$$

$$= a \left[\sin(2\pi f t) - \sin(2\pi f(t - \Delta t)) \right]$$

Where f is the roll frequency

t is time

Δt is the time delay

a is the amplitude scaling factor

The roll error is proportional to the roll amplitude. It does not take much of a time delay to get a large roll error: 0.12 sec time delay with a 30° roll amplitude would produce a 5° peak roll error. The roll error is also proportional to the frequency of the motion (Figure 3.15). For example, the maximum roll error obtained with the parameters used in Figure 3.14 (0.2 Hz and 0.1 sec time delay) is 3.6° while it reaches 17.7° if we increase the frequency to 1 Hz.
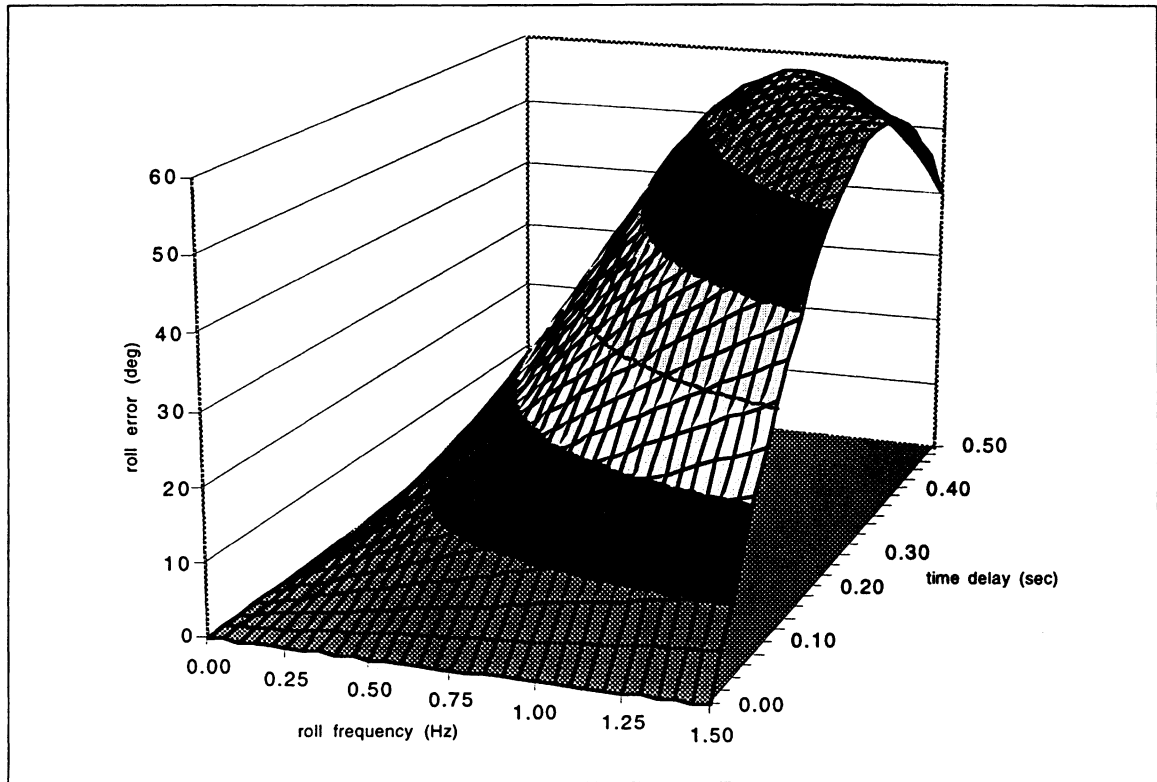
Figure 3.15 Sensitivity analysis for the roll error (peak) with varying VRU time delay and roll frequency. To generate this graph the roll amplitude was fixed to 30°.

3.1.6 Dynamic Draught and Vertical Offsets

The position of the transducer below the mean water surface is the transducer draught, which is measured prior to acquisition of data. A static correction is applied either in real time or in the post-processing to account for this. Section 2.2.4 outlines the causes for changes in transducer elevation that may occur. The vertical movements discussed here are the long term changes in transducer's draught which can be caused by:

- ship settlement (defined in § 3.1.6.1)

- changes in vessel's displacement

- changes in water density

- bad calibration of the heave sensor

- changes in transducer draught caused by a constant heel or trim angle

3.1.6.1 Ship Settlement (Squat and Lift)

Ship settlement is here defined as the change of the mean draught caused by the interaction between the hull, the water and the nearby seafloor or another vessel. Squat is the vertical changes where the mean draught of a vessel increases. It can be due to the displacement of the watermass because of an increase in pressure caused by the forward movement of the vessel, pressure which increases with increasing speed. It can also be caused by a Bernoulli effect when the seafloor (or a shoal) is close to the hull, creating an increase in water flow and a corresponding depression which attracts the hull downward (or toward the feature). Conversely, lifting occurs when aquaplaning takes place or by the actions of foils on hydrofoils.

One must assess the settlement of the survey vessel, in different operating conditions, if one is to correct for the variations that occur in the

vertical position of the transducer (or the reference point) relative to the water surface. For settlement caused by the hull's dynamics (displacement-based squat or aquaplaning), a look-up table can be created for the vessel, which would give the correction in transducer draught to be applied with a corresponding change of speed on the water (or RPM).

3.1.6.2 Changes in Vessel's Displacement

Changes in transducer draught can also be introduced by changes in the displacement (weight) of the survey platform. These changes in displacement are caused by fuel and fresh water depletion, the taking in of equipment or boats, or from ballasting. The hydrographer must be aware of any changes in displacement in order to compute the new mean draught and derive the new transducer draught. The mean draught of a vessel can be calculated using the TPI (Ton Per Inch) factor, as indicated in the ship stability tables.

3.1.6.3 Changes in Water Density

If the hydrographic vessel is moored in a river (fresh water) and if the survey area is offshore (sea water), a change in water density will be experienced which will affect the draught of the vessel. For this reason the

cargo vessel has two sets of loading marks (the Plimsoll Marks) that indicate the maximum loading draught in fresh or sea water. The specific gravity of the water at the dock is measured and the corresponding loading mark is verified before departure. The volume of water displaced by the mass of the vessel varies with the density of the water:

$$mass = volume * density$$

If the ship's mass, length and breadth remain unchanged (as with a box-shaped vessel) the change in draught is explained as follows:

$$volume = length * breadth * draught$$

$$\frac{new\ volume}{old\ volume} = \frac{old\ density}{new\ density}$$

$$\frac{new\ draft}{old\ draft} = \frac{old\ density}{new\ density} \tag{3.33}$$

As expected, ships have deeper draught in fresh water and will move up as they proceed into sea water. For ship-shaped vessel, the exact volume of displacement must be obtained for any given draught. The change can be substantial (10 - 30 cm) for a deep sea survey vessel. Obviously, the difference is negligible if the ship is to survey in ocean depths but is worth considering for very shallow water.

3.1.6.4 Bad Calibration of the Heave Sensor

Although rarely encountered, a DC offset in the heave output will affect all depth measurements and a constant error will be present in soundings. Another problem can occur if the cut-off frequency of the high-pass filter is set too high for the prevailing sea conditions. The problem would occur when the ship is sailing with the sea (at or close to the traveling speed of waves) and surfing on the crests. The heave sensor will be able to track the change in elevation until the cut-off frequency is reached and the heave output will decay down toward zero afterward. Proper calibration and configuration of the Heave sensor will minimize these situations.

3.1.6.5 Changes in Transducer Draught Caused by a Constant Heel or Trim Angle

This effect was mentioned in section 2.2.4.2 where erroneous heave values are used in the calculation of depth measurements relative to the mean water surface. Lets take the example where the transducer is located away from the ship's attitude axes and where the heave sensor is installed right above it so as to observe the total heave motion experienced by the transducer. A constant heel and/or trim of the vessel due to ballasting or to wheather conditions may change the elevation of the transducer and this

change will be undetected by the heave sensor. The vertical displacement is undetected because the change is constant over a time period longer than the cut-off period of the heave high-pass filter. Hence, the correct change in elevation will be measured at first, but as the static component of the heave output decays down (or up), this will introduce an error in the pre-defined transducer draught. If an attempt is made to correct the total heave observed at the location of the heave sensor by subtracting the roll-pitch induced heave, the error occurs for all short period motions after the constant attitude angle is attained and after the cut-off period of the heave high-pass filter is reached, because the correction will be applied on top of the "sensed" heave.

3.1.7 Sensors' static Offsets

These are the static offsets that separate the antennae (transducer and positioning) and the ship's reference point. If they are not correctly accounted for, position errors will be present in soundings and on roll/pitch induced heave. The effect of an error in the along ship offset will be similar to the errors generated by a positioning time delay (explained next) while an error in the athwart ship offset (less noticeable) will act on the relative transverse position (y values) of sonar vectors. The static offsets (2.5), as illustrated in Figure 2.3, are defined in the Body-Frame.

If the static sensor offsets are not correctly taken into account, it will affect each step in the computation of the sounding position (c.f. § 2.2.4.1). If the offsets are ignored, the position error for each epoch is obtained by the rotation of the offset:

$$\mathcal{E}p = \begin{bmatrix} \mathcal{E}x \\ \mathcal{E}y \\ \mathcal{E}z \end{bmatrix}_{LL} = P^{-1} \begin{bmatrix} x_{sub} \\ y_{sub} \\ z_{sub} \end{bmatrix}_{BF} \qquad (3.34)$$

If the static offsets are used but are erroneous, the position error for each step in the horizontal transformation will be:

$$\mathcal{E}p = \begin{bmatrix} \mathcal{E}x \\ \mathcal{E}y \\ \mathcal{E}z \end{bmatrix}_{LL} = P^{-1} \begin{bmatrix} \mathcal{E}x_{sub} \\ \mathcal{E}y_{sub} \\ \mathcal{E}z_{sub} \end{bmatrix}_{BF} \qquad (3.35)$$

Where - $\mathcal{E}prefix$ are the position error components

  - x_{sub} y_{sub} z_{sub} are the offset components for the antenna or the transducer

  - $\mathcal{E}prefix_{sub}$ are the errors in the offsets components obtained by subtracting the erroneous offset vectors from the good ones

An error in the vertical static offset between the transducer and the ship's reference point will produce errors in roll/pitch induced heave; i.e. an erroneous lever arm will be used to compute the remote heave. The error in

roll/pitch induced heave is the z component of the transformation error vector:

$$\mathcal{E}h = \begin{bmatrix} - \\ - \\ \mathcal{E}z \end{bmatrix}_{LBF} = R_y^T(\theta)R_x^T(\psi) \begin{bmatrix} \mathcal{E}x_t \\ \mathcal{E}y_t \\ \mathcal{E}z_t \end{bmatrix}_{BF} \tag{3.36}$$

$$= -\sin(\theta)\mathcal{E}x_t + \sin(\psi)\cos(\theta)\mathcal{E}y_t + \cos(\psi)\cos(\theta)\mathcal{E}z_t$$

3.1.8 Positioning Time delay

The positioning time delay is the time difference between the positioning system clock and the echo-sounder or the logging system clock. If the positions are time tagged by the echo-sounder or the integration unit, the time delay can be introduced by unaccounted transmission or computing time lags (coordinate transformation, etc.). A time delay (< 2 sec) will be meaningful only in shallow water (< 100 m) and where the accuracy of the positions is high (0.1 to 3 m RMS).

The effect of a positioning time delay in the horizontal transformation (c.f. § 2.2.4.1) is two fold:

1) wrong interpolated attitude values will be used to compute the position of the RP at time **t** (2.10), resulting in position errors of the RP (randomly distributed because driven by the sea)

2) position displacement along the course made good CMG because the observed position is behind the position of the ship at transmit time (Figure 3.16).
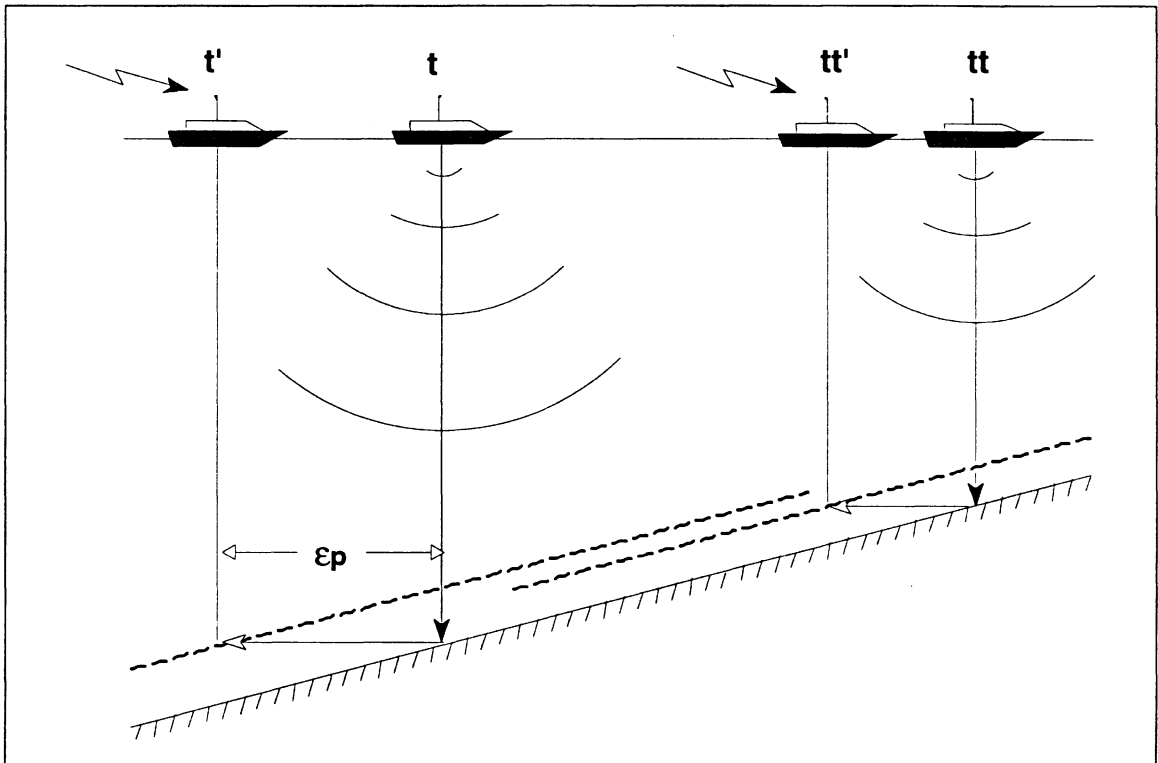
Figure 3.16 Profile view of a survey line run at two different speeds along a slope showing the effect of time delay on the relative position of sounding in the CMG direction. The highest speed is represented by the single letter case. t and tt are the time at transmission while t' and tt' are the positions at time t and tt minus the time delay. The dash lines represent the apparent seafloor and $\mathcal{E}p$ is the position displacement.

Figure 3.16 illustrates the effect of a positioning time delay when running a line perpendicular to a slope. Notice that the position displacement εp is larger at the highest speed. Using the speed over ground (**SOG**), the course made good (**CMG**) and the time delay (Δ_t), the position displacement can be computed as follows:

$$\begin{bmatrix} \varepsilon_{x_{td}} \\ \varepsilon_{y_{td}} \\ 0 \end{bmatrix}_{LL} = \begin{bmatrix} \Delta t * SOG * \sin(CMG) \\ \Delta t * SOG * \cos(CMG) \\ 0 \end{bmatrix} \tag{3.37}$$

3.1.9 Echo Sounder Errors

So far, the systematic errors originated from external sensors or from their misalignment relative to the transducer. Systematic errors can also be inherent to the echo-sounder itself. This is the case when the calibration of the transducer has not been done properly or when the algorithms implemented in the beam forming, the bottom detection or the signal processing are inappropriate.

It is rather hard and tedious to estimate errors associated with incorrect algorithms and we assume they are working properly. The case where the transducer is not calibrated correctly is nevertheless possible. A wrong

calibration is usually associated with errors in beam pointing angle. Figure 3.17 shows a curl present in a Simrad EM100 across-track profile caused by errors in the pointing angles of a group of beams.
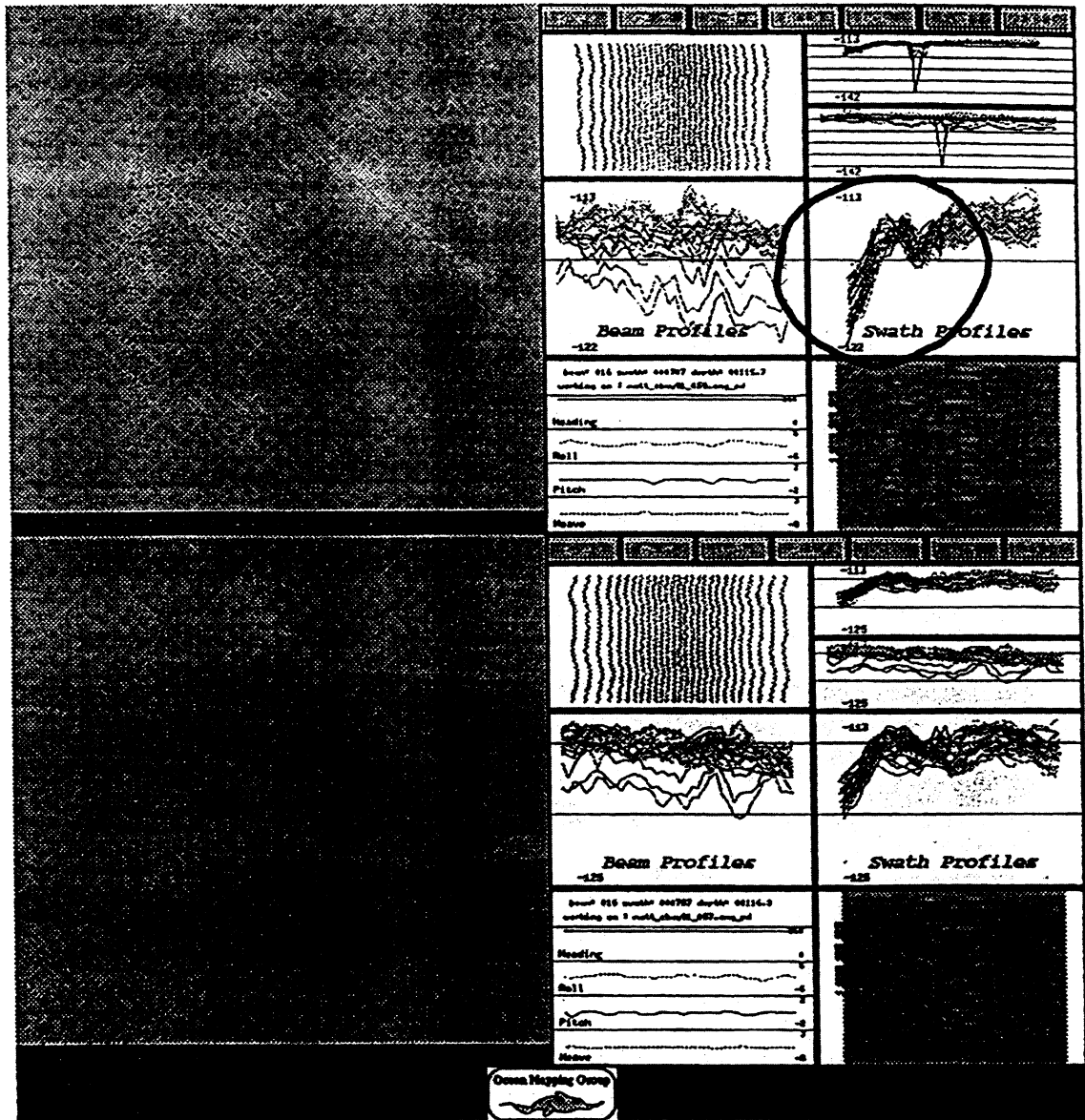
Figure 3.17 Curled across-track profile from the CSS Matthew Simrad EM100 [from Hughes Clarke J. (1993a)].

When the beam pointing angles from the transducer's normal are biased, systematic proportional errors in depth and position of soundings occur, just as in the case of a roll offset. This can happen for a particular beam or for a group of beams. A systematic erroneous depth measurement for one beam is easily detected in the bathymetry and a group of erroneous beams will change the shape of the across-track profile made by the echo-sounder.

3.1.10 Variations of the speed of sound in the water column

It was mentioned in section 2.2.3 that vertical variations in the speed of sound in the water column would cause beam refraction and that a good knowledge of the sound velocity structure in the water mass is needed to correct the depth measurements for this effect. Based on the sound velocity casts and the measurements at the surface, three aspects are to be considered:

1) the accurate location of the boundaries between layers in the water mass (accuracy of depth measurement) and their spatial and temporal variations

2) the speed of sound for each water mass layer at the measurement site (accuracy of sound velocity measurement or of its derivation) and their spatial and temporal variations

3) the speed of sound at the location of the transducer (accuracy of sound velocity measurement or of its derivation)

The first two factors are used to build the look-up tables for relative radial distance and depth for specific travel times and launch angles. The speed of sound at the transducer must be measured in real time when using flat transducers in order to perform accurate beam steering (for those beams which are not at right angles to the acoustic elements).

Errors in the sound velocity profiles will produce proportional errors in both depth and position of soundings. Thus, in order to calibrate for these sources of error, one should ensure the sound velocimeters (or STD) are well calibrated (for both sound velocity and depth measurements) and that spatial and temporal changes in the sound velocity structure of the water mass are well monitored.

3.2 Uncertainty Brought by the Simplified Approach

It was stated in the introduction of this report that calibration for beam refraction and for temporal and/or spatial changes in the sound velocity structure of the water column will not be covered. Furthermore, in order to simplify the derivation of biases, the transformation adopted in the system integration assumes no sound velocity gradient in the watermass (c.f. § 2.2.5). This assumption increases the uncertainty level of the position and depth

error derived in this chapter. In order to accurately assess these errors, one would need to incorporate refraction models in the derivations. To make accurate error derivations and to assign them a confidence level using a refraction model would be extremely complex because of the many parameters involved: water depth, number of water mass layers, bottom slope, accuracy of depth, accuracy of sound velocity measurements, and accuracy of the beam steering, if any. Making the assessment of the uncertainty brought by the simplified approach is also not simple and we will not try to achieve it in this report.

Most of the problems associated with refraction errors reside in the fact that the roll and pitch biases are interrelated in the refraction solution. Even if we assume there is no error in the corrections for beam refraction (no errors in the sound velocity profile), one still has to correct the original launch angle for roll and pitch biases and recompute a new refraction solution. One might then end up with new values for roll and pitch biases. This process could take several iterations before solving the angular offsets to the required level of accuracy. Errors in heave, induced heave and dynamic draught would also contribute in refraction solution errors. One must resolve these before attempting to decipher the roll and pitch offsets.

In presence of error in the refraction solutions caused by errors in the sound velocity profile, position and depth error in the soundings would

occur that would leak in both roll and pitch biases (if any). The approach used in Chapter 4 for quantifying the individual biases is to evaluate them independently (uncorrelating them in the same way) and in an iterative process that minimizes the uncertainty level. This is true, provided that the refraction solution errors are minimal; i.e. using calibrated sound velocimeters and using bathymetric data acquired in the same sound velocity structure of the water column. One would then perform a comparison survey so as to assess the overall performance of the MBES and verify that the bathymetric data comply with accuracy requirements.

4. Field Procedures for the Calibration of Multibeam Echo-sounding Systems

The correct integration of multibeam system data (echo-sounder and external sensors output) is the most important aspect of hydrographic swath surveying. An adequate integration will guarantee accurate and reliable depth measurements. Integration parameters will be assessed after installation of the sounding system on the survey platform.

This document considers two aspect of the calibration of MBES. Sections 4.1 to 4.5 deal with the assessment of the integration parameters pertaining to the installation of the MultiBeam Echo-sounding System (MBES) on the survey platform. Sections 4.6 and 4.7 describe the field procedures for determining the residual biases and the corrections that will be used to fine tune the calibration of the MBES. These field procedures have been developed specifically for the calibration of Simrad MBES, as owned by the Canadian Hydrographic Service, and for use with the HIPS post-processing package [Universal Systems Ltd., 1994].

A calibration report form, herein called the "ship's profile", is provided in Appendix II. A ship's profile should be associated with each MBES in particular, and should be updated every time a new calibration is performed.

Appendix III illustrates a calibration survey, made in June 1993 off Rimouski (Québec, Canada). The survey was done by the CHS with the NSC Frederick G. Creed, equipped with a Simrad EM1000 multibeam echo-sounder. The various figures are screen dumps made from HDCS sessions. The field procedures for the calibration survey include a "Performance Check" which is carried out after the assessment of the residual biases and which leads to the production of "Quality reports". Examples of quality reports are provided in Appendix IV. Procedures for using the OMG 's DelayEditor, developed to detect and quantify roll errors, have been reproduced in Appendix V.

Some procedures that use GPS measurements have not yet been tested and implemented by the CHS and are herewith presented as potential means for achieving the required error source assessment. This is the case for the evaluation of the dynamic draught and the gyro offset, using DGPS carrier phase measurements techniques. These methods should be adopted only after adequate experimental verification.

The coordinate reference system and the related rotations employed in this document are the ones adopted by the Simrad multibeam echo-sounders, which correspond to the ones used in Chapter 2. The Simrad EM series operator manuals should be consulted along with this document. The coordinate system and transformation conventions used for the post-processing are the ones defined for the HIPS package and the HIPS (and

HDCS) operator manual should be referred to when dealing with the data post-processing section.

4.1 Assessment of the Integration Parameters

The integration parameters consist of the parameters peculiar to the survey platform (static offsets, dynamic draught, sensor misalignment with respect to Body-Frame) and parameters intrinsic to the multibeam echo-sounding system (VRU or positioning time delay, beam pointing angle, beam refraction solution, etc.).

The following sub-sections describe the actions that must be taken after the installation of the MBES on the survey platform in order to determine the integration parameters. These parameters will further be used, both during the acquisition and in the post-processing, to perform the integration of the multibeam echo-sounder data with the other external sensor outputs.

The assessment of the integration parameters can be outlined as follows:

- Determination of the reference point location

- Assessment of the sensor static offsets

- Determination of the transducer mount angles with respect to the Body-Frame

- Determination of the transducer draught with respect to ship's draught marks

- Determination of the VRU alignment with respect to the Body-Frame and to the transducer

- Verification of the gyro readings vs. the ship's heading

- Determination of the ship settlement (squat or lift) with respect to the ship speed on the water

- Determination of the draught changes with respect to fuel/water consumption and ballasting

- Assessment of errors in roll data

- Determination of the positioning time delay

- Post-installation calibration

The integration parameters will be compiled in a ship's profile form that belongs to each installation in particular, and which will help to keep track of the development of the system. A sample of such form is provided in Appendix II.

4.1.1 Ship's Reference Frame and Sensor Static Offsets

In order to integrate the sonar vectors with the other sensor outputs, the static offsets between the VRU, the sonar arrays and the positioning system antennae must be measured accurately and referred to a common reference point.

4.1.1.1 Determination of the Reference Point Location

The Reference Point (RP) can be arbitrarily located anywhere on the survey platform. Nonetheless, it must be chosen so it is readily accessible and in a place from which sensor offsets can easily be measured. If the multibeam echo-sounder requires so (e.g. Simrad EM systems), the RP can be located at the intersection of the roll and pitch axes or alternatively, at the centre of gravity of the vessel.

(a) **Intersection of the roll and pitch axes.** The position of the intersection of the roll and pitch axes is not often obvious. Customarily, the roll axis is coincident with the water plane (varies with loading conditions) while the pitch axis passes through the centre of floatation, the one that is used to calculated the moment to change trim (MTCI). Check with the ship's builder for accurate location of these two axes.

(b) Centre of Gravity. Obtained from the stability table of the ship. The centre of gravity is usually referred to the keel (KG) and varies with loading conditions. The location chosen as RP must represent the loading condition most often encountered when surveying.

4.1.1.2 *The Marking of the Reference Point*

The ship's reference point must be physically marked and identified on the vessel for further reference. The marking should be made permanent (with a drill, a chisel, or by mounting some kind of monument) and distinctly painted. If it is not possible to mark the exact location of the point (e.g. into a void space), a remote point can be marked and the actual Reference Point be referred to this remote point by XYZ offsets. The offsets should be physically indicated (magnitude and direction) near the remote reference point.

4.1.1.3 *Determination of the Body-Frame Orientation*

Some platforms operate better with a constant trim. This is the case with the CHS vessel "Frederick G. Creed" which surveys with a 3° trim angle by the stern and where the transducer and the VRU have been tilted accordingly. The orientation of the Body-Frame must also account fore such trim settling.

One must thus define the orientation of the Body-Frame within the rigid body of the survey platform. Rotations with respect to ship's structure can be defined, which will be useful if the sensor static offsets are measured relative to it.

4.1.1.4 Assessment of the Sensor Static Offsets

1) Obtain or accurately determine (± 1 cm) reference centre of each sensor.

2) Offsets can be physically measured using a surveying tape. Measurements must be made along longitudinal and transversal beams to ensure perpendicularity and accuracy. When measuring through bulkheads, the plate thickness must be accounted for.

3) When physical measurements can't be made, use the ship's drawings, supplied by the shipbuilder. If possible, use originals (non shrinkable medium) and accurately locate the RP and each sensor on the drawings.

4) If the Body-Frame has a different orientation than the ship's structure, the static offsets must be rotated accordingly.

5) Record the sensor offsets, including a diagram showing the location of each sensor, in the SHIP'S PROFILE form (sample in Appendix II).

4.1.2 Transducer Mount Angles with respect to the Body-Frame

The assessment of the transducer mount angles with respect to the Body-Frame is part of the installation routine. It will be accomplished while the ship is in dry-dock, preferably during the fixing of the transducer onto the hull. Measurements must be performed accurately (within ± 0.1°), using surveying equipment.

1) Follow the manufacturer's instructions for the determination of the transducer mount angles.

2) Refer to the ship's keel and transverse beams for assessing the mount angles.

3) Pay particular attention to the determination of the azimuthal alignment of the transducer, as beam steering is not usually done about the z-axis.

4) Record the transducer mount angles in the SHIP'S PROFILE form, provided in Appendix II.

4.1.3 Transducer Draught with respect to Ship's Draught Marks

When the transducer elevation with respect to the water surface (static transducer draught) is assessed from the ship's draught, the draught marks, which are referred to the keel, must be verified carefully.

1) With ship in dry dock and with leveling instruments, verify draught marks and record any deviation for each one. Report the deviations to the ship owner (draught and Plimsol marks are covered by shipping act when ships are duly registered) to correct the situation and/or produce a draught marks correction table, for your own use.

2) With leveling instruments, measure the elevation of the transducer face with respect to the ship's keel.

3) Verify with the multibeam echo-sounder manufacturer where the reference centre of the transducer is located with respect to its face.

4) Calculate the correction to be applied to the elevation of the transducer if the Body-Frame coordinate axes have been rotated, to account for a particular operating trim.

5) Record the elevation of the transducer reference centre with respect to the ship's keel, in the SHIP'S PROFILE form, provided in Appendix II. Produce also a table showing the draught mark errors, to be adjoined to the SHIP'S PROFILE.

4.1.4 VRU Alignment with respect to the Body-Frame and to the Transducer

Ideally, the VRU's sensitive axes would be perfectly aligned with the transducer axes. In practice, unless the MBES is installed on a launch or a ROV, the alignment of the VRU with respect to the transducer is quite hard to obtain. Hence, this operation will be performed so as to minimise (as much as possible) the offsets between both sensor axes. The residual angular

offsets between the VRU and the transducer will be subsequently assessed, by comparing sets of bathymetric data (Calibration Survey). We will here use the ship's axes as reference to match the VRU and the transducer axes.

1) Follow the manufacturer's instructions to align the VRU with the ship's axes, using the longitudinal and transverse beams.

2) If necessary, install the VRU with the same mount angles found for the transducer.

3) Pay particular attention to aligning the VRU and the transducer's x-axes, because the VRU azimuthal offset is not easily detected from the bathymetry. Azimuthal misalignment of the VRU would lead to proportional cyclic errors in the depth measurements.

4) Record the VRU mount angles in the SHIP'S PROFILE form, provided in Appendix II.

4.1.5 Gyro Reading vs. Ship's Heading

This procedure is needed to verify the gyro alignment with respect to the ship's x-axis. It must be accomplished in port, under calm weather conditions, using total stations and geodetic control points.

1) Three persons, at least, are required to perform this operation.

2) Ensure the ship is tightly moored against the wharf and that wave or surge action has no or very little effect on the azimuthal movement of the vessel. For a launch, this procedure should preferably be performed out of the water; i.e. launch sitting on its cradle.

3) Ensure the gyro has gone through the recommended warm-up duration before commencing with the measurements. Verify corrections for latitude and speed have been appropriately applied (where applicable).

4) If a digital gyro repeater is used for gyro readings, ensure there is no offset or significant time lag (> 0.2s) with the master. If the multi-beam echo-sounder provides instantaneous gyro readings from the gyro output, this value should be recorded instead for it will be the ones used by the MBES. Recording gyro readings from the MBES integration unit can also be done, provided good synchronization is achieved.

5) Locate two (or more) points on the deck, passing through the ship centre line, and mark them. Position a target on each of these points.

6) Observe the targets with two total stations, using mobile radios to synchronize the readings. The person recording the ship's heading will coordinate the timing of the measurements. Make several observation sets (at least 25) to ensure redundancy.

7) From the observations, compute the ship's azimuth and compare with the gyro readings. Compute the mean and standard deviation of the differences and decide if more measurements are needed based on these statistical values.

8) In the presence of an offset (more than 1°), have the gyro physically realigned with the ship centre line and redo the observations. Otherwise, apply the correction to the gyro output, accounting for transducer azimuthal misalignment (c.f. § 4.1.2).

9) Record the gyro misalignment in the SHIP'S PROFILE form, provided in Appendix II.

NOTE: the observations can also be done with On-The-Fly GPS positioning, synchronized on UTC or GPS time. Two GPS receivers would be needed, one at each target on the ship.

4.1.6 Ship Settlement (squat or lift) with respect to Ship's Speed on the Water

The establishment of the ship's settlement, when underway, is crucial since the long term change in elevation of the transducer will not be measured by the heave sensor (c.f. § 2.2.4.2). The evaluation of the ship's settlement should be made for various speeds (or RPMs) and a look-up table should be produced, to be used for correcting the transducer draught. Since the settlement varies with the speed of the vessel on the water, surface velocity (not the speed over ground) should be obtained with the aid of an accurate log.

The change in elevation can be obtained by GPS carrier phase

measurements using the "On-The-Fly" cycle ambiguity resolution technique.

In Figure 4.1, the heights (a) and (b) are known, (c) and (Δh) are measured.

The antenna elevation over the water surface (f) is computed using the other

values.
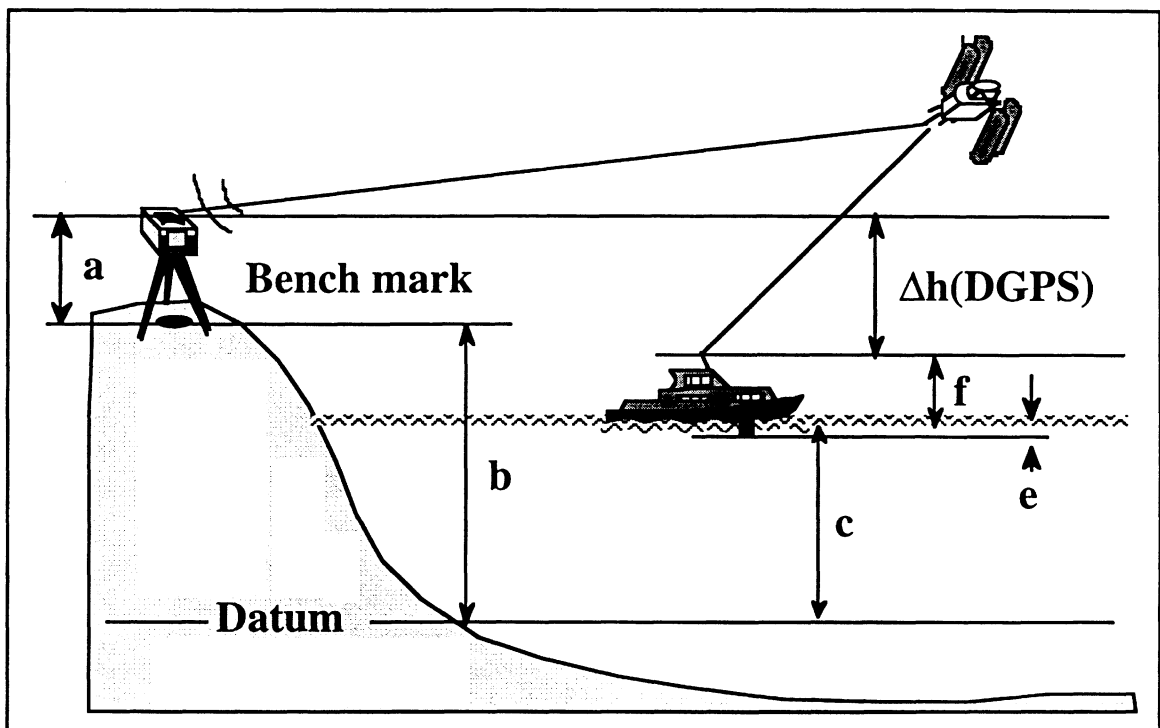
Figure 4.1   DGPS technique, using carrier phase measurements to acquire antenna heights above the water surface (from a figure used by Dr. D. E. Wells in an oral presentation in Norfolk [1994]).

4.1.6.1 Acquisition of Data

Ships settlement is generally at the centimetre level and acquisition of data must be performed with a corresponding accuracy. To reduce the noise level, attitude data will be recorded and used to correct for roll and pitch induced heave of the GPS antenna. When observing GPS altitudes, the following possible effects must be accounted for:

- River slope

- Bathymetric effects on sea surface topography

- Short period tidal signatures (e.g. seiche)

- Constant angle of heel and trim of the survey platform

1) Position the GPS antenna on the ship, close to the centre but not too high, so as to minimize its motions with the ship's roll and pitch. Measure the offsets between the antenna and the ship's reference point (RP).

2) Install a tide gauge, preferably a digital one, as close as possible to the test area. If an analog pressure gauge is utilized, ensure a stilling well is used or that the location of the pressure sensor is sheltered from sea states. Ensure the sensors are below low water. Carry out a GPS static baseline survey to determine the ellipsoidal height of the tide gauge zero.

3) If one suspects the presence of a significant slope in the tidal datum with respect to the ellipsoid, one should use two (or more) tide gauges, installed at each end of the survey line. If only one tide gauge is used, data will be recorded (during 2 min with a 1 sec sampling interval) with the ship drifting at each end of the survey line, the difference in elevation determining the slope of the river. This technique will provide the water current as well, used to derived the surface speed from the SOG.

4) Carry out the test survey. Wait for calm weather to run the test lines. Make test lines at different speeds, starting at dead slow ahead, incrementing by one knot up to full sea speed. Always use the same survey line and verify that the speed on the water is constant throughout the line. Repeat the test line with different (say 3) loading conditions.

5) Record, on a common datum and a common time:

   - GPS 3-D positions (sampling rate: 1 to 10 Hz)
   - Ship's heave, roll and pitch
   - Ship's speed on the water (sampling rate: 1 Hz) or engine RPM
   - Water levels (sampling rate: 1 to 15 min.)

6) If ship's movements are rapid and important (> 10°), such as with hydrographic launches, the highest possible sampling rates must be used (10 Hz for GPS and 100 Hz for attitude data). Low sampling rate (1 Hz for GPS and 10 Hz for attitude data) can be adopted for larger vessels. High sampling rate (1 min) for water level measurements will be used for large tidal ranges.

4.1.6.2 Data Post-Processing

1) Data samples must be adjusted to correspond in time, either during logging, or by interpolation during post-processing. If interpolation is performed, polynomial or spline curve fitting is preferred to linear interpolation. Use GPS events as the reference and interpolate the motion data. Linear interpolation can be used for tidal data.

2) Compute the average elevation for each end of line (ship adrift) and derive the river slope for each survey line. The current direction and speed can be computed from the positions.

3) Use the GPS antenna offsets and the attitude data to compute the roll and pitch induced heave and correct the antenna elevations (processed Z values) accordingly. Subtract water level data and heave data from GPS antenna elevation. Correct for the river slope using the positions along the line (height differences are linearly interpolated).

4) For each test line, compute the average speed on the water, and the average antenna elevation (corrected for motions, water levels and river slope) with respect to the water level.

5) Produce a look-up table that will be used to correct transducer draught and add it to the SHIP'S PROFILE.

NOTE: another method, less accurate, can be used to assess ship's settlement, using ground truth testbed [Hughes Clarke, 1993c]. The changes in elevation for various test lines are obtained by producing a difference DTM of the surveyed swath and the ground truth data. A statistical mean computed from

the differences between the inner beams and the DTM will be used for assessing changes in transducer elevation with respect to the water plane. Very accurate tide measurements (and corrections) are of paramount importance for this technique.

4.2 Draught Changes with respect to Fuel/Water Consumption and Ballasting

Once again, variations in the transducer elevation caused by changes in loading conditions are determined. The period of these variations are quite long and they will be undetected by the heave sensor. Thus, it is important to quantify the amplitude of the ship settlement with changes in its displacement. The ship stability tables contain information on the TPI (Ton Per Inch) factor, which will be used to assess the change in draught with fuel and water consumption or ballasting, while underway. Other relevant information will be provided by the ship's chief engineer or the shipyard. If the ship's draught can be accurately assessed during the survey day, then the following procedure is not necessary.

1) Get from the chief engineer, a series of tank readings for fresh water, in order to estimate the average daily consumption. Determine the fuel consumption for various engine RPM values, and the density of the fuel used.

2) Define the most probable amount of fresh water consumption throughout a regular survey day and convert the used water to change in draft, using the TPI. Build a look-up table showing hourly draught corrections. Make a look-up table for the fuel consumption according to RPM. A combined look-up table can be produced if the ship always surveys with a constant engine RPM.

3) Adjoin the look-up tables to the SHIP'S PROFILE.

4.3 Errors in Roll Data

It has been observed in the past (CSS Matthew and NCS Frederick G. Creed motion sensor trials) that time delay and scaling errors in attitude data will result in roll errors that can strongly degrade the accuracy of the outer beams. Horizontal accelerations in cornering can also affect attitude measurements from the VRU which will also result in erroneous depth measurements. The following sections, although not exhaustive procedures to quantify these source of errors, have been included to indicate to hydrographers their existence, and to guide them toward ways to resolve them.

4.3.1 Time Delay and Scaling Errors

The basic principle for the detection of roll errors is to observe, from the bathymetric data, short period changes in the across-track seafloor slope when surveying flat and smooth terrain. The technique was developed in 1993 by the Ocean Mapping Group [Hughes Clarke, 1993b] when investigating residual roll artifacts present in the Matthew EM100 data.

In order to quantify any existing biases in the motion data, it will be necessary to employ specific tools. In the CHS, the UNIX-based "SwathEd" and "DelayEditor" software, developed by the OMG, are used to assess time delay and scaling errors, present in the swath data [Hughes Clarke, 1993b].

1) If induced roll errors are suspected from horizontal accelerations (easily noticeable during turns), speed should be reduced significantly (4 to 6 knots) and sufficient time should be allowed after a turn for the motion sensor to settle down (typically 3 min with a TSS-335B and up to 15 min with a Hippy 120B).

2) Survey a small area (1 to 3 km²) of flat, sedimentary seabed, in shallow water (20 to 100 m). The surveyed area should be large enough to detect from the bathymetry and the acoustic backscatter data, regions with no short period variations in the seafloor slope. Lines are run parallel to the contour lines. Heavy inter-swath overlap is not necessary. Some roll motion (> 5°) is required for the artifact to be easily detected and quantified.

3) Process the data first with the SwathEd tool in order to get the
*.merged files. One can use a script file (example in Appendix V),
invoked with the line number (variable $1).

4) Analyze the survey line with the DelayEditor. A scaling error and/or
time delay would be easily detected by comparing the traces "Sum of
Low Pass Roll and High Pass Bottom Slope" and "Scaled and Delayed
Roll" (trace window 5 in FIX mode). The example provided in the
Appendix V shows both errors. It also shows that the time delay is
not constant, which is an indication that something was wrong with
the attitude sensor. A variable time delay should by all means be
avoided and the motion sensor be repaired or changed.

4.4 Azimuthal Misalignment of the VRU

If azimuthal misalignment of the motion sensor with respect to the Body-
Frame is present, motions about the pitch axis will result in a response in the
roll data (cross-talk). Similarly, induced pitch values will result from
motions about the roll axis (c.f. § 3.1.4). Since roll errors are most critical with
MBES, one should inspect, in presence of heavy pitch motions, the residual
roll errors from the apparent across-track slope. This investigation should be
made after time delay and scaling errors are resolved (c.f. § 4.3.1) and applied.
The magnitude and sign of the misalignment γ could be derived from the
logged roll and pitch values and from the roll error, using the equation:

$$\sin(roll) = \cos(\gamma) \sin(\text{true } roll) - \sin(\gamma) \sin(\text{true } pitch) \qquad (4.1)$$

The "true roll" is made up of the measured roll and the roll error. Similarly, the "true pitch" is made up of the measured pitch and the pitch error. The azimuthal misalignment γ could be detected and quantified on a launch when it is sitting on its cradle. The attitude angles (true roll and pitch) are obtained from theodolite measurements of the dependent roll (β) and pitch (α) angles, transformed to obtain the Euler angles (see Appendix I). The azimuthal misalignment is computed from the biased angles observed by the attitude sensor (internally transformed to Euler angles) and using equation 4.1.

On larger platforms, the azimuthal misalignment has to be derived from the bathymetry and the observed attitude data. One can assess the roll error using the Delay Editor (c.f. § 3.1.4). The true roll is obtained from the observed roll and the roll error. The pitch is assumed unbiased and the observed pitch will be used instead of true pitch. An approximated value for the azimuthal misalignment is then obtained from numerical methods (e.g. Newton's method) and equation 4.1. Several measurements should be used to come up with a reliable average value.

4.5 Positioning Time Delay

Two possible situations can be encountered with positioning time delay:

A) when the positions are time tagged by the integration unit or the logging system clock, the positioning time delay is the time lag between the instant at which positioning data are received (e.g. reception of the GPS pseudo-ranges) and the time the computed position reaches the logging or the multibeam integration unit.

B) when the time tag within the position telegram is kept, accurate synchronization between the positioning system and the multibeam logging or integration unit must be ensured. In this case, the positioning time delay is the time difference between both systems clock.

Positioning time delay results in a negative along-track displacement of the depth measurements. Processing and transmission time can be measured beforehand for each specific installation in order to evaluate the positioning time delay. It is nonetheless necessary to verify it by field testing (c.f. § 4.7 and § 4.7.2.1), for unaccounted internal delay, in the logging or in the multibeam operator unit, may still be present.

1) One should get from the manufacturer the time required to compute a position, for a particular positioning system. With GPS positioning,

the problem resides in the fact that the processing time will vary with the number of pseudo-ranges used in the final solution. One might want to regulate the output by some gating system, using the 1 PPS signal commonly available on most GPS survey receivers.

2) The kind of factors to be considered when computing transmission time would be the length (in bytes) of the transmitted telegram and the communication port settings (baud rate, parity, etc.).

3) If the time embedded in the output GPS message is to be used, then proper synchronization between this time (UTC, GPS or Local time) and the multibeam echo-sounder clock must be achieved. A time telegram and the 1 PPS signal provided by a GPS receiver can be used to synchronize the multibeam logging or integration unit clock.

4) Whatever timing scheme is chosen, the hydrographer must be aware of the situation and verify if a time delay is still present in the system when performing the calibration survey (c.f. § 4.7). Whenever changes are made to the installation, whether it is hardware or software, the positioning time delay must be reassessed

4.6 Post-Installation Calibration

The next step is to perform a post-installation calibration survey in order to verify if the misalignment angles have been accurately determined and in order to assess the misalignment errors and the associated corrections that will permit fine tuning of the swath system. This test survey consists of

running a series of specific test lines over various terrains. The test line

pattern, the acquisition and the post-processing procedures are explained in

detail, in section 4.7. The purpose of this survey is to investigate:

- Residual pitch offset

- Residual roll offset

- Residual positioning time delay

- Residual azimuthal offset

- Overall system performance check

Large angular biases (> 1°), found from the processed post-installation

survey test data, **should be corrected mechanically** (e.g. rotating/adjusting

motion sensor or gyro synchro motor on their mounting frame). **The test**

lines should then be run again.

4.7 The Calibration Survey

The following procedures have been developed to help the hydrographer

perform the calibration of a multibeam echo-sounding system after its

installation on the sounding platform and periodically during the survey

season. The calibration survey aims at quantifying the following potential residual biases:

- Residual pitch offset

- Residual roll offset

- Residual positioning time delay

- Residual azimuthal offset

These values will be used to rectify the initial misalignment corrections and calibrate the sounding system. The calibration survey must be done carefully to ensure acquisition of accurate and reliable depth measurements. A performance check should be done after the residual biases have been assessed and entered in the system to verify the overall calibration. This verification requires specific procedures which are described in section 4.7.2.5 (the Performance Check). The calibration survey should be performed when these events occur:

- Start and end of a survey

- During a survey when one suspects a drift of the misalignement angles

- Each time a sensor has been moved, changed or modified

4.7.1 Acquisition of Data

Before carrying out the test survey, one must ensure that all integration parameters have been entered in the MBES integration unit. Some parameters can be used during the post-processing instead of at the time of acquisition. With swath systems that perform real-time beam refraction correction, it is strongly recommended to **apply draught corrections and offsets (e.g. transducer or VRU misalignment) at the time of acquisition**, in order to obtain the correct refraction solution. The sound velocity profiler must be calibrated and the VRU scaling factors and heave filter parameters adequately adjusted. The following check list, along with the ship's profile, can be used to verify if the proper values are used:

- Sensor static offsets

- Pitch, roll & gyro offsets

- Positioning time delay

- VRU time delay

- Static transducer draught

- Transducer draught correction for ship settlement

- VRU configuration parameters

- Sound velocity profile on the site

It is also essential to have **good positioning** ($\leq$ 1.7 m @ 90% confidence

level) and **good water level corrections** ($\leq$ 5 cm @ 90% confidence level). If

horizontal accelerations affect the VRU performance, one must ensure

sufficient time is given for the motion sensor to settle down after a turn,

before acquiring usable data. Calm weather is obviously preferable, to ensure

good bottom detection and limited motions. Gentle line keeping is also of

paramount but even more important is that the **vessel does not deviate too**

far (> 5 m) from the planned survey line, since beams of reciprocal lines will

be compared.

4.7.1.1 Calibration Test Lines

Except for the assessment of the roll bias, the test lines will be run in

shallow water; i.e. less then 100 m (which makes sense, since we are

evaluating a shallow water swath system). The order in which the lines must

be run is not particularly important. The test line patterns consist of:

(a) Test lines for positioning time delay and pitch bias. Two pairs (or more)

of reciprocal lines are run, at different speeds, over a slope (10° to 20°),

perpendicular to the contours. Figure 4.2 illustrates the line pattern. To

determine the time delay, a conspicuous topographic feature on the bottom

could also be used, as long as it is swept by the beam at nadir.
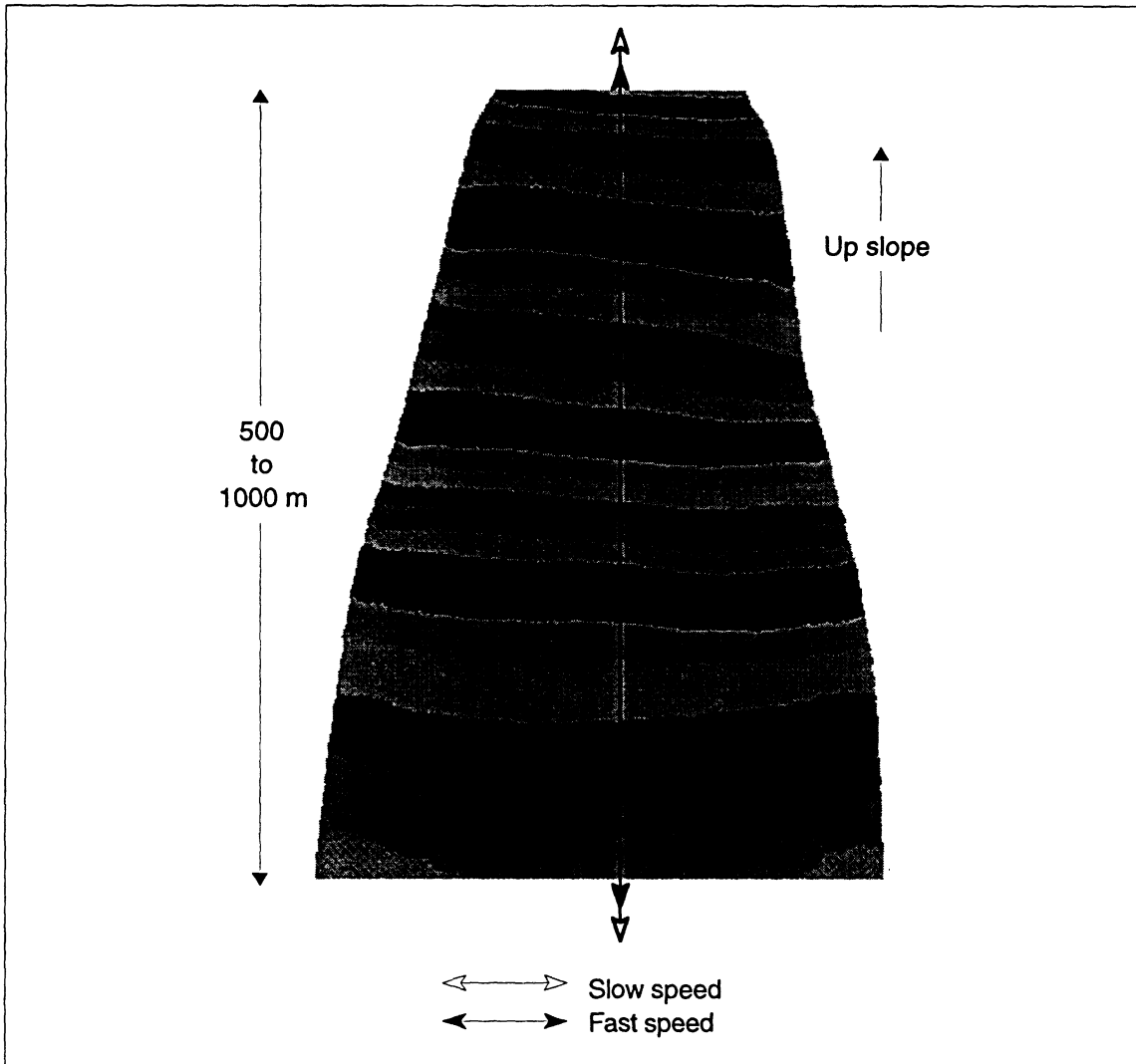
Figure 4.2   Test line for assessing pitch bias and positioning time delay.

• The slope must be long enough (500 to 1000 m) to obtain a good
  sample and it must be as regular and smooth as possible (not inclined
  transversally and/or bumpy).

- The difference in speed between the two pair of reciprocal lines should be at least 5 knots in order to assess easily the positioning time delay.

- Use equi-angular beam spacing mode in order to have a high density of depth measurements in the central part of the swath.

(b) Test lines for roll bias. One pair (or more) of reciprocal lines are run, over a flat or nearly flat seafloor, in relatively deep water (50 to 250 m). A roll bias will show up better in deep water, at the limit where one starts losing the outer beams.

- The length of the survey lines range from 500 to 1000 m, depending on the ping rate and along-track beam overlap.

- Lines must be run at a speed that will ensure significant forward overlap ($\geq$ 100%) and provide a good sample of data for the assessment of the roll bias.

- If available, use equi-distance beam spacing mode in order to have a constant density of depth measurements in the outer part of the swath.

- The maximum speed of the vehicle should be adjusted to ensure 100% forward overlap of the beams footprint. For example, the maximum speed for a 150° MBES (e.g. Simrad EM1000) can be calculated by the equation:

$$v = S * d * \tan(\beta/2) \tag{4.2}$$

Where v is the speed in m/s

S is the echo-sounder sampling rate (ping/s)

d is the depth in m

β is the fore-aft beamwidth

(c) **Test lines for azimuthal offset.** Two adjacent pairs of reciprocal lines are run, on each side of a submerged and conspicuous bathymetric feature (e.g. shoal), in shallow water (20 to 50 m). One should avoid using a bathymetric feature having sharp edges (such as wrecks), since an ambiguity in comparing the two different passages, will likely occur on these edges. Figure 4.3 depicts the test line pattern for assessing azimuthal offsets.

- Adjacent lines must overlap slightly (~15%), while covering the shoal.

- The surveyed feature should be wide enough (> 1/4 swath width) to ensure adequate sampling.

- The above mentioned rule (c.f. § 4.7.1.1.c) for defining the speed of the vehicle is also recommended here.

- If available, use equi-distance beam spacing mode in order to have a constant density of depth measurements in the outer part of the swath.
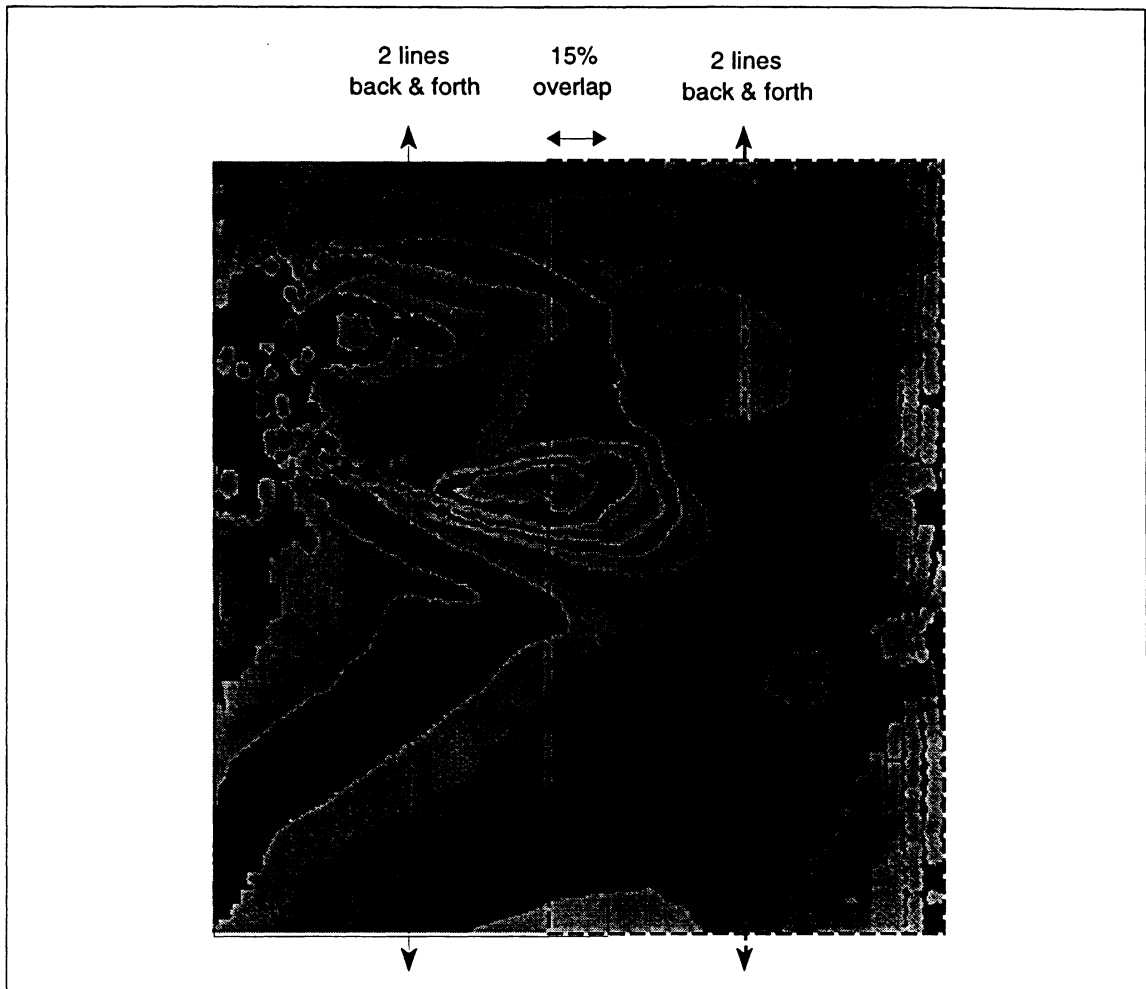
Figure 4.3   Test lines pattern for the assessment of azimuthal offsets.   The swaths are represented by the enclosing rectangles.

4.7.1.2 The Performance Check Survey Data

This procedure is to assess the overall calibration and verify whether the data meets the accuracy requirements. Once the calibration survey data have been processed and the final residual offsets obtained, the new corrections are entered in the integration unit and the performance survey is performed.

Nevertheless, it can be accomplished right after the calibration test lines if time is a constraint, the performance check being made with the corrections applied in the post-processing; this technique will be less accurate, for the reason mentioned in the introduction of this chapter (c.f. §4.1).

4.7.1.3 The Reference Surface

1) Select an area of flat or near-flat and smooth seabed.

2) Run four or five parallel lines (> 300 m long), in shallow water (20 to 50 m), with 115% to 160% inter-swath overlap (Figure 4.3). Ensure the area is covered with the inner beams, with a swath width representing 2 or 3 times the water depth (e.g. 2*d for the Simrad EM100 and 3*d for the Simrad EM1000).

3) Run four or five parallel lines (> 300 m long), perpendicular to the previous lines, with 115% to 160% inter-swath overlap.

4) examples:

   - Simrad EM1000 in 20 m = four 300 m and five 250 m lines, 160% overlap

   - Simrad EM100 in 30m = five 300 m and five 300 m lines, 115% overlap

5) If available, use equi-angular beam spacing mode.

6) The maximum speed of the vehicle will be adjusted to ensure 100% forward overlap. Equation 4.2 can be used to determined the survey speed.
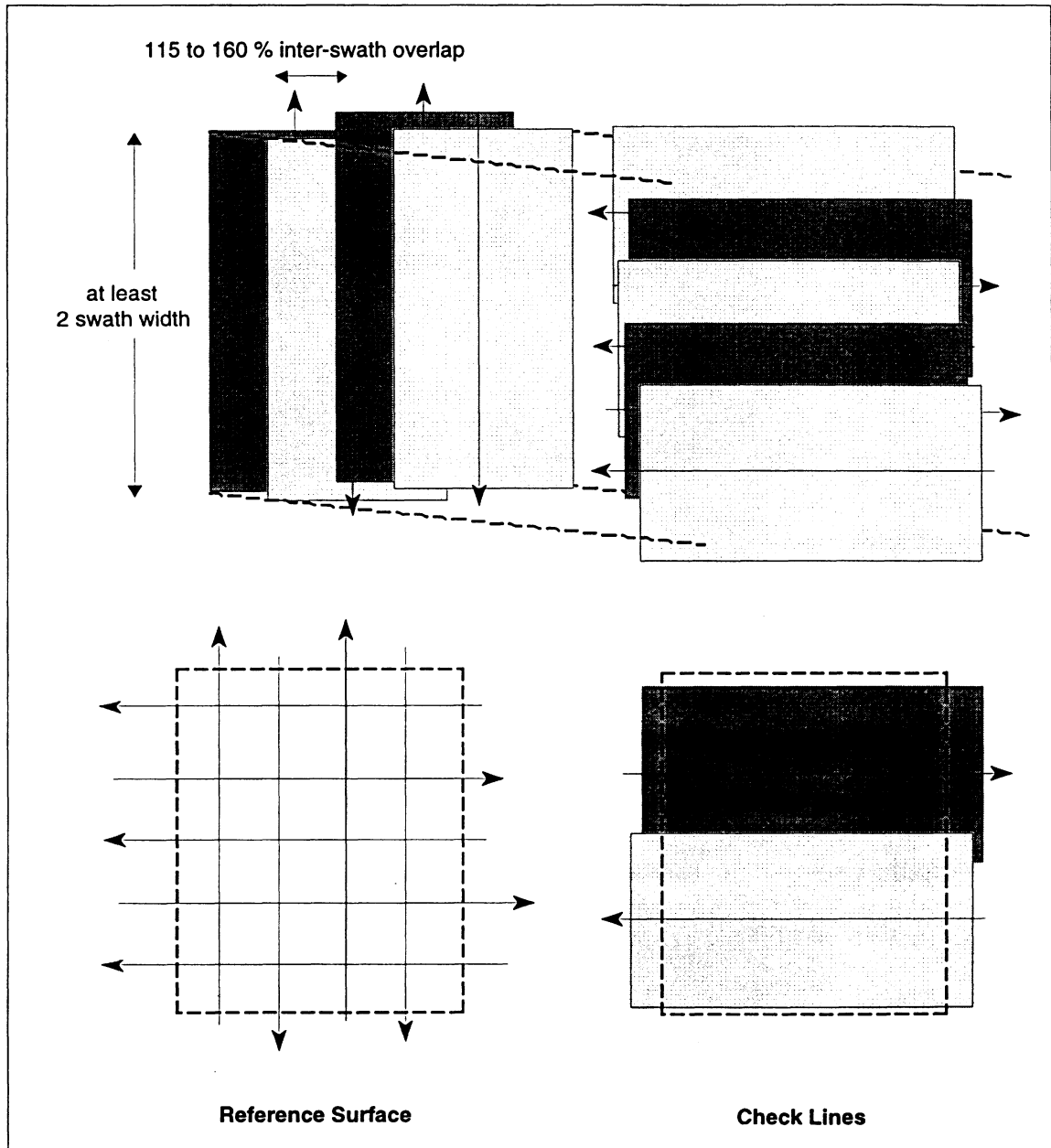
Figure 4.4   Test lines pattern for the performance check. The upper part shows the inter-swath overlap of the reference surface. Different level of grey is used to delineate the individual lines.

4.7.1.4 *The Check lines*

1) Perform a new sound velocity cast, within the reference surface.

2) Run a pair of parallel lines (> 300 m long), inside the reference surface, as shown in Figure 4.4. Inter-swath overlap is not needed.

3) Run other pairs of check lines, in other operating modes (if available).

4) Ship speed will be as above.

4.7.2 Data Post-Processing

The method employed to assess the different system biases uses direct measurements of the observed depth readings (as opposed to gridded data). Thus, one needs post-processing tools that allow visualization of observed depth measurements, with cross-section capabilities. The calibration steps are sequentially ordered and the procedures should be followed as they are presented. The post-processing package used in this report and for these procedures is the HDCS (Hydrographic Data Cleaning System), summer 1995 version [Universal Systems Ltd., 1994].

When processing calibration data, it is most important that position and attitude data are thoroughly cleaned. Look carefully for bad time tags and discard suspicious data. Permit interpolation (no breaks) between positions

only when the time gaps are less than five (or so) ship lengths. It is not important to clean the bathymetry since we will work on clouds of data points rather than on individual soundings. Hence, no data thining will be performed. Outliers will be identified within the various cross-sections used, and ignored.

4.7.2.1 Positioning Time Delay

The best way to detect and quantify a positioning time delay is to measure the along-track displacements of soundings, acquired by a pair of coincident lines, run at different speeds over a sloping terrain or a conspicuous topographic feature. Figure 4.5 illustrates the displacement caused by a positioning time delay. In order to eliminate the effect of a potential pitch offset, which would leak in the along-track displacements, lines run in the same direction will be used. Also, one must ensure that linear static offsets between the positioning system antenna and the transducer, are appropriately applied.

- With lines run in the same direction, the time delay can be computed using the following equation:

$$TD = \frac{d_a}{\left(v_h - v_l\right)} \tag{4.3}$$

Where TD is the time delay in seconds

d_a is the along-track displacement in metres

v_h is the higher speed in m/s

v_l is the lower speed in m/s
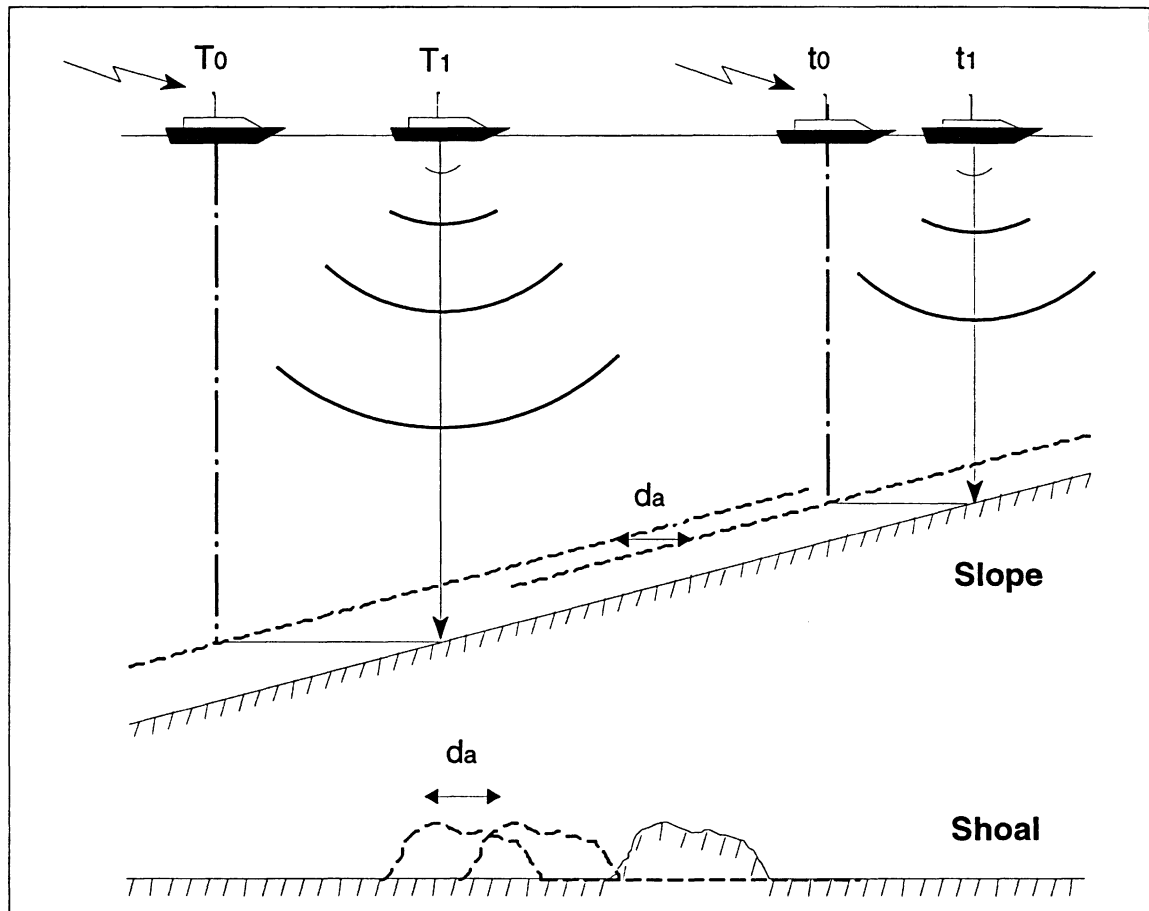
Figure 4.5 Profile view of a survey line run at two different speeds along a slope or over a shoal, showing the along-track displacement da in the apparent seafloor (dashed lines), caused by a positioning time delay. The highest speed is symbolized by the upper case letters T0 and T1. T0 (t0) is the time at which the position is observed while T1 (t1) is the time and position at which the sound signal is transmitted.

1) Process the survey lines, making sure no corrections for positioning time delay, pitch error, roll error and gyro error are entered in the

vessel configuration file (VCF) and that appropriate corrections for sensors static offsets are applied.

2) In HDCS Subset mode, work on two lines at a time.

3) Define a subset where the slope is the most pronounced or where the topographic features have been surveyed. In the *Magnified Window*, capture a narrow strip (with bounding box) that contains the beam readings at nadir, in the direction of the survey lines (illustrated in Figure III.3).

4) In the *Operations Window*, measure **horizontally** the displacements between the two along-track profiles, at different places. Make several measurements (≥ 10) and compute the mean, residual time delay, using formula 4.3.

5) Repeat the measurements on the other pair of lines, run in the opposite direction.

6) Verify that the along-track profile obtained by the highest speed, precedes the lowest speed profile, otherwise the time delay will be positive (echo-sounder clock is late with respect to positioning system clock) or the time delay applied during acquisition was overestimated. Save the session with a session name that corresponds to the line numbers.

7) Re-merge the lines with the time delay correction entered in the VCF (Figure III.4) and replot the along-track profiles. Fine tune the time delay correction until one obtains the best match (Figure III.5). This process may require several iterations.

8) Record in the SHIP'S PROFILE (sample in Appendix II), the exact time delay (initial ± residual).

4.7.2.2 Assessment of Pitch Offset

The two pairs of reciprocal lines, run over a slope at two different speeds, will be used to assess the pitch offset. The along-track displacements of soundings caused by a pitch offset is proportional to depth: the deeper the water depth, the larger the displacement. Figure 4.6 illustrates the apparent along-track profiles, in the presence of a pitch offset.

1) Process the survey lines, entering only the positioning time delay correction in the vessel configuration file (VCF) and the appropriate corrections for sensor static offsets.

2) Define a subset that encloses a portion of the survey lines (1/4 to 1/2). In the *Magnified Window*, capture a narrow strip that contains the beam readings at nadir, in the direction of the survey lines (illustrated in Figure III.6).

3) In the *Operations Window*, measure **horizontally** the displacements in the two along-track profiles, at different places, noting the depth at the location of the measurement. Make several measurements (≥10) and compute the mean, residual pitch offset. Save the session with a session name that corresponds to the line numbers.

4) The pitch offset can be computed using the following equation:

$$\alpha = \tan^{-1}\left(\frac{d_a/2}{depth}\right) \tag{4.4}$$

Where α is the pitch offset in degrees

d_a is the along-track displacement in metres

$depth$ is in metres
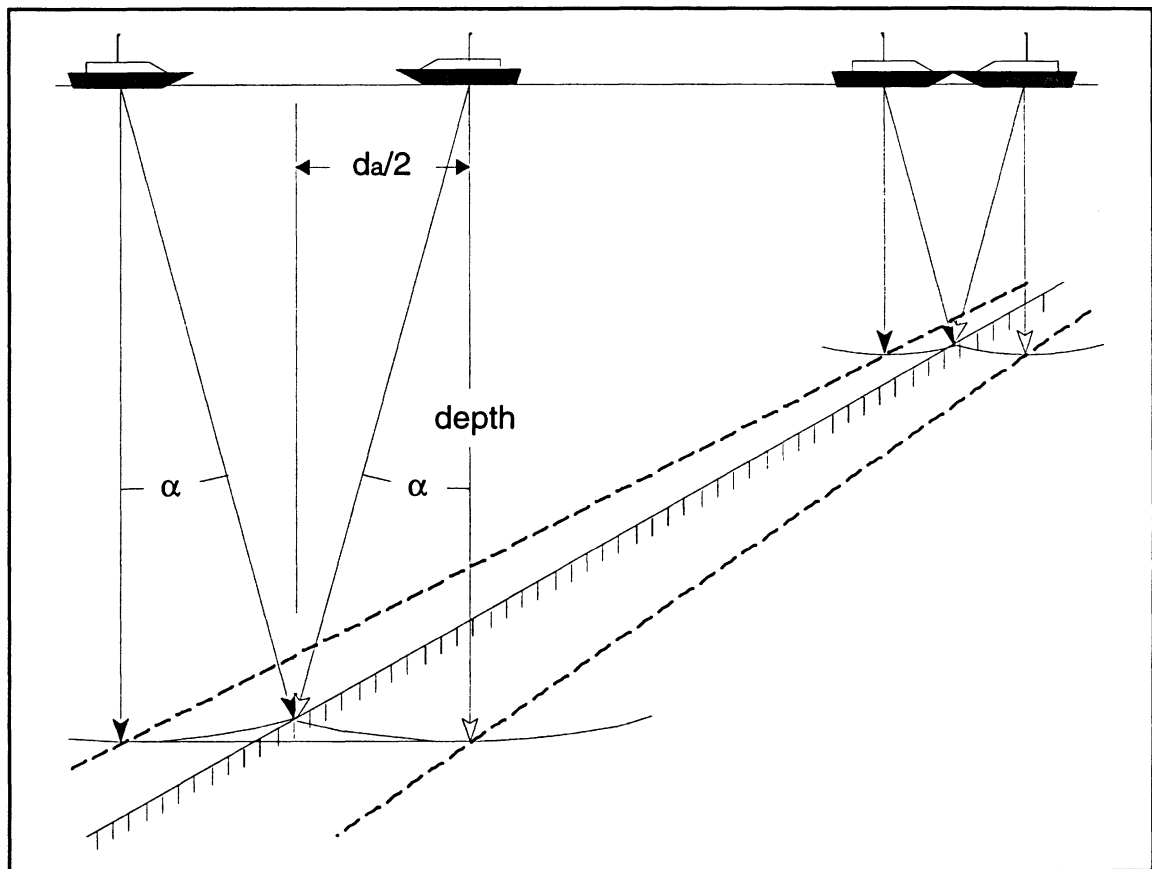
Figure 4.6   Profile view of two survey lines run over a slope, at the same speed and in opposite
direction, showing the along-track displacement da in the apparent seafloor (dash
lines) caused by a positive pitch offset α.

5) Repeat the measurements on the other pair of lines, run at a different

speed. Verify the sign of the pitch offset. In Figure 4.6, the pitch offset

is positive and the apparent seafloor is closer to a ship moving upslope. One must enter a negative correction in the OPU (or in the VCF) to correct this situation.

6) Re-merge the lines with the pitch offset correction entered in the VCF and replot the along-track profiles. Fine tune the pitch offset correction until the best match is obtained. Several iterations of this process might be needed.

7) Record in the SHIP'S PROFILE (sample in Appendix II) the exact pitch offset (initial ± residual).

4.7.2.3 Assessment of Azimuthal Offset

The two pairs of adjacent lines, run on each side of a conspicuous topographic feature, will here be used. Work on one pair of adjacent lines at a time, run in the opposite direction, to remove the effect of a potential roll offset. Figure 4.7 shows the effect of an azimuthal offset (exaggerated) on the along-track profiles measured by outer beams.

1) Process the survey lines, using only the positioning time delay and pitch offset corrections in the VCF, and the appropriate corrections for sensors static offsets.

2) Define a subset that encloses the topographic feature covered by the outer beams. In the *Operations Window*, query the beams over the shoal to locate the place where the scanning line should pass (i.e.

beams of equal across-track distance). In the *Magnified Window*,
capture a narrow strip, across the entire area, in order to measure in
the *Operations Window* the relative across-track distance for the
selected beams.
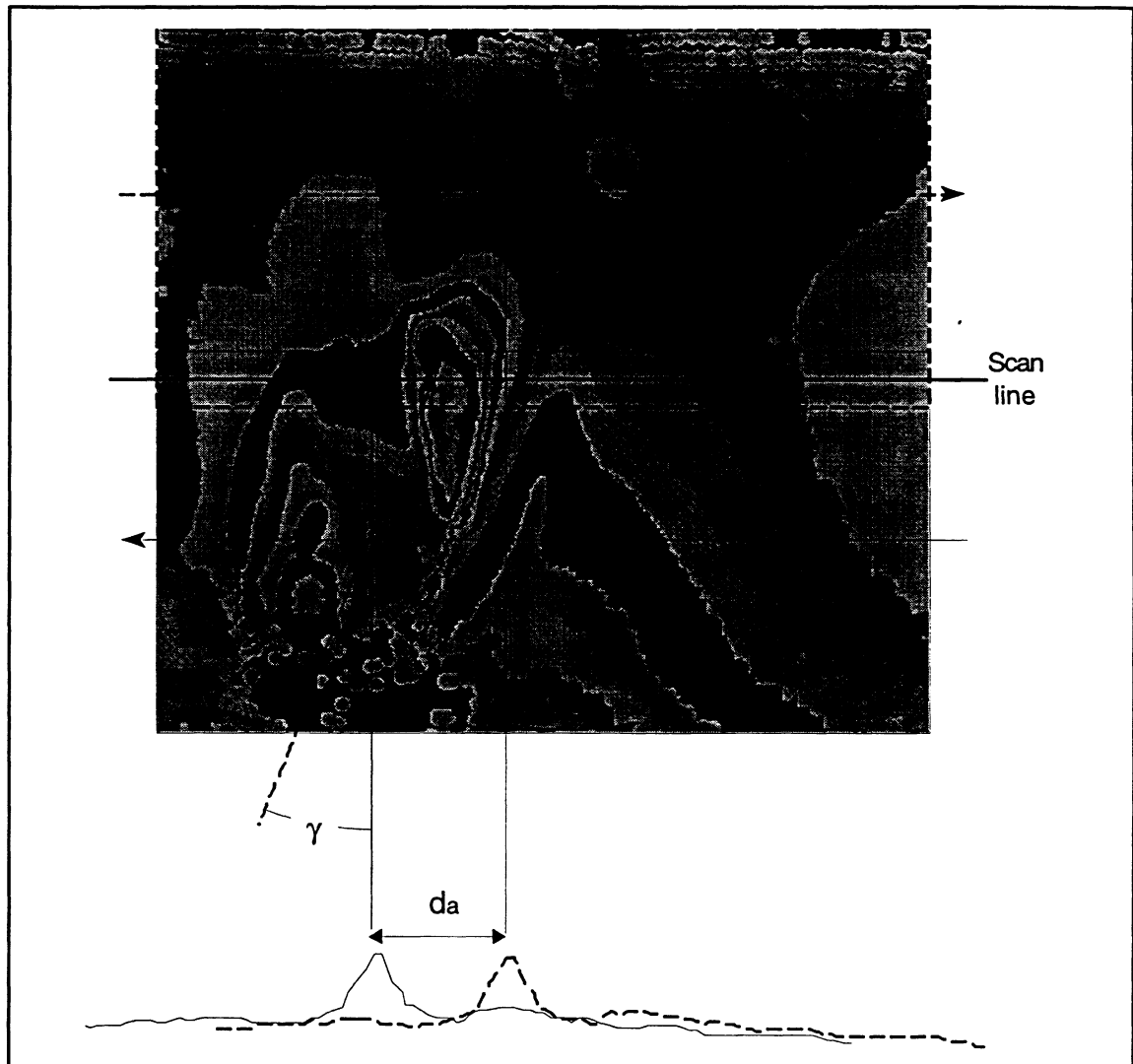
Figure 4.7   Plan view and along-track profiles for two adjacent survey lines run in the same
direction, on either side of a shoal. The along-track profiles represent the
apparent seafloor swept by the outer beams, along the scan line. The along-track
displacement da in the apparent seafloor is caused by the azimuthal offset γ.

3) Then, in the *Magnified Window*, rotate the bounding box and place a narrow strip over the shoal and along the scanning line (illustrated in Figure III.7), that produces the desired along-track profiles.

4) In the *Operations Window*, measure **horizontally** the displacements in the two along-track profiles, at different places along the shoal. Make several measurements (≥10) and compute the mean, residual azimuthal offset. Save the session with a session name that corresponds to the line numbers.

5) The azimuthal offset can be obtained, using the following equation:

$$\gamma = \sin^{-1}\left(\frac{d_a/2}{X_i}\right)$$

(4.5)

Where γ is the azimuthal offset in degrees

d_a is the along-track displacement in metres

X is the relative across-track distance for beam i, in metres

6) Repeat the measurements on the other pair of lines, run in opposite direction. Verify the sign of the azimuthal offset. In Figure 4.7, the azimuthal offset is positive and a negative correction should be entered in the OPU (or in the VCF) to correct the situation.

7) Re-merge the lines with the azimuthal offset correction entered in the VCF (Figure III.8) and replot the same along-track profiles. Fine tune the azimuthal offset correction until obtain the best match

(Figure III.9) between the two along-track profiles is obtained; several iterations of this process might be needed.

8) Record in the SHIP'S PROFILE (sample in Appendix II) the exact azimuthal offset (initial ± residual).

4.7.2.4 Assessment of Roll Offset

Reciprocal lines run over a flat terrain are used to detect and quantify the roll offset. Figure 4.8 shows the general principle of a roll offset from reciprocal lines, greatly exaggerated here for clarity.
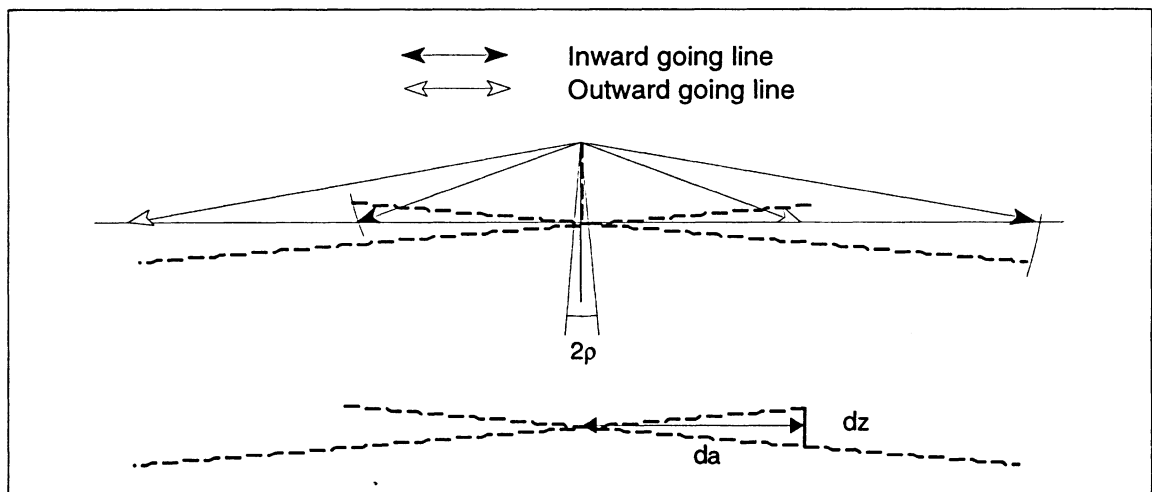
Figure 4.8   Profile view of two survey lines run in opposite direction over a flat seafloor. The apparent across-track profiles (dash lines) show a negative roll offset ρ of 5°. The depth difference dz and across-track distance da can be used to compute the roll offset.

1) Process the survey lines, entering only the positioning time delay, pitch offset and gyro offset corrections in the VCF, and the appropriate corrections for sensors' static offsets.

2) Define subsets that enclose half the lines, in the sailing direction (see Figure III.10). In the *Magnified Window*, bound a narrow strip of soundings, across the swaths. In the *Operations Window*, measure the depth difference at the outermost beams and the across-track distance from the location of the measurement to nadir. Make several measurements (≥10) along the lines and compute the average residual roll offset. Save the session with a session name that corresponds to the line numbers. Repeat the measurements on the other subset.

3) For small angles, the roll offset can be approximated, using the following equation:

$$\rho = \frac{\tan^{-1}\left(d_z / d_a\right)}{2} \tag{4.6}$$

Where ρ is the roll offset in degrees

d_z is the depth difference in metres

d_a is the across-track distance in metres

4) Verify the sign of the roll offset. In Figure 4.8, the roll offset is negative and a positive correction should be entered in the OPU (or in the VCF) to correct the situation.

5) Re-merge the lines with the roll offset correction entered in the VCF (Figure III.11) and replot the same profiles. Fine tune the roll offset correction until the best match between the across-track profiles is obtained (Figure III.12); several iterations of this process might be needed.

6) Record in the SHIP'S PROFILE (sample in Appendix II) the exact roll offset (initial ± residual).

4.7.2.5 The Performance Check

"Performance check" data are composed of (a) reference surface data, and (b) check line data. The post-processing of these data sets is done in two steps:

A) the data cleaning

B) the gridding and differencing

The reference surface represents the ground truth data. Hence, it should be free of biases and outliers. On the other hand, check lines will be used to verify the overall performance of the sounding system, and thus thinning and/or smoothing is avoided. During differencing, check lines will be processed one at a time and a "Quality Report" will be created for each check line (examples in Appendix IV).

1) Using HDCS, process the reference surface data first. At conversion, remove the outer beams that are outside 3*depth by disabling beams in the VCF (none for EM100). Thoroughly clean positions, attitude and bathymetric data. Interactive editing is preferred to automatic detection (and rejection!) of outliers. In the HDCS subset mode, **DO NOT** perform bathymetric data thinning.

2) Using HDCS, process the check lines next. Keep all beams at conversion. Remove obvious positional and bathymetric outliers only. If you have a systematic artifact in the profiles, do not clean it since it will be used to quantify its variance.

3) In HIPS, create a work file that encloses the reference surface area (one can get the coordinates in a HDCS window). Graticule and projection grid can be added to the work file but they will not be used. The choice for a scale depends only on whether you want to plot on paper or not. Import (into a work file) the reference surface lines, passing on accepted soundings only, **WITHOUT** data thinning. **DO NOT** import check line data now.

4) In *Work File Processing - Interactive Edit*, plot the data to make sure it is what you expect. Zoom in to enclose only the plotted data.

5) Create a **regular** DTM of the reference surface, from the visible area, using a grid size as big as the average beam footprint size. Once the DTM is produced, visualize it in 3-D to make sure it is free of excessive noise and outliers (use large vertical exaggeration).

6) Import (into *Checkline File*) the first check line, passing on accepted soundings only, **WITHOUT** data thinning. Visualize it in *Interactive edit*, to make sure it is what you expect. Create a *Quality report*.

In the HIPS *Import* routine, new data are appended to existing ones. It is thus not possible to import into a work file a second check line and have it compared against the reference surface without including the previously imported check line into the statistical calculation. Also, the existing quality report file (makehist.lis) will be overwritten by the incoming new one. Hence, before creating a new quality report, one must remove the checkline files (checkline.*) and move elsewhere the report file as follow:

1) After creation of the quality report, open a window (option menu: *System*). You will need the write permission for removing checkline files unless you are the owner of the files. Go into the work file directory (cd workfile) and move the report file one level up (mv makehist.lis ../checkline_1.lis) and remove the checkline files (rm -f checkline.*).

2) Follow the same sequence for creating the other quality reports.

5. Conclusions and Recommendations

This Master of Engineering report discusses the calibration of multibeam echo-sounding systems when operating in shallow water. Herewith, we approach the subject by considering the acquisition platform and the auxiliary sensors as a whole. The system to be dealt with is thus an entity, composed of the vessel, the multibeam echo-sounder and the complementary instruments (motion sensors, gyro, etc).

We know that techniques have already been developed for performing MBES calibration (e.g. Hughes Clarke et al. [1995], Simrad Subsea [1995], Herlihy et al. [1989], but they usually discuss the adjustment of the echo-sounding instrument itself and do not cover the other problems brought by the acquisition platform. In this report, an attempt was made to depict all sources of systematic error that are relevant to shallow water operations. In particular, one must consider:

- the ship's dynamics

- the misalignments between the transducer and the attitude sensors

- a means to assess the transducer draught or to refer the depth measurements to the instantaneous mean water level

- the static offsets between the sensors

- the behavior of each sensor in all operating conditions

- the beam refraction caused by imperfect knowledge of the sound velocity structure of the watermass

Hence, a description of sources of error is provided and indications are given as to their effects on MBES measurements. Although listed above, the errors produced by beam refraction and erroneous mean of the speed of sound for each beam path are not addressed by the report. Because of the unpredictable nature of the surveyed element (shallow water mass) it was deemed impractical to try calibrating the MBES for these sources of error using the existing calibration techniques. As for the identification of the other sources of error, they lead to the determination of a set of "system parameters" that are used during the integration of the various inputs.

This report provides a set of field procedures for calibrating the shallow water MBES. The procedures include the assessment of systematic errors pertaining to shallow water MBES. Guidelines are provided for the acquisition of calibration data, the "Calibration Survey", and a demonstration of bias assessment is incorporated, using Simrad EM1000 data and HIPS post-processing package. The methods take advantage of various features on the

seafloor, to help identifying the system biases. The procedures end with a proposed method for evaluating the efficiency of the calibration, the "Performance Check", which can also be used to certify the data comply with accuracy standards.

Although demonstrated with the use of a particular post-processing software package (HIPS), these procedures present a non-specific approach for the system's calibration. While tools already exist on the market that automate the assessment of biases, the procedures described herein can help those who are not equipped with such tools as well as helping in the understanding of the overall calibration.

The procedures provide a specific sequence in which biases must be assessed. The end product of the system integration is the geo-referenced soundings, in which all system biases contributed in the total position and depth error. Hence, system biases are interrelated in the final measurement. The biases need to be isolated before being detected and quantified. They then need to be corrected for, systematically in an orderly sequence. The sequence adopted in the field procedures for segregating and removing the biases is as follows:

- determining positioning time delay

- determining pitch offset (data corrected for time delay)

- determining azimuthal offset (data corrected for time delay and pitch offset)

- determining roll offset(data corrected for time delay, pitch and azimuthal offsets)

-

Once biases have been removed, one should conduct the Performance Check. This routine consists of surveying a small area (0.1 km^2) of flat and smooth seabed, building from it a reference surface. Check lines are then made over that surface and each beam reading is compared against the reference surface. Statistics of the differences are made, indicating the confidence level one can get for each beam of the MBES. The differencing stage requires the ability to produce a DEM from the reference data, the differences being generated from the interpolated gridded surface. Obviously, a good understanding of the gridding techniques and of the algorithm used by the post-processing software is needed before performing the differencing. The quality assessment is here limited to the overall accuracy of the sounding system and the resolution at which the DEM can be meaningfully produced.

Possible future development in MBES calibration includes the implementation of a fully automated calibration tool, in which the user would just survey a specific parcel of terrain, in a specific manner, leaving to

the program to come up with required system parameters. The estimation of system biases could certainly be made through least squares techniques.

Another possible field of development, which is actually being investigated, is the real time calibration for beam refraction caused by improper knowledge of the sound velocity structure of the surveyed waters. This source of error already limits our ability to perform the MBES calibration for common system biases. Such real time calibration for beam refraction is required for a complete characterization of MBES biases and errors.

References

Blouin, G., D. Davesne, J. Giard, C. Laliberté and P. Lavoie (1982). *Algèbre linéaire et géométrie*. gaëtan morin éditeur, réimpression 1985, Chicoutimi.

Canadian Hydrographic Service (1986). *Survey Standing Order 5.2-86*, Section 4 - Depth Measurement Accuracy, 3 p.

Derrett, D.R. (1964). Ship stability for Masters and Mates. 4th rev. ed. (1990), Butterworth-Heinemann, Oxford.

Forrester, W.D. (1983). *Manuel Canadien des Marées*. Ministère des Pêches et des Océans, Service hydrographiques du Canada, Ottawa (Ontario), 148 p.

Hare, R. and B. Tessier (1995). *Water level accuracy estimation for real-time navigation in the St. Lawrence River*. Department of Fisheries and Oceans, Canadian Hydrographic Service internal report, Laurentian region, 147 p.

Hare, R., A. Godin, and L. Mayer (1995). *Accuracy estimation of Canadian Swath (multibeam) and Sweep (multi-transducer) sounding systems*. Department of Fisheries and Oceans, Canadian Hydrographic Service internal report, Laurentian region.

Herlihy, D.R., B.F. Hillard, and T.D. Rulon (1989). *National Oceanic and Atmospheric Administration Sea Beam System "Patch Test"*. International Hydrographic Review, Monaco, LXVI(2), July 1989, pp. 119-138.

Hughes Clarke, J., L. Mayer, D. Wells, C. de Moustier and B. Tyce (1996). *Cosatal Multibeam Sonar Training Course*. Lecture notes, Department of Geodesy and Geomatics Engineering, University of New Brunswick.

Hughes Clarke, J., L. Mayer, D. Wells, C. de Moustier and B. Tyce (1995). *Multibeam Sonar: Theory, measurement and analysis*. Lecture notes, Department of Geodesy and Geomatics Engineering, University of New Brunswick.

Hughes Clarke, J. (1993a). *Insvestigation of the residual roll artifact present in Matthew 92-008 EM100 data*. Department of Fisheries and Oceans, Canada, DFO contract report FP962-2-6001.

Hughes Clarke, J. and A. Godin (1993b). *Investigation of the roll and heave errors present in Frederick G. Creed - EM1000 data when using a TSS 335B motion sensor.* Department of Fisheries and Oceans, Canada, DFO contract report FP707-3-5731.

Hughes Clarke, J. (1993c). *Analysis of residual roll and heave errors identified during the "Matthew Motion Sensor Trials".* Department of Fisheries and Oceans, Canada, DFO contract report FP962-3-4602.

International Hydrographic Organisation (1987). *IHO Standards for Hydrographic Surveys.* Special Publication No. 44, 3rd Edition, 1987. International Hydrographic Bureau, Monaco.

Mayer, L., J. Hughes Clarke, D. Wells, and the HYGRO-92 Team (1993). *A Multi-faceted Acoustic Ground-truthing experiment on the Bay of Fundy.* Proceedings of Acoustic Classification and Mapping of the Seabed Internal Conference, 18p.

Mikhail, E.M., G. Gracie (1981). *Analysis and Ajustment of Survey Measurements.* Van Nostrand Reinhold Company, Toronto

Mimkler, G. and J. Mimkler (1990). *Aerospace Coordinate Systems and Transformations.* Magellan book company, Baltimore, MD.

Pøhner, F. (1993). *Model for calculation of uncertainty in multibeam depth sounding.* Proceedings of the FEMME 93 conference, 16 pp.

Simrad Subsea A/S (1995). *NEPTUNE Operator Manual.* Simrad publication.

Simrad Subsea A/S (1994). *Simrad EM1000 Operator Manual.* Simrad publication.

The Royal Naval Surveying Service (1990). *The Assessment of the Precision of Sounding.* Hydrographic Department, Ministry of Defence, U.K. - Professional Paper No 25.

TSS (UK) Ltd. (1993). *335B Roll-Pitch-Heave Sensor - Operating Manual.* TSS (UK) Ltd publication.

Universal Systems Ltd. (1994). *CARIS HIPS & SIPS Instruction Manual.* USL publication.

Wheaton, G.E. (1988), *"Patch Test, a system check for multibeam survey system"*. Third biennial U.S. Hydrographic Conference Proceedings, April 12-15 1988, Baltimore, MD, pp. 85-90.

Appendix I

Theory of Ship-borne Motion Sensors and

Derivation of the Azimuthal Misalignment

This Appendix provides complementary information on ship-borne motion sensor and describes the way roll and pitch errors are produced when a azimuthal misalignment of the motion sensors is present. For convenience, the Body-Frame is represented with the z-axis up. No changes have been made to the conventions adopted in this report. The leveled coordinate system employed in the derivation is different from the Local-Level reference frame and they should not be mistaken for one another.

I.1   Ship-borne Motion Sensors

There are several types of inertial sensors that can be installed on ships for attitude measurements. Amongst these are the rate gyro platforms (e.g. POS/MV), the motion sensors equipped with "solid-state" angular rate sensors (e.g. TSS-335B), liquid ball (e.g. Hippy 120) or Coriolis force based vibrating gyro (e.g. MRU). Most motion sensors are also equipped with an orthogonal array of linear accelerometers that provides orientation with respect to the Local-Level frame. The working principle greatly varies from one type of sensor to another but they all measure the same basic quantities:

- Roll angle β

- Pitch angle α

- Heave h

- Yaw (and some, heading)

For example, the TSS motion sensors use the low-pass filtered output of an array of three linear accelerometers to assess the long term orientation of the platform with respect to the true vertical Z. The accelerometers are mounted orthogonally on the Body- Frame (Figure I.1) and provide a measure of the acceleration vector $\underline{a}$ which
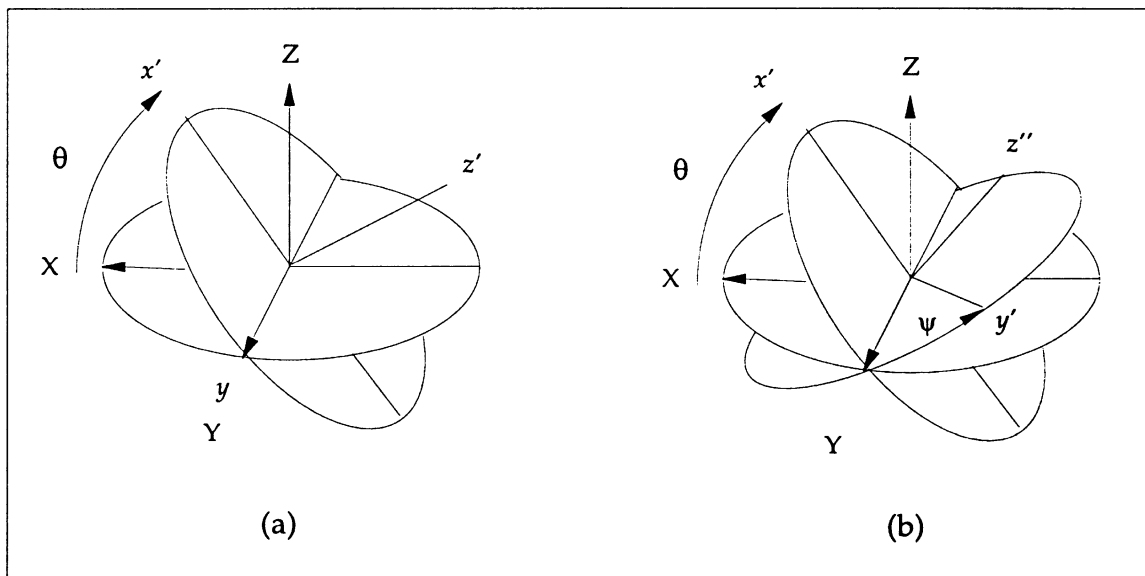
Figure I.1   The two independent Euler angles θ (rotation of the Body-Frame about the y-axis) and ψ (rotation of the Body-Frame about the transformed x'-axis) shown here with respect to a leveled reference system (upper case letters). Notice the rotation sequence of pitch (a) and roll (b) which follow the Tate-Bryant convention.

can be projected on the platform x and y axis using the following set of equations [TSS (UK) Ltd, (1992)]:

$$a_x = a \sin \alpha \qquad \text{(I.1)}$$

$$a_y = a \sin \beta \qquad \text{(I.2)}$$

Where - $a = \left(a_x^2 + a_y^2 + a_z^2\right)^{1/2}$

  - α is the angle made by the once rotated BF x-axis (x' in Figure I.1) with the horizontal plane, after pitchl rotation

  - β is the angle made by the once rotated BF y-axis (y' in Figure I.1) with the horizontal plane, after pitch and roll rotation

In order to combine the motion sensors output with the multibeam echosounder, it is necessary to get from the motion sensor (or computed by the integration unit) the two independent Eulerian angles θ and ψ (Figure I.1). The rotation matrices $\mathbf{R_x}$ and $\mathbf{R_y}$ will define the rotation operator $\mathbf{Q}$ as follows:

$$R_x = \begin{pmatrix} 1 & 0 & 0 \\ 0 & \cos \psi & \sin \psi \\ 0 & -\sin \psi & \cos \psi \end{pmatrix} \qquad \text{(I.3)}$$

$$R_y = \begin{pmatrix} \cos \theta & 0 & -\sin \theta \\ 0 & 1 & 0 \\ \sin \theta & 0 & \cos \theta \end{pmatrix} \qquad \text{(I.4)}$$

$$Q = R_x R_y = \begin{pmatrix} \cos\theta & 0 & -\sin\theta \\ \sin\theta\sin\psi & \cos\psi & \cos\theta\sin\psi \\ \sin\theta\cos\psi & -\sin\psi & \cos\theta\cos\psi \end{pmatrix} \qquad (I.5)$$

In order to express the position of a vector $\underline{x}'$ on the Body-Frame (BF) in the leveled coordinate system (LS), one must multiply the vector by the inverse of Q (which is transpose because Q is orthogonal) as in the following linear relationships:

$$\underline{x}' = Q\underline{x} \qquad \Leftrightarrow \qquad \underline{x} = Q^{-1}\underline{x}'$$

$$Q^{-1} = \begin{pmatrix} \cos\theta & \sin\theta\sin\psi & \sin\theta\cos\psi \\ 0 & \cos\psi & -\sin\psi \\ -\sin\theta & \cos\theta\sin\psi & \cos\theta\cos\psi \end{pmatrix} \qquad (I.6)$$

The dependent angle α is equal in radians to $\pi/2$ minus the angle between true vertical and BF x-axis. The angle β is obtained similarly with the BF y-axis. These angles are related to the Eularian angles as follow:

Pitch angle α

$$Q^{-1}x' = \begin{pmatrix} \cos\theta & \sin\theta\sin\psi & \sin\theta\cos\psi \\ 0 & \cos\psi & -\sin\psi \\ -\sin\theta & \cos\theta\sin\psi & \cos\theta\cos\psi \end{pmatrix} \begin{pmatrix} 1 \\ 0 \\ 0 \end{pmatrix}_{BF}$$

$$Q^{-1}x' = \begin{pmatrix} \cos\theta \\ 0 \\ -\sin\theta \end{pmatrix}_{LS} \tag{I.7}$$

For a unit vector on the BF x-axis, the sine of the angle from the horizontal plane (illustrated in Figure I.2) to that rotated vector ($\underline{x}'$) represents the z component in the LS coordinate system, and thus:

$$\sin\alpha = -\sin\theta \tag{I.8}$$
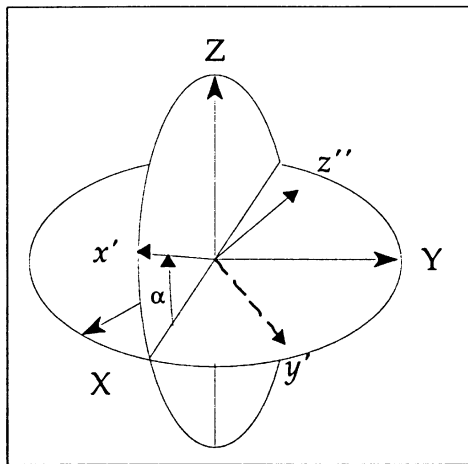
Figure I.2   Representation of the pitch angle α with respect to the LS coordinate system. Notice the once rotated x-axis (x', after pitch), the once rotated y-axis (y', after roll) and the doubly rotated z-axis (z'', after pitch and roll).

<u>Roll angle β</u>

$$Q^{-1}y' = \begin{pmatrix} \cos\theta & \sin\theta\sin\psi & \sin\theta\cos\psi \\ 0 & \cos\psi & -\sin\psi \\ -\sin\theta & \cos\theta\sin\psi & \cos\theta\cos\psi \end{pmatrix}\begin{pmatrix} 0 \\ 1 \\ 0 \end{pmatrix}_{BF}$$

(I.9)

$$= \begin{pmatrix} \sin\theta\sin\psi \\ \cos\psi \\ \cos\theta\sin\psi \end{pmatrix}_{LS}$$

and
$$\sin\beta = \cos\theta\,\sin\psi$$
(I.10)

I.2 Azimuthal Misalignment of the Motion Sensor

As stated above, an azimuthal offset of the sensitive axes (orthogonal array of accelerometers) with respect to the ship's rotation axes will result in errors in the attitude outputs. Figure I.3 illustrates the azimuthal offset γ, which is hereafter mathematically derived.
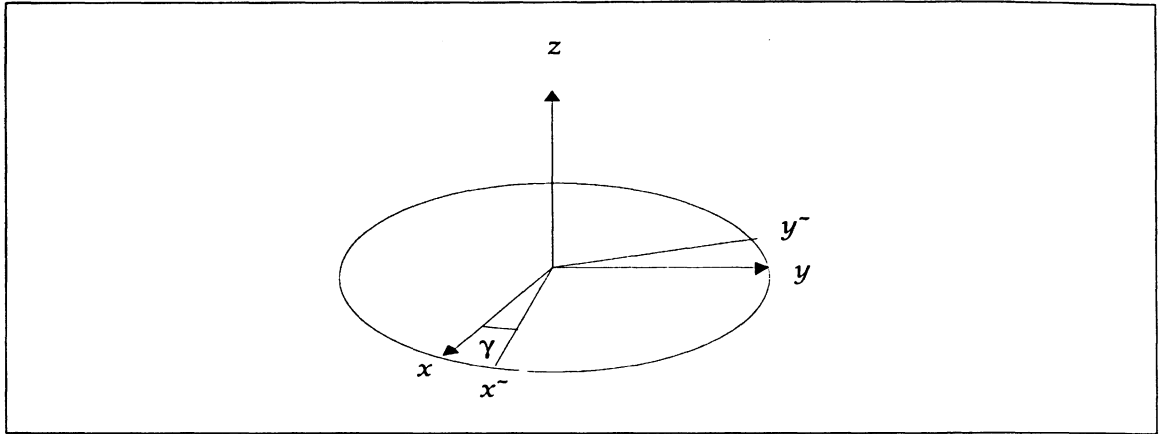
Figure I.3 Azimuthal offset γ between the Body-Frame x and y axes and the sensitive x˜ and y˜ axes of the motion sensor.

The $\underline{x}^{\sim}$ and $\underline{y}^{\sim}$ vectors can be expressed in the BF coordinate system after a rotation about the BF z-axis, using the rotation matrix R_z.

$$R_z = \begin{pmatrix} \cos\gamma & -\sin\gamma & 0 \\ \sin\gamma & \cos\gamma & 0 \\ 0 & 0 & 1 \end{pmatrix} \qquad (I.11)$$

$$\underline{x}^{\sim} = \begin{pmatrix} \cos\gamma & -\sin\gamma & 0 \\ \sin\gamma & \cos\gamma & 0 \\ 0 & 0 & 1 \end{pmatrix} \begin{pmatrix} 1 \\ 0 \\ 0 \end{pmatrix}$$

$$= \begin{pmatrix} \cos\gamma \\ \sin\gamma \\ 0 \end{pmatrix}_{BF} \qquad (I.12)$$

$$\underline{y}^{\sim} = \begin{pmatrix} \cos \gamma & -\sin \gamma & 0 \\ \sin \gamma & \cos \gamma & 0 \\ 0 & 0 & 1 \end{pmatrix} \begin{pmatrix} 0 \\ 1 \\ 0 \end{pmatrix}$$

and   (I.13)

$$= \begin{pmatrix} -\sin \gamma \\ \cos \gamma \\ 0 \end{pmatrix}_{BF}$$

The $\underline{x}^{\sim}$ and $\underline{y}^{\sim}$ vectors are then expressed in the LS coordinate system

using the transformation operator Q^{-1}:

$$Q^{-1}\underline{x}^{\sim} = \begin{pmatrix} \cos \theta & \sin \theta \sin \psi & \sin \theta \cos \psi \\ 0 & \cos \psi & -\sin \psi \\ -\sin \theta & \cos \theta \sin \psi & \cos \theta \cos \psi \end{pmatrix} \begin{pmatrix} \cos \gamma \\ \sin \gamma \\ 0 \end{pmatrix}_{BF}$$

(I.14)

$$\underline{x}^{*} = \begin{pmatrix} \cos \gamma \cos \theta + \sin \gamma \sin \theta \sin \psi \\ \sin \gamma \cos \psi \\ -\cos \gamma \sin \theta + \sin \gamma \cos \theta \sin \psi \end{pmatrix}_{LS}$$

$$Q^{-1}\underline{y}^{\sim} = \begin{pmatrix} \cos \theta & \sin \theta \sin \psi & \sin \theta \cos \psi \\ 0 & \cos \psi & -\sin \psi \\ -\sin \theta & \cos \theta \sin \psi & \cos \theta \cos \psi \end{pmatrix} \begin{pmatrix} -\sin \gamma \\ \cos \gamma \\ 0 \end{pmatrix}_{BF}$$

and   (I.15)

$$\underline{y}^{*} = \begin{pmatrix} -\cos \gamma \sin \theta + \cos \gamma \sin \theta \sin \psi \\ \cos \gamma \cos \psi \\ -\sin \gamma \sin \theta + \cos \gamma \cos \theta \sin \psi \end{pmatrix}_{LS}$$

But substituting with equations I.5 and I.7 and from the fact that vectors

$\underline{x}^{\sim}$ and $\underline{y}^{\sim}$ are unit length vectors, the sine of the output pitch and roll (biased)

correspond to the z component of the transformed $\underline{x}^*$ and $\underline{y}^*$ vectors and can be expressed by the equations:

$$\sin\alpha' = \cos\gamma \sin\alpha - \sin\gamma \sin\beta \qquad (I.16)$$

$$\sin\beta' = \cos\gamma \sin\beta - \sin\gamma \sin\alpha \qquad (I.17)$$

Appendix II

The SHIP'S PROFILE

SHIP'S PROFILE   MBES Integration Parameters

LINEAR OFFSETS		ANGULAR OFFSETS			TIME DELAYS		
X VRU :		**Pitch**	VRU:		**VRU**	estimated:	
Y VRU :			Transducer:			residual:	
Z VRU :			residual:				
X trans :		**Roll**	VRU:		**Positioning**	estimated:	
Y trans :			Transducer:			residual:	
Z trans :			residual:				
						Meta Data	
X anten :		**Azimuthal**	VRU:		**Vessel :**		
Y anten :			Transducer:				
Z anten :			residual:		**Location :**		
					Project:		
RP to Keel :							
Transducer to Keel :					**Date :**		
Transducer draft coor. :					**Engineer :**		

Ship: ———————

MBES Configuration

SHIP'S PROFILE
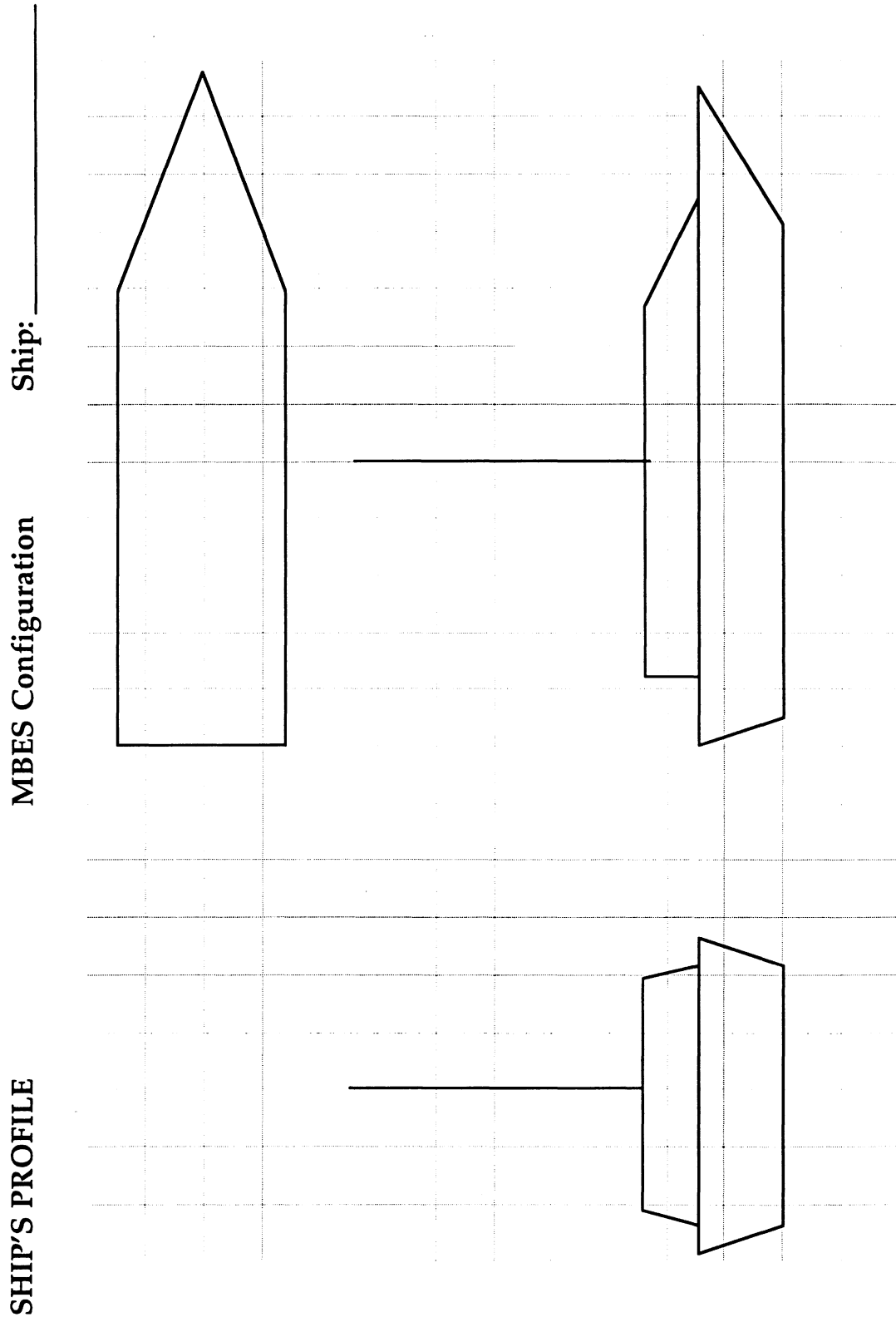
Appendix III

Example of a Calibration Survey

(From Simrad EM1000 data and using
HIPS post-processing s/w)

This appendix depicts a calibration survey that was performed on 29 June 1993, off Rimouski (Québec) on the NSC "Frederick G. Creed", before a hydrographic survey in 1993. The multibeam echo-sounding system was composed of:

- Simrad EM1000 multibeam echo-sounder

- TSS335B motion sensor

- Anshutz North Star gyrocompass

- Navitronics SVM-1 sound velocity profiler

- DGPS positioning system
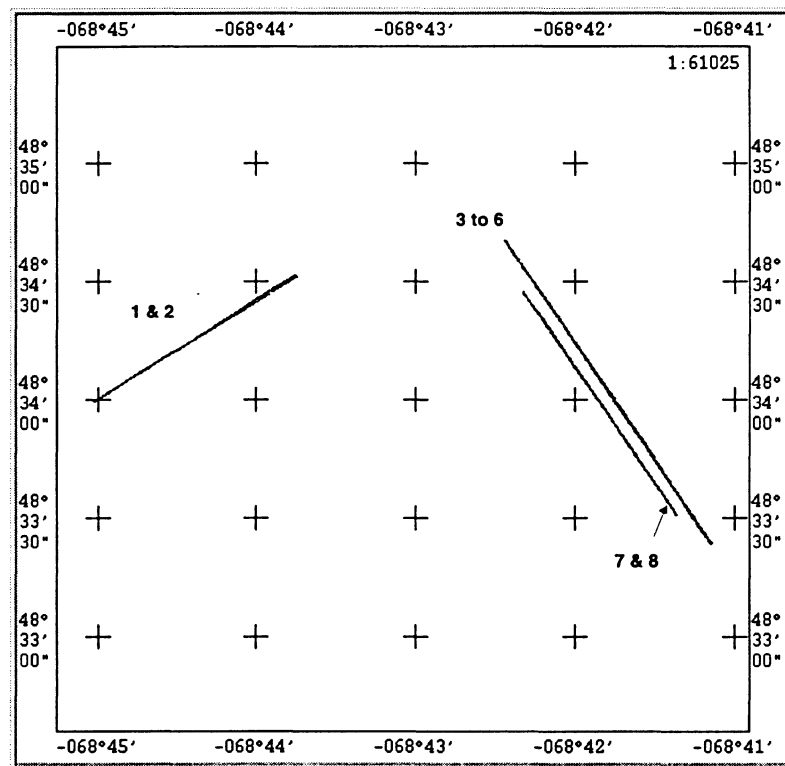
Figure III.1 The calibration survey tracklines. Lines 1 and 2 are the Roll offset test lines. Lines 3 to 6 are the Time delay/Pitch offset lines and lines 5 to 8 are used for assessing the azimuthal offset.

The tide gauge used was a Socomar TMS-1000, installed at Rimouski's wharf, within 3 km of the testbed. Figure III.1 illustrates the line pattern which are also detailed in table B1. The general bathymetric configuration of the test area is illustrated in Figure III.2. As one can see, all necessary testbed features for a calibration survey are located close to each other. Hence, we have a flat seafloor in deep water for the roll offset assessment, a slope (± 10° with max of 25°) and two topographic features on the bottom, as indicated by the arrows, for the time delay, the pitch and gyro offsets assessment. Some integration parameters have been entered in the EM1000 OPU, as shown in the following printout of the "start datagram".

EM Start Datagram --------------------
Date: 93:06:29 Time: 18:53:27.00 Position Input System: 4   Time Delay: 1
Motion Sensor Roll Offset: -0.44 Pitch Offset: -3 Gyro Offset: 0
EM100   Transducer Depth: 0 Alongship Offset: 0 Athwartships Offset: 0
EM12   Transducer Depth: 0 Alongship Offset: 0 Athwartships Offset: 0
EM1000 Transducer Depth: 2 Alongship Offset: 0 Athwartships Offset: 0
Survey Line: 0001
Comment: Calibration_Creed_93

Table III.1   Calibration lines run off Rimouski (Québec), day 180 1993.

	SOL			EOL			Speed	(SMG)	Course
Line	Time	Lat	Long	Time	Lat	Long	(m/s)	(kn)	(CMG)
1	18h53m26s	48°34'31"289N	68°43'45"389W	18h58m41s	48°33'59"465N	68°45'01"193W	5.8	11.3	237.6
2	19h05m29s	48°34'00"071N	68°44'59"718W	19h09m31s	48°34'31"073N	68°43'44"795W	7.4	14.5	58.2
3	19h17m26s	48°34'38"993N	68°42'25"397W	19h22m18s	48°33'23"766N	68°41'08"399W	9.6	18.7	145.9
4	19h29m15s	48°33'24"228N	68°41'09"143W	19h34m26s	48°34'40"176N	68°42'26"256W	9.1	17.7	325.9
5	19h41m47s	48°34'39"018N	68°42'25"337W	19h49m13s	48°33'24"726N	68°41'09"588W	6.2	12.1	146.0
6	19h56m45s	48°33'23"399N	68°41'08"795W	20h04m32s	48°34'40"337N	68°42'26"561W	6.1	11.9	326.2
7	20h10m39s	48°34'27"239N	68°42'19"698W	20h16m05s	48°33'30"689N	68°41'21"666W	6.5	12.6	145.6
8	20h22m13s	48°33'30"918N	68°41'21"641W	20h27m20s	48°34'22"643N	68°42'14"496W	6.3	12.2	325.9
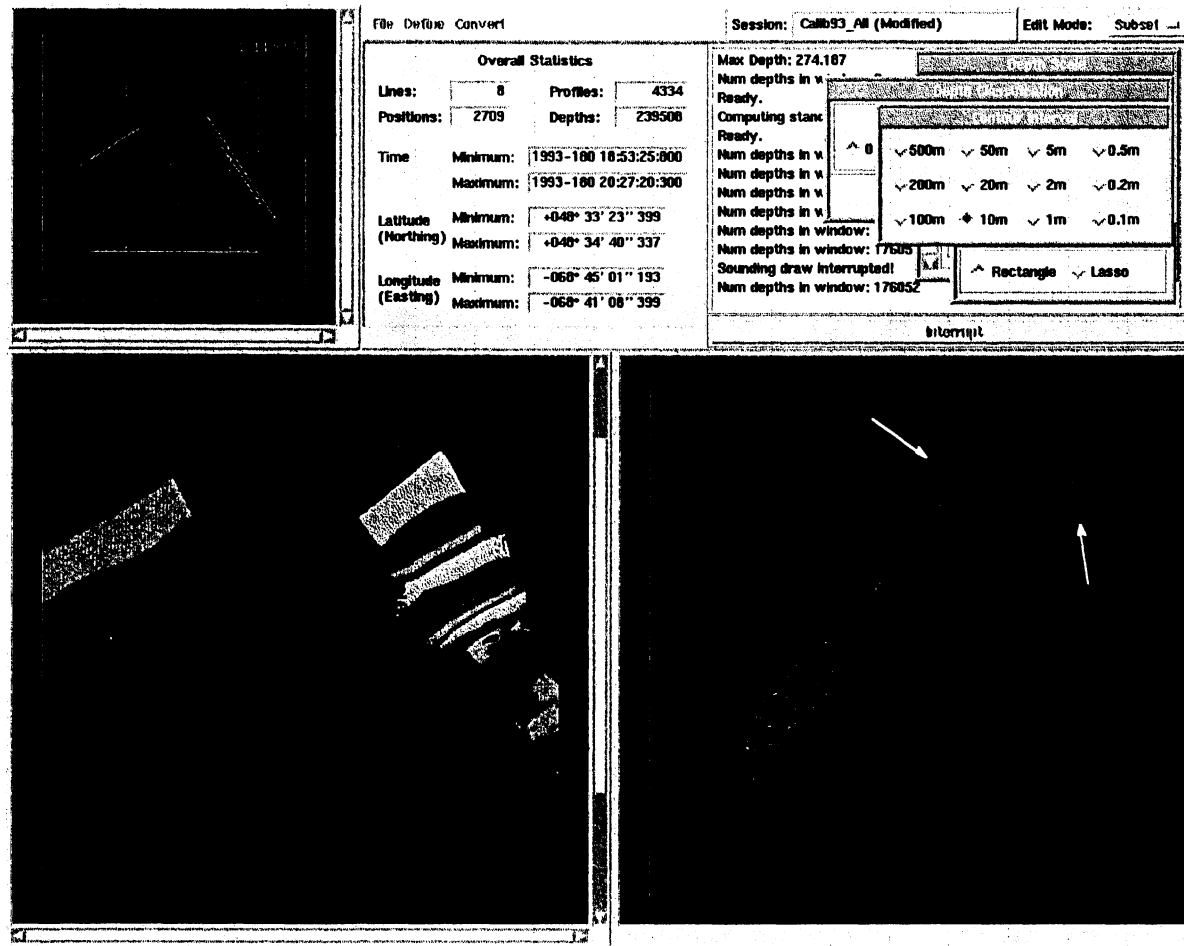
Figure III.2 Bathymetric configuration of the calibration survey area. For azimuthal offset assessment, two conspicuous features on the bottom are used (indicated by arrows). The cross-section (right view) is seen from west. The mean slope, greatly exaggerated here, is 10° with a maximum of ~ 25°.
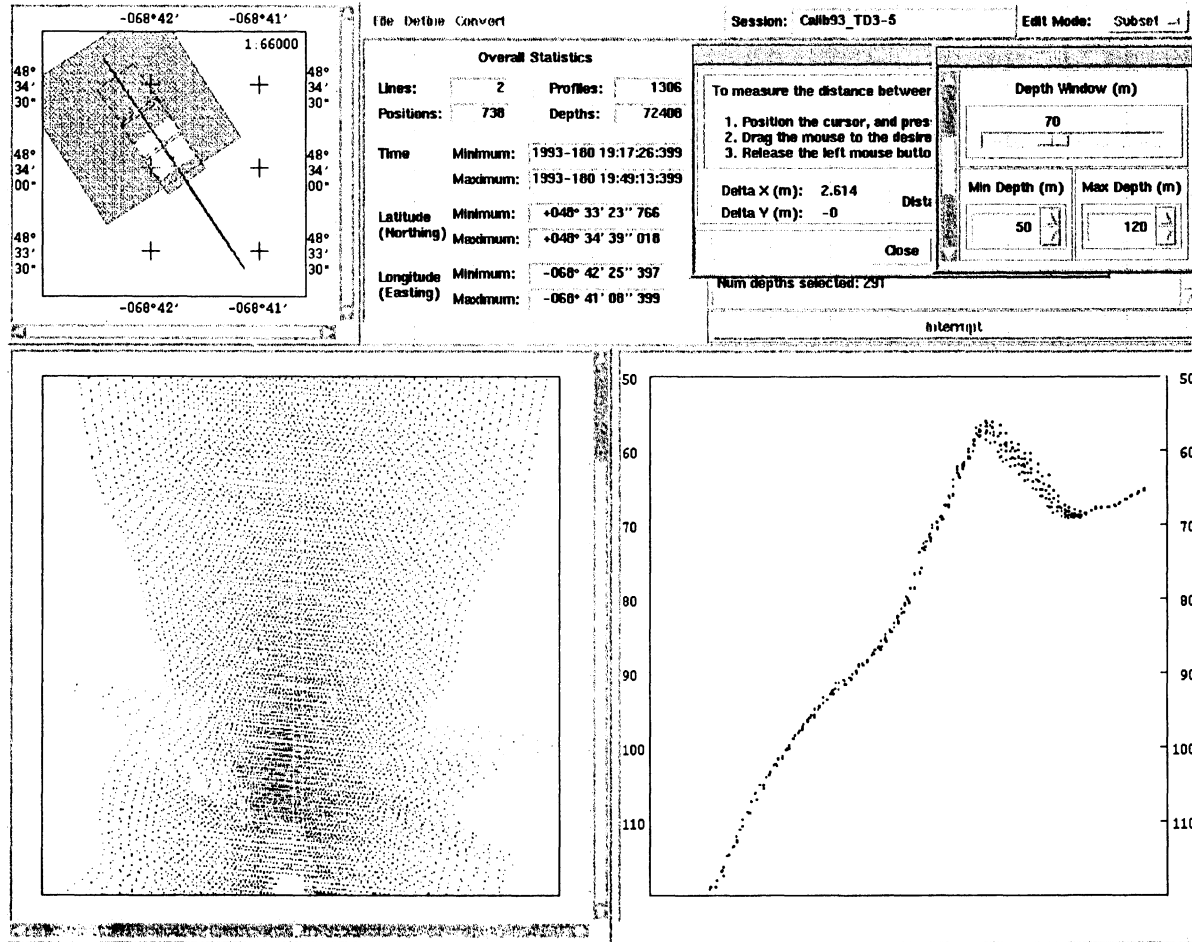
Figure III.3 Lines 3 (blue) and 5 (red) are plotted to show the residual (negative) time delay. The lower left window is a plan view of the survey lines. The lower right window is a cross-section of the surveyed area contained in the yellow bounding box shown in the plan view. A larger speed difference would have help measuring the along-track displacements.

File   Vessel: Creed   Status: Modified

Depth Sensor   1993-180 18:45 —| New Entry Remove Entry

#	1	2	3	4	5	6	7	8	9	10	11	12	13	14	15	16	17	18	19	20	21	22	23	24
X																								
Y																								
Z																								
S	♦ E	♦ E	♦ E	♦ E	♦ E	♦ E	♦ E	♦ E	♦ E	♦ E	♦ E	♦ E	♦ E	♦ E	♦ E	♦ E	♦ E	♦ E	♦ E	♦ E	♦ E	♦ E	♦ E	♦ E

◄ ►

Time Error: 0.60   Delta X: 3.87   Delta Y: 5.43   Delta Z: 0.00   Roll: 0.00   Pitch: 0.00   Azimuth: 0.00   Draft: 0.00

Navigation   1993-180 18:45 —| New Entry Remove Entry

Time Error: 0.00   Delta X: 0.74   Delta Y: 2.45   Delta Z: -11.8   Ellipsoid: WG84 —|

Gyro   1992-100 00:00 —| New Entry Remove Entry

Time Error: 0.00   Delta X: 0.00   Delta Y: 0.00   Delta Z: 0.00   Error: 0.00

Heave   1992-100 00:00 —| New Entry Remove Entry

Time Error: 0.00   Delta X: 0.00   Delta Y: 0.00   Delta Z: 0.00   Error: 0.00

Pitch   1992-100 00:00 —| New Entry Remove Entry

Time Error: 0.00   Delta X: 0.00   Delta Y: 0.00   Delta Z: 0.00   Error: 0.00

Roll   1992-100 00:00 —| New Entry Remove Entry

Time Error: 0.00   Delta X: 0.00   Delta Y: 0.00   Delta Z: 0.00   Error: 0.00

Figure III.4   A time delay correction is entered in the VCF. The fact that the residual time delay is negative indicates that an overestimated positioning time delay was entered in the OPU at acquisition. A time delay correction of 0.6s has been entered in the Depth sensor time error window, to be subtracted from the soundings time. A correction of -0.6s in the Navigation time error window would have had the same effect.
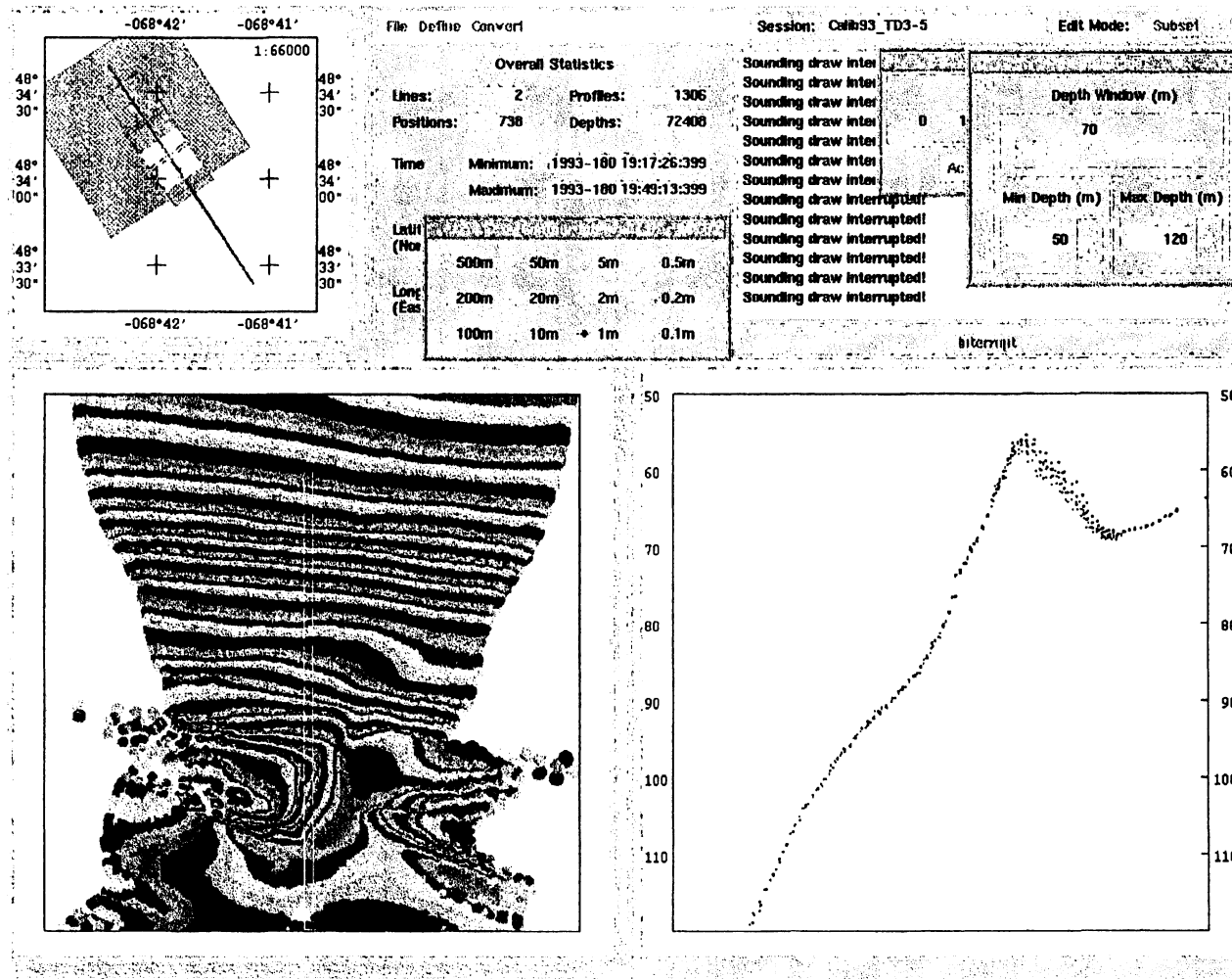
Figure III.5   Bathymetric representation (color-coded by depth) and cross-section view of lines 3 & 5, corrected for the residual time delay. The mismatch between soundings at the top of the hill is caused by across-track slope of the hump.
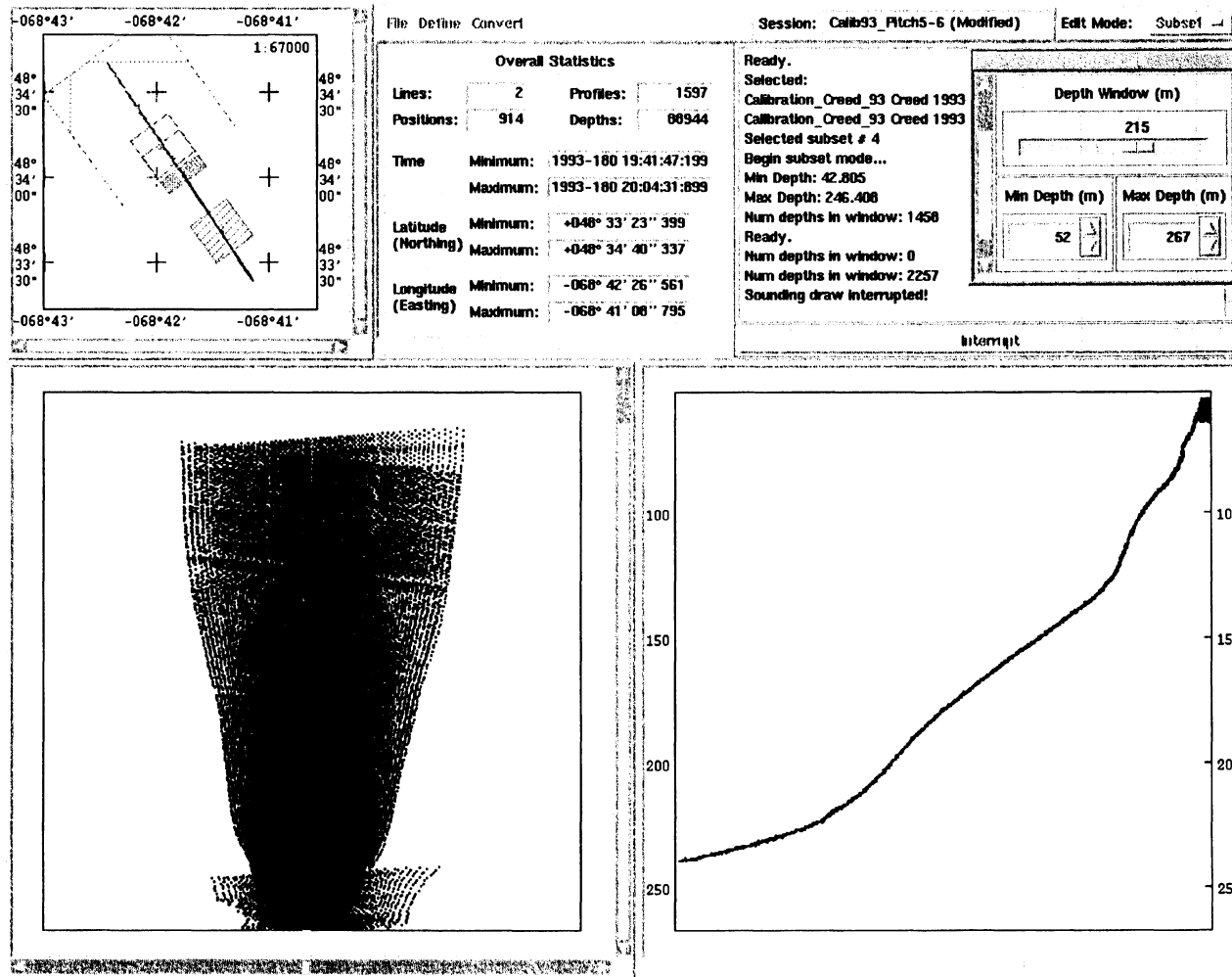
Figure III.6   Lines 5 (blue) and 6 (red) are plotted to assess the pitch offset. No significant along-track displacements are present between the two lines, indicating there is no residual pitch offset.
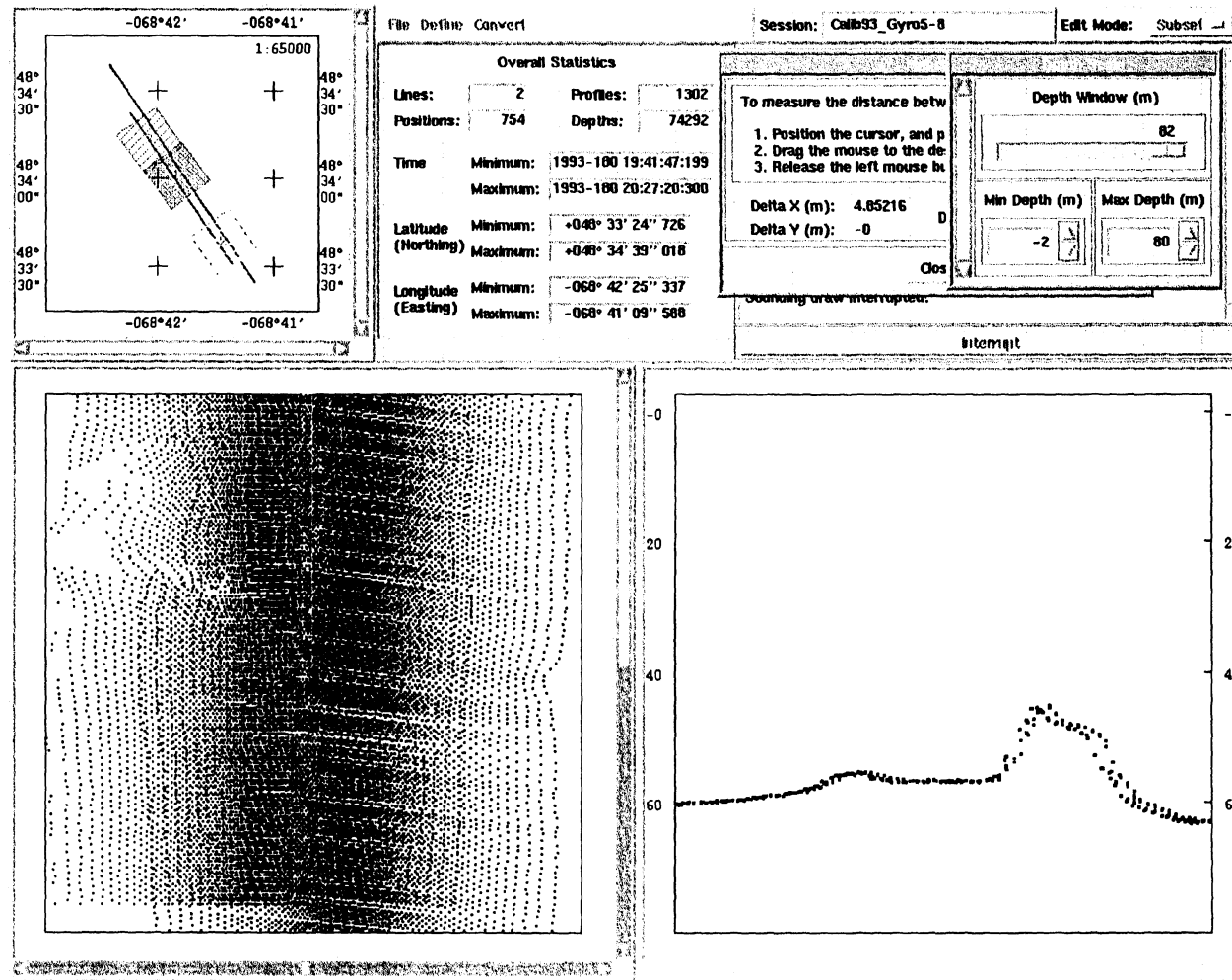
Figure III.7   Lines 5 (red) and 8 (blue) are plotted to show a negative azimuthal offset.

| File | | Vessel: | Creed | | Status: | Modified |

Depth Sensor `1993-180 18:45` ▭ New Entry Remove Entry

| # | 1 | 2 | 3 | 4 | 5 | 6 | 7 | 8 | 9 | 10 | 11 | 12 | 13 | 14 | 15 | 16 | 17 | 18 | 19 | 20 | 21 | 22 | 23 | 24 |

Time Error: `0.60`   Delta X: `3.87`   Delta Y: `5.43`   Delta Z: `0.00`   Roll: `0.00`   Pitch: `0.00`   Azimuth: `0.00`   Draft: `0.00`

Navigation `1993-180 18:45` ▭ New Entry Remove Entry

Time Error: `0.00`   Delta X: `0.74`   Delta Y: `2.45`   Delta Z: `-11.8`   Ellipsoid: `WG84` ▭

Gyro `1993-180 18:45` ▭ New Entry Remove Entry

Time Error: `0.00`   Delta X: `0.00`   Delta Y: `0.00`   Delta Z: `0.00`   Error: `2.65`

Heave `1992-100 00:00` ▭ New Entry Remove Entry

Time Error: `0.00`   Delta X: `0.00`   Delta Y: `0.00`   Delta Z: `0.00`   Error: `0.00`

Pitch `1992-100 00:00` ▭ New Entry Remove Entry

Time Error: `0.00`   Delta X: `0.00`   Delta Y: `0.00`   Delta Z: `0.00`   Error: `0.00`

Roll `1992-100 00:00` ▭ New Entry Remove Entry

Time Error: `0.00`   Delta X: `0.00`   Delta Y: `0.00`   Delta Z: `0.00`   Error: `0.00`

Figure III.8   An important correction of 2.65° must be entered in the VCF to correct the azimuthal offset. This residual offset is unusually large. The captain had rotated the gyrocompass to compensate for a misalignment (known to be approximately -1.9°) without notifying the hydrographer. The azimuthal offset was well detected by the calibration survey. This initial gyro misalignment has been measured after installation and corrected for by adjusting the gyro's synchro motor accordingly. Rotating the gyro casing induced a new azimuthal offset in the sounding system. Accurate manual adjustment for gyro misalignment is rather hard to obtain and the rotation of the gyro casing made here had overcompensated for the misalignment. Notice that the correction is entered in the gyro error, because the transducer azimuth adjustment is currently inactive in the VCF.
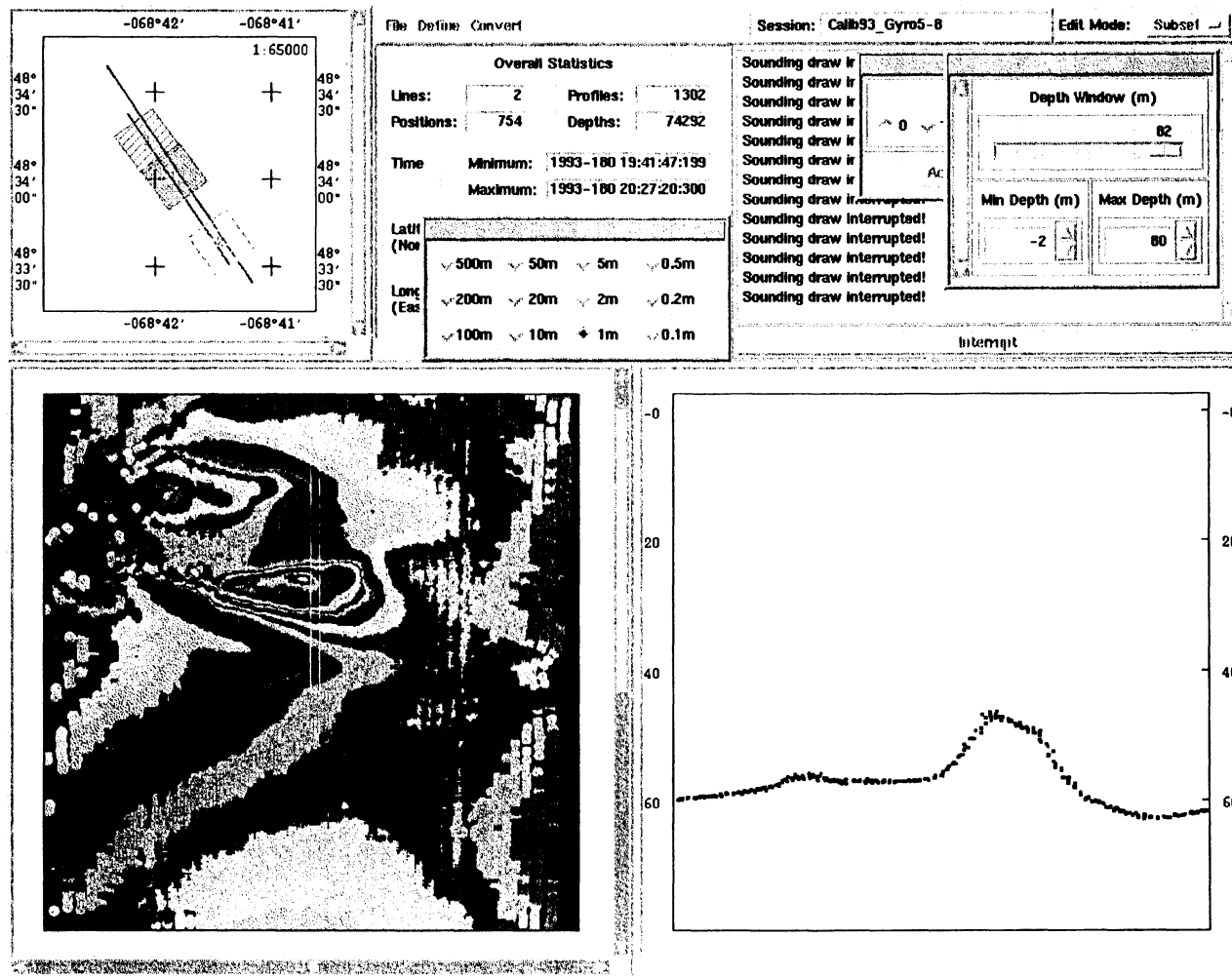
Figure III.9   Bathymetric representation and cross-section view of lines 5 & 8, corrected for the azimuthal offset.

-068°45'00"-068°44'30"-068°44'00"

1:44000

48°
34'
30"

48°
34'
30"

48°
34'
00"

48°
34'
00"

-068°45'00"-068°44'30"-068°44'00"

File Define Convert

Session: Calib93_Roll (Modified)   Edit Mode: Subset

Overall Statistics

Lines: 2   Profiles: 598
Positions: 558   Depths: 26704

Time   Minimum: 1993-180 18:53:25:800
         Maximum: 1993-180 19:09:31:300

Latitude   Minimum: +048° 33' 59" 465
(Northing) Maximum: +048° 34' 31" 289

Longitude   Minimum: -068° 45' 01" 193
(Easting)   Maximum: -068° 43' 44" 795

To measure the distance between
1. Position the cursor, and pres
2. Drag the mouse to the desire
3. Release the left mouse butto

Delta X (m):   -0
Delta Y (m):   2.76923   Dist

Close

Num depths in window: 323

Depth Window (m)

72

Min Depth (m)   Max Depth (m)

208   280

Interrupt

210
220
230
240
250
260
270

210
220
230
240
250
260
270

Figure III.10   Lines 1 (blue) and 2 (red) illustrating a positive roll offset. The cross-section is used to measured both the depth differences and the across-track distance between the beams of interest and nadir.

| File | | Vessel: | Creed | | | Status: | Modified |

Depth Sensor 1993-180 18:45 [New Entry] [Remove Entry]

#	1	2	3	4	5	6	7	8	9	10	11	12	13	14	15	16	17	18	19	20	21	22	23	24
X																								
Y																								
Z																								
S	◇ E	◇ E	◇ E	◇ E	◇ E	◇ E	◇ E	◇ E	◇ E	◇ E	◇ E	◇ E	◇ E	◇ E	◇ E	◇ E	◇ E	◇ E	◇ E	◇ E	◇ E	◇ E	◇ E	◇ E

◀ ▶

Time Error: 0.60   Delta X: 3.87   Delta Y: 5.43   Delta Z: 0.00   Roll: -0.14   Pitch: 0.00   Azimuth: 0.00   Draft: 0.00

Navigation 1993-180 18:45 [New Entry] [Remove Entry]

Time Error: 0.00   Delta X: 0.74   Delta Y: 2.45   Delta Z: -11.8   Ellipsoid: WG84

Gyro 1993-180 18:45 [New Entry] [Remove Entry]

Time Error: 0.00   Delta X: 0.00   Delta Y: 0.00   Delta Z: 0.00   Error: 2.65

Heave 1992-100 00:00 [New Entry] [Remove Entry]

Time Error: 0.00   Delta X: 0.00   Delta Y: 0.00   Delta Z: 0.00   Error: 0.00

Pitch 1992-100 00:00 [New Entry] [Remove Entry]

Time Error: 0.00   Delta X: 0.00   Delta Y: 0.00   Delta Z: 0.00   Error: 0.00

Roll 1992-100 00:00 [New Entry] [Remove Entry]

Time Error: 0.00   Delta X: 0.00   Delta Y: 0.00   Delta Z: 0.00   Error: 0.00

Figure III.11   A correction of -0.14° is entered in the VCF to correct for the roll offset.

-068°45'00"-068°44'30"-068°44'00"

44000

48° 34' 30"
48° 34' 30"

48° 34' 00"
48° 34' 00"

-068°45'00"-068°44'30"-068°44'00"

File Define Convert

Session: Calib93_Roll (Modified)   Edit Mode: Subset

Overall Statistics

Lines: 2   Profiles: 598
Positions: 558   Depths: 28704

Time   Minimum: 1993-180 18:53:25:800
        Maximum: 1993-180 19:09:31:300

Latitude   Minimum: +048° 33' 59" 465
(Northing) Maximum: +048° 34' 31" 289

Longitude   Minimum: -068° 45' 01" 193
(Easting)   Maximum: -068° 43' 44" 795

Calibration_Creed_9
Calibration_Creed_9
Selected subset # 2
Begin subset mode.
Min Depth: 250.506
Max Depth: 274.189
Num depths in wind
Ready.
Num depths in window: 536
Num depths in window: 576
Num depths in window: 361
Computing standard deviation...
Ready.

0   1

Ac

Depth Window (m)

72

Min Depth (m)   Max Depth (m)

208   280

Interrupt

Figure III.12   Cross-section view of lines 1 & 2, corrected for the roll offset.

Appendix IV

Quality Report Examples

The following quality reports were obtained from a performance check survey, carried out on May 19th 1995 off Tadoussac (Québec), by the NCS "Frederick G. Creed". The ship was equipped with a Simrad EM1000 multibeam echo-sounder. As shown in the first page of the first quality report, the depth range was from 105 to 127 metres. Three check lines were made, in three different operating modes, to produce the three following quality reports:

- **Shallow mode** (equi-angular beam spacing with a 150° fan opening)

- **EDBS150 mode** (equi-distance beam spacing with a 150° fan opening)

- **EDBS140 mode** (equi-distance beam spacing with a 140° fan opening)

The quality reports are generated by the HDCS application. The differences are calculated from the reference DTM and the check line observed data. The quality report is divided into two sections. The first section shows the general statistics for the differences. The second section shows the percentage of depth readings that meet the prescribed tolerance criteria (1% of water depth here for a depth window of 30 to 3000 m). Since the survey was deeper than 30 m, the 1.6% tolerance level for the beam readings, as shown in the first section of the quality report, would here indicate which beams meet the CHS accuracy requirements (90% confidence level). For instance, beams 1 to 4 in Shallow mode would have not pass the 1.6% repeatability test. The sign of the mean difference could also indicate the presence of a roll offset.

Simrad EM1000 Shallow Mode

Quality Control Report for file : checkline

Depth Range is :   127.16(m)   105.51(m)

Total number of 3D points used: 14208

Starting Time: 19-MAY-1995 15:49:02.74
Ending Time: 19-MAY-1995 15:52:15.72

Minimum tidal reduction: 1146 (mm)
Maximum tidal reduction: 1180 (mm)

User#	Total	Max(+)	Max(-)	Mean	Std.	3dm(%)	5dm(%)	1%(%)	1.6%(%)
1	83	0.23	-9.60	4.45	1.0150	2.	4.	6.	10.
2	104	0.47	-5.75	2.69	0.5460	4.	6.	13.	25.
3	145	1.56	-3.83	1.56	0.2710	10.	14.	41.	57.
4	220	1.51	-2.91	1.23	0.1690	11.	20.	43.	76.
5	240	2.16	-1.87	0.89	0.1130	15.	27.	65.	96.
6	240	1.40	-1.72	0.67	0.0850	25.	40.	82.	100.
7	241	1.06	-1.53	0.53	0.0640	31.	51.	95.	100.
8	241	1.15	-1.18	0.46	0.0560	37.	56.	99.	100.
9	241	1.18	-1.02	0.40	0.0440	42.	66.	98.	100.
10	241	1.87	-0.90	0.35	0.0350	55.	78.	98.	100.
11	242	1.91	-0.54	0.34	0.0270	53.	78.	97.	100.
12	242	1.49	-0.90	0.33	0.0290	58.	76.	98.	100.
13	242	1.64	-0.65	0.39	0.0250	49.	69.	96.	100.
14	243	1.26	-0.76	0.32	0.0220	56.	79.	98.	100.
15	243	1.39	-0.60	0.35	0.0210	53.	74.	97.	100.
16	243	1.25	-0.60	0.28	0.0230	64.	84.	98.	100.
17	242	1.64	-2.84	0.33	0.0290	62.	80.	96.	99.
18	243	1.29	-0.64	0.35	0.0220	53.	78.	96.	100.
19	244	1.27	-0.71	0.31	0.0220	62.	80.	98.	100.
20	244	1.37	-0.60	0.30	0.0220	63.	80.	99.	100.
21	244	1.35	-1.13	0.29	0.0220	64.	82.	99.	100.
22	244	1.07	-0.86	0.28	0.0290	61.	85.	100.	100.
23	244	1.22	-0.61	0.26	0.0200	68.	84.	100.	100.
24	244	1.62	-0.49	0.26	0.0200	66.	85.	99.	100.
25	244	1.24	-0.82	0.26	0.0220	70.	85.	99.	100.
26	244	1.15	-1.21	0.27	0.0250	67.	84.	99.	100.
27	245	1.33	-0.72	0.28	0.0270	64.	83.	99.	100.
28	244	1.21	-1.91	0.27	0.0270	69.	85.	98.	100.
29	242	0.93	-3.30	0.50	0.0700	49.	71.	89.	93.
30	238	1.06	-3.33	0.32	0.0380	58.	78.	99.	100.

31	241	1.14	-2.28	0.27	0.0290	66.	82.	99.	100.
32	243	1.12	-0.56	0.24	0.0220	72.	88.	99.	100.
33	245	1.10	-2.80	0.25	0.0230	71.	88.	100.	100.
34	246	1.31	-1.89	0.32	0.0300	64.	82.	97.	99.
35	246	1.10	-1.47	0.27	0.0270	70.	85.	98.	100.
36	246	1.08	-0.86	0.24	0.0190	70.	84.	100.	100.
37	246	1.11	-0.48	0.21	0.0180	76.	89.	100.	100.
38	246	1.05	-0.56	0.22	0.0190	76.	88.	100.	100.
39	246	0.93	-0.68	0.25	0.0230	70.	86.	100.	100.
40	245	0.97	-0.73	0.25	0.0220	71.	84.	100.	100.
41	245	1.03	-0.70	0.23	0.0210	72.	87.	100.	100.
42	246	1.02	-0.63	0.23	0.0210	73.	88.	100.	100.
43	246	1.14	-0.58	0.22	0.0220	75.	89.	100.	100.
44	246	1.36	-0.73	0.25	0.0240	71.	86.	100.	100.
45	246	0.99	-0.86	0.29	0.0320	61.	85.	100.	100.
46	246	0.94	-0.81	0.27	0.0290	66.	86.	100.	100.
47	246	0.77	-0.82	0.29	0.0330	53.	86.	100.	100.
48	246	0.98	-0.79	0.25	0.0250	65.	88.	100.	100.
49	246	0.99	-0.94	0.30	0.0340	54.	82.	100.	100.
50	246	1.08	-0.90	0.32	0.0320	52.	82.	100.	100.
51	246	0.93	-1.22	0.36	0.0430	46.	71.	100.	100.
52	246	1.23	-1.45	0.47	0.0590	35.	57.	96.	100.
53	246	0.73	-1.70	0.64	0.0820	19.	39.	90.	100.
54	246	0.84	-1.79	0.79	0.1020	17.	30.	72.	100.
55	246	0.83	-2.05	0.98	0.1290	12.	23.	55.	95.
56	246	1.16	-2.71	1.17	0.1520	13.	22.	49.	76.
57	246	0.92	-3.94	1.56	0.2040	8.	14.	35.	54.
58	244	0.77	-4.34	2.10	0.2770	6.	9.	24.	40.
59	236	0.76	-5.65	2.89	0.3880	3.	5.	17.	29.
60	240	1.23	-7.68	4.27	0.5650	2.	2.	7.	14.

Classification report 2 of 2

Depth Range is :   3000.00   30.00

Percentage tolerance is :   1.0%

User#	Total	# fail	% fail	# pass	% pass
1	83	78	93.98	5	6.02
2	104	90	86.54	14	13.46
3	145	85	58.62	60	41.38
4	220	126	57.27	94	42.73

5	240	84	35.00	156	65.00
6	240	44	18.33	196	81.67
7	241	13	5.39	228	94.61
8	241	3	1.24	238	98.76
9	241	4	1.66	237	98.34
10	241	5	2.07	236	97.93
11	242	7	2.89	235	97.11
12	242	6	2.48	236	97.52
13	242	9	3.72	233	96.28
14	243	4	1.65	239	98.35
15	243	7	2.88	236	97.12
16	243	5	2.06	238	97.94
17	242	10	4.13	232	95.87
18	243	10	4.12	233	95.88
19	244	5	2.05	239	97.95
20	244	3	1.23	241	98.77
21	244	3	1.23	241	98.77
22	244	0	0.00	244	100.00
23	244	1	0.41	243	99.59
24	244	2	0.82	242	99.18
25	244	2	0.82	242	99.18
26	244	3	1.23	241	98.77
27	245	2	0.82	243	99.18
28	244	4	1.64	240	98.36
29	242	26	10.74	216	89.26
30	238	3	1.26	235	98.74
31	241	3	1.24	238	98.76
32	243	2	0.82	241	99.18
33	245	1	0.41	244	99.59
34	246	8	3.25	238	96.75
35	246	5	2.03	241	97.97
36	246	1	0.41	245	99.59
37	246	1	0.41	245	99.59
38	246	0	0.00	246	100.00
39	246	0	0.00	246	100.00
40	245	0	0.00	245	100.00
41	245	0	0.00	245	100.00
42	246	0	0.00	246	100.00
43	246	0	0.00	246	100.00
44	246	1	0.41	245	99.59
45	246	0	0.00	246	100.00
46	246	0	0.00	246	100.00
47	246	0	0.00	246	100.00
48	246	0	0.00	246	100.00
49	246	0	0.00	246	100.00
50	246	0	0.00	246	100.00
51	246	1	0.41	245	99.59

52	246	10	4.07	236	95.93
53	246	25	10.16	221	89.84
54	246	70	28.46	176	71.54
55	246	110	44.72	136	55.28
56	246	126	51.22	120	48.78
57	246	161	65.45	85	34.55
58	244	186	76.23	58	23.77
59	236	197	83.47	39	16.53
60	240	224	93.33	16	6.67

Simrad EM1000 EDBS 150 Mode

Quality Control Report for file : checkline

Depth Range is :   125.76(m)   105.19(m)

Total number of 3D points used: 12406

Starting Time: 19-MAY-1995 15:55:30.13
Ending Time: 19-MAY-1995 15:58:19.98

Minimum tidal reduction: 1083 (mm)
Maximum tidal reduction: 1112 (mm)

User#	Total	Max(+)	Max(-)	Mean	Std.	3dm(%)	5dm(%)	1%(%)	1.6%(%)
1	137	2.41	-7.76	4.82	0.8390	2.	4.	5.	6.
2	172	3.41	-4.92	2.98	0.4630	3.	3.	11.	17.
3	185	1.66	-3.45	1.88	0.2820	4.	9.	23.	38.
4	206	2.73	-3.17	1.35	0.1910	7.	16.	37.	67.
5	208	2.01	-2.23	0.94	0.1310	17.	26.	58.	95.
6	208	1.57	-1.78	0.71	0.0980	25.	35.	81.	100.
7	208	1.84	-1.57	0.56	0.0730	28.	47.	94.	100.
8	209	1.26	-1.39	0.51	0.0640	28.	47.	99.	100.
9	209	1.22	-0.98	0.41	0.0470	38.	64.	100.	100.
10	209	1.25	-0.69	0.33	0.0350	53.	79.	100.	100.
11	209	1.86	-0.62	0.35	0.0290	57.	77.	97.	100.
12	210	1.96	-0.57	0.33	0.0290	60.	79.	98.	100.
13	210	1.46	-0.29	0.37	0.0240	52.	69.	97.	100.
14	210	1.36	-0.40	0.33	0.0240	57.	77.	98.	100.
15	210	1.36	-0.39	0.33	0.0240	60.	77.	98.	100.
16	210	1.16	-0.59	0.26	0.0250	69.	84.	100.	100.
17	210	1.44	-0.71	0.28	0.0260	69.	81.	98.	100.
18	210	1.45	-0.56	0.32	0.0250	61.	78.	97.	100.
19	210	1.16	-0.39	0.25	0.0210	70.	84.	99.	100.
20	210	1.10	-0.41	0.26	0.0210	69.	82.	99.	100.
21	210	1.20	-0.36	0.26	0.0230	70.	81.	99.	100.
22	211	1.35	-1.50	0.31	0.0330	55.	82.	99.	100.
23	211	1.21	-0.41	0.26	0.0220	69.	82.	99.	100.
24	211	1.23	-0.38	0.27	0.0220	67.	84.	98.	100.
25	210	1.08	-0.92	0.25	0.0240	72.	85.	100.	100.
26	210	1.15	-0.70	0.26	0.0260	69.	84.	99.	100.
27	210	1.15	-2.44	0.29	0.0310	66.	84.	99.	100.
28	210	1.21	-2.20	0.26	0.0300	74.	85.	98.	99.
29	208	1.21	-3.00	0.33	0.0450	65.	81.	97.	98.
30	210	1.11	-1.71	0.31	0.0360	59.	80.	99.	100.
31	209	1.14	-0.84	0.28	0.0310	64.	83.	99.	100.

32	209	1.18	-0.79	0.26	0.0280	70.	85.	98.	100.
33	210	1.31	-0.90	0.28	0.0260	70.	82.	98.	100.
34	210	1.48	-0.65	0.31	0.0250	66.	81.	95.	100.
35	210	1.61	-0.64	0.26	0.0270	72.	84.	97.	100.
36	210	1.47	-0.62	0.26	0.0250	76.	84.	97.	100.
37	210	1.34	-0.88	0.27	0.0280	70.	84.	97.	100.
38	210	1.45	-0.61	0.26	0.0280	69.	88.	97.	100.
39	210	1.71	-0.61	0.27	0.0300	66.	88.	97.	100.
40	209	1.52	-0.77	0.28	0.0310	65.	87.	97.	100.
41	208	1.53	-0.98	0.29	0.0320	67.	84.	97.	100.
42	209	1.48	-2.46	0.29	0.0330	68.	83.	96.	100.
43	209	1.07	-1.65	0.29	0.0320	63.	85.	100.	100.
44	209	1.41	-0.68	0.29	0.0310	61.	84.	99.	100.
45	208	0.85	-0.99	0.31	0.0370	51.	84.	100.	100.
46	209	0.86	-1.17	0.31	0.0380	52.	85.	100.	100.
47	208	0.96	-0.95	0.38	0.0490	37.	74.	100.	100.
48	209	0.85	-0.86	0.31	0.0380	52.	86.	100.	100.
49	209	0.93	-0.86	0.37	0.0480	38.	73.	100.	100.
50	208	0.82	-0.98	0.35	0.0430	48.	75.	100.	100.
51	211	0.98	-1.30	0.45	0.0590	33.	62.	98.	100.
52	209	0.96	-1.35	0.54	0.0760	32.	47.	94.	100.
53	210	0.73	-1.43	0.70	0.0980	19.	36.	83.	100.
54	210	0.43	-1.74	0.87	0.1240	15.	25.	63.	100.
55	210	0.71	-2.11	1.07	0.1520	9.	15.	50.	95.
56	209	0.58	-2.40	1.32	0.1870	8.	12.	40.	73.
57	209	1.10	-3.22	1.71	0.2410	4.	6.	24.	50.
58	208	0.55	-4.01	2.30	0.3260	2.	5.	17.	31.
59	204	0.13	-5.59	3.13	0.4480	1.	2.	8.	20.
60	192	1.11	-7.37	4.83	0.7080	1.	1.	3.	6.

Classification report 2 of 2

Depth Range is :   3000.00   30.00

Percentage tolerance is :   1.0%

User#	Total	# fail	% fail	# pass	% pass
1	137	130	94.89	7	5.11
2	172	153	88.95	19	11.05
3	185	143	77.30	42	22.70
4	206	130	63.11	76	36.89
5	208	88	42.31	120	57.69

6	208	40	19.23	168	80.77
7	208	13	6.25	195	93.75
8	209	3	1.44	206	98.56
9	209	1	0.48	208	99.52
10	209	1	0.48	208	99.52
11	209	7	3.35	202	96.65
12	210	4	1.90	206	98.10
13	210	7	3.33	203	96.67
14	210	4	1.90	206	98.10
15	210	4	1.90	206	98.10
16	210	0	0.00	210	100.00
17	210	4	1.90	206	98.10
18	210	7	3.33	203	96.67
19	210	2	0.95	208	99.05
20	210	2	0.95	208	99.05
21	210	2	0.95	208	99.05
22	211	2	0.95	209	99.05
23	211	2	0.95	209	99.05
24	211	4	1.90	207	98.10
25	210	1	0.48	209	99.52
26	210	2	0.95	208	99.05
27	210	3	1.43	207	98.57
28	210	5	2.38	205	97.62
29	208	6	2.88	202	97.12
30	210	2	0.95	208	99.05
31	209	2	0.96	207	99.04
32	209	4	1.91	205	98.09
33	210	4	1.90	206	98.10
34	210	10	4.76	200	95.24
35	210	7	3.33	203	96.67
36	210	7	3.33	203	96.67
37	210	6	2.86	204	97.14
38	210	6	2.86	204	97.14
39	210	7	3.33	203	96.67
40	209	7	3.35	202	96.65
41	208	6	2.88	202	97.12
42	209	8	3.83	201	96.17
43	209	1	0.48	208	99.52
44	209	3	1.44	206	98.56
45	208	0	0.00	208	100.00
46	209	1	0.48	208	99.52
47	208	0	0.00	208	100.00
48	209	0	0.00	209	100.00
49	209	0	0.00	209	100.00
50	208	0	0.00	208	100.00
51	211	5	2.37	206	97.63
52	209	12	5.74	197	94.26

53	210	36	17.14	174	82.86
54	210	78	37.14	132	62.86
55	210	104	49.52	106	50.48
56	209	126	60.29	83	39.71
57	209	158	75.60	51	24.40
58	208	173	83.17	35	16.83
59	204	187	91.67	17	8.33
60	192	187	97.40	5	2.60

Simrad EM1000 EDBS 140 Mode

Quality Control Report for file : checkline

Depth Range is :   128.04(m)   105.11(m)

Total number of 3D points used: 8806

Starting Time: 19-MAY-1995 16:02:35.24
Ending Time: 19-MAY-1995 16:05:50.79

Minimum tidal reduction: 1012 (mm)
Maximum tidal reduction: 1042 (mm)

User#	Total	Max(+)	Max(-)	Mean	Std.	3dm(%)	5dm(%)	1%(%)	1.6%(%)
1	1	0.00	-3.40	3.40	******	0.	0.	0.	0.
3	2	0.00	-7.60	6.93	******	0.	0.	0.	0.
4	1	0.00	-1.38	1.38	******	0.	0.	0.	100.
5	1	0.00	-3.07	3.07	******	0.	0.	0.	0.
6	6	0.00	-4.15	3.24	3.2030	0.	0.	0.	17.
7	2	0.00	-3.64	3.50	9.9120	0.	0.	0.	0.
8	3	0.00	-2.81	1.68	3.0040	0.	0.	33.	67.
9	8	0.00	-5.16	2.30	1.9420	12.	12.	12.	38.
10	88	0.35	-4.23	1.76	0.3900	8.	9.	28.	52.
11	117	1.06	-3.50	1.54	0.2950	8.	14.	34.	59.
12	146	0.89	-2.62	1.34	0.2270	6.	11.	44.	72.
13	158	1.41	-2.69	1.09	0.1760	10.	18.	53.	85.
14	174	1.32	-2.21	0.92	0.1410	14.	27.	65.	95.
15	177	1.28	-2.03	0.76	0.1140	20.	33.	73.	98.
16	178	1.25	-1.65	0.67	0.0980	24.	36.	81.	100.
17	177	1.41	-1.56	0.58	0.0830	28.	43.	94.	100.
18	177	1.17	-1.51	0.50	0.0720	32.	53.	97.	100.
19	178	1.22	-1.61	0.44	0.0620	40.	63.	96.	100.
20	177	1.12	-1.59	0.36	0.0460	48.	73.	99.	100.
21	178	1.21	-1.08	0.35	0.0380	50.	76.	99.	100.
22	178	1.33	-0.57	0.35	0.0300	55.	75.	98.	100.
23	178	1.31	-0.48	0.37	0.0280	52.	72.	98.	100.
24	178	1.33	-1.45	0.33	0.0290	58.	78.	97.	100.
25	178	1.50	-2.96	0.34	0.0360	58.	79.	96.	99.
26	178	1.73	-0.59	0.35	0.0300	58.	77.	97.	99.
27	178	1.64	-1.38	0.31	0.0370	59.	83.	98.	100.
28	179	1.30	-0.59	0.27	0.0260	67.	87.	97.	100.
29	179	1.25	-0.78	0.29	0.0280	64.	82.	97.	100.
30	179	1.17	-0.82	0.26	0.0310	69.	82.	99.	100.
31	180	1.16	-0.78	0.26	0.0280	67.	87.	99.	100.
32	180	1.41	-0.40	0.29	0.0260	64.	83.	97.	100.

33	180	1.11	-0.60	0.22	0.0240	78.	89.	99.	100.
34	180	1.52	-0.72	0.23	0.0280	73.	90.	98.	100.
35	178	1.11	-1.54	0.26	0.0310	70.	86.	98.	100.
36	180	1.31	-0.66	0.27	0.0340	66.	86.	98.	100.
37	179	1.40	-1.11	0.31	0.0420	54.	85.	98.	100.
38	180	1.12	-0.81	0.29	0.0360	58.	84.	99.	100.
39	180	0.98	-1.05	0.29	0.0390	61.	84.	100.	100.
40	180	1.19	-1.05	0.33	0.0430	55.	78.	99.	100.
41	180	0.82	-1.15	0.44	0.0630	31.	59.	99.	100.
42	181	1.17	-1.32	0.54	0.0790	25.	44.	97.	100.
43	181	1.26	-1.71	0.66	0.0990	23.	32.	91.	100.
44	181	1.26	-1.70	0.82	0.1240	15.	25.	74.	100.
45	181	0.71	-2.18	0.96	0.1450	11.	20.	60.	98.
46	181	0.45	-1.94	1.02	0.1560	12.	19.	51.	96.
47	181	1.18	-2.42	1.13	0.1710	12.	17.	45.	87.
48	181	1.17	-2.53	1.26	0.1920	8.	17.	37.	77.
49	181	0.80	-2.95	1.51	0.2300	4.	7.	32.	58.
50	181	0.83	-3.12	1.75	0.2660	3.	7.	24.	46.
51	180	1.32	-3.15	1.95	0.2960	3.	5.	16.	41.
52	180	2.45	-3.58	2.20	0.3340	2.	3.	13.	29.
53	178	2.49	-4.00	2.50	0.3790	1.	2.	6.	25.
54	178	1.38	-4.32	2.71	0.4120	1.	1.	6.	17.
55	177	1.11	-4.50	2.94	0.4500	2.	3.	7.	18.
56	170	0.58	-5.26	3.33	0.5210	1.	2.	5.	11.
57	169	0.42	-7.83	3.73	0.5850	0.	2.	5.	11.
58	157	0.68	-7.16	4.17	0.6760	1.	1.	2.	6.
59	132	0.00	-7.26	4.82	0.8510	0.	0.	0.	1.
60	125	0.00	-8.07	5.31	0.9650	0.	0.	0.	2.

Classification report 2 of 2

Depth Range is :   3000.00   30.00

Percentage tolerance is :   1.0%

User#	Total	# fail	% fail	# pass	% pass
1	1	1	100.00	0	0.00
3	2	2	100.00	0	0.00
4	1	1	100.00	0	0.00
5	1	1	100.00	0	0.00
6	6	6	100.00	0	0.00
7	2	2	100.00	0	0.00

8	3	2	66.67	1	33.33
9	8	7	87.50	1	12.50
10	88	63	71.59	25	28.41
11	117	77	65.81	40	34.19
12	146	82	56.16	64	43.84
13	158	75	47.47	83	52.53
14	174	61	35.06	113	64.94
15	177	48	27.12	129	72.88
16	178	33	18.54	145	81.46
17	177	10	5.65	167	94.35
18	177	5	2.82	172	97.18
19	178	8	4.49	170	95.51
20	177	1	0.56	176	99.44
21	178	1	0.56	177	99.44
22	178	3	1.69	175	98.31
23	178	4	2.25	174	97.75
24	178	6	3.37	172	96.63
25	178	7	3.93	171	96.07
26	178	6	3.37	172	96.63
27	178	3	1.69	175	98.31
28	179	6	3.35	173	96.65
29	179	5	2.79	174	97.21
30	179	1	0.56	178	99.44
31	180	2	1.11	178	98.89
32	180	5	2.78	175	97.22
33	180	2	1.11	178	98.89
34	180	3	1.67	177	98.33
35	178	3	1.69	175	98.31
36	180	3	1.67	177	98.33
37	179	3	1.68	176	98.32
38	180	1	0.56	179	99.44
39	180	0	0.00	180	100.00
40	180	1	0.56	179	99.44
41	180	1	0.56	179	99.44
42	181	6	3.31	175	96.69
43	181	17	9.39	164	90.61
44	181	47	25.97	134	74.03
45	181	72	39.78	109	60.22
46	181	88	48.62	93	51.38
47	181	100	55.25	81	44.75
48	181	114	62.98	67	37.02
49	181	123	67.96	58	32.04
50	181	137	75.69	44	24.31
51	180	151	83.89	29	16.11
52	180	157	87.22	23	12.78
53	178	168	94.38	10	5.62
54	178	167	93.82	11	6.18

55	177	165	93.22	12	6.78
56	170	161	94.71	9	5.29
57	169	160	94.67	9	5.33
58	157	154	98.09	3	1.91
59	132	132	100.00	0	0.00
60	125	125	100.00	0	0.00

Appendix V

Instructions for using the OMG's SwathEditor and DelayEditor

when investigating Errors in Roll Data

```
# This is done in the directory /drives/solomon/disk22/agodin/Calibration93

RT\
    -packdown \
    -background \
    -prefix /home/omg3/agodin/Patch_Test_93/ \
    -suffix .Patch_Test1_Riki \
    -svtd \
    -onetype \
    -WRITE\
    -out /drives/solomon/disk22/agodin/Calibration93/Calib93_ \
    << enough
$ 1
enough

mv \
    /drives/solomon/disk22/agodin/Calibration93/Calib93_$1.depth \
    /drives/solomon/disk22/agodin/Calibration93/Calib93_$1.merged

removeRedundantNav \
    -comp temp \
    /drives/solomon/disk22/agodin/Calibration93/Calib93_$1.nav

mv /drives/solomon/disk22/agodin/Calibration93/Calib93_$1.nav \
    /drives/solomon/disk22/agodin/Calibration93/Calib93_$1.nav_orig

mv temp /drives/solomon/disk22/agodin/Calibration93/Calib93_$1.nav

checkNav /drives/solomon/disk22/agodin/Calibration93/Calib93_$1.nav

jview region.blank \
    -rejectnav \
    -navedit /drives/solomon/disk22/agodin/Calibration93/Calib93_$1.nav

mergeNav \
    -delay 0.0 \
    -ahead 7.3 \
    -right 3.4 \
    /drives/solomon/disk22/agodin/Calibration93/Calib93_$1

getBounds /drives/solomon/disk22/agodin/Calibration93/Calib93_$1.merged

swathed /drives/solomon/disk22/agodin/Calibration93/Calib93_$1.merged

DelayEditor -norollfilter /drives/solomon/disk22/agodin/Calibration93/Calib93_$1.merged
```

Figure V.1 Example of a script file for processing a survey line with the OMG's RT tool. The script starts the swathed application (Figure V.2) and the other necessary programs that perform the data cleaning. The script file then opens the line with the DealayEditor which permits the analysis of the data.

Use of the "DelayEditor" tool
(from Hughes Clarke, J. [1993, Appendix C]).

The interactive graphical tool "DelayEditor" takes in an fully merged EM100 (or EM1000) data file in Extended Ocean Mapping Group Format. The tools consists of a X Window interface with 6 graphical windows and 18 buttons and manipulative widgets (Figure V.3).

The top window represents the entire data file and two attributes are plotted to help you select a sub-area (the high pass across track slope (white trace) and the nadir depth (green trace). The yellow rectangle indicates the subset revealed in detail below. In order to select an different subset, move the cursor into the upper window and pressing down the left mouse button, draw out a rectangle to cover as much of the file as you wish to view.

The lower five window give you a time series of a selection of parameters derived from the raw EM100 data. there are six selection options available, which can be chosen using the top buttons:

(1) - *Ship*

(2) - *Navi*

(3) - *Roll*

(4) - *Image*

(5) - *Fix*

(6) - *Seabed*

All the parameters are plotted according to their location in time, within the window subset (in contrast the file window is plotted by record number). The time duration is indicated by vertical markers: complete markers correspond to 1 minute boundaries (from start of subset), smaller markers correspond to 30 second, then 5 second and (if the subset is short) the smallest correspond to 1 second marks. The resultant parameter selections plotted are thus:

(1) *Ship*
- heading
- rate of change of heading
- pitch and transducer pitch
- roll
- heave

(2) *Navi*
- heading derived from navigation fixes
- rate of change of navigation derived heading (needs filtering!)
- velocity derived from navigation.(can see fix spacing!)
- roll
- not used

(3) *Roll*

- shot interval (average shot interval is listed)

- high pass filtered roll (from a 3 ping boxcar filter).

- low pass filtered roll (")

- raw roll

- EM100 pulse length and mode

(4) *Image*

- Power Gain level

- EM100 Attenuation Gain Level

- EM100 TVG gain level

- plan view of EM100 imagery (press spacebar to enable/disable)

- beam profile of EM100 echo strength

(5) *Fix*

- "corrected" residual seafloor slope. (RMS and average envelope level is calculated, note, the average envelope algorythm (Hilbert Transform) needs at least 40 samples to be useful).

- high-pass seafloor slope and predicted error

- high-pass seafloor slope and "corrected" residual slope.

- Raw Roll

- Scaled/Delayed Roll against sum of raw roll and high-pass seafloor slope (for comparison of measured vs. "true")

(6) *Seabed*

-across track seafloor slope

-same high pass filtered (20 ping boxcar filter0

-same low pass filtered (")

-raw roll

-nadir and one port and starboard profile option of color coded depth plot (press spacebar) .

Options *Ship, Navi, Roll, Seabed* are all just for information.

Option *Fix* allows user interaction in three ways:

Using the Delay, Lag or Scale widget, one can apply arbritrary roll delay, lag and scaling to try and remove the residual roll artifact. (The logic behind this is explained in the main report). Manual selection of parameter values is achieved by pressing any mouse button in the relevant parameter widget at the level required. There is the option of automated parameter selection. These are operated by pressing the "Corr ." or "Auto" buttons next to the corresponding parameter widget. Before starting these automated steps, it is necessary to set all values to their default values. This is done by pressing the "Z" key in each of the parameter widgets.

Option *Image*:

This is a developmental tool designed to correct the raw echo strength values. For the purpose of this report it is sufficent to just set all the gain options to *on* (should be the default, else press the six buttons) and then hit the space bar in window 4 to see the corresponding imagery.

X-Plot options:

There are three ways of using the X-Plot window:

> - 1 Xplot roll and corrected roll by sweeping out a rectangle with the right cursor button in option *Fix*, window 5.
>
> -2 Xplot pitch and transducer pitch by doing same in option *Ship*, window 3.
>
> -3 Xplot backscatter as a function of grazing angle by doing the same in option *Image* window 4.

Another method for selecting a subset within a subset, rather than using the top window is to define a rectangle using the left mouse button in any of windows 1-5. This is useful when one wishes to focus in on problems within small time series.

Print Option:

If the top left hand button is pressed a file in created (filename.merged.**aspect**) which contains a listing of all the values presented for the time series viewed (the subset of the total file examined). This ASCII file can easily be incorporated into any standard plotting package to get custom plots. It is also a useful facility for dumping out the roll and residual roll time series for analysis using different tools.

The exact format for the listing is as follows:

```
filename
minimium_time maximum_time/* seconds since 1970
0.0 difftime/* time range in seconds
start_rec end_rec/* start and end record in file (first rec. is 0)
num_rec/* number of records
delay/* delay in seconds
lag/* lag in seconds
scale_factor/* scale_factor

/* then num_rec lines containing the following listing :
/* all floats */
        time_since start_of_window /* seconds
        roll
        pitch
        transducer_pitch
        heave
        heading
        delta_heading/* rate of change of heading deg/sec
        bottom_slope/* average across track bottom slope for this ping
        low_bottom_slope/* low pass filter of above
        high_bottom_slope/* high pass filter of same
        raw_bottom_slope/* high_bottom_slope+low_pass_filtered_roll
        corrected_residual
        delayed_scaled_roll
```

```
                roll -delayed_scaled_roll
                lagged_(roll-delayed_scaled_roll)
                centre_beam_depth
                stbd7_depth
                port7_depth
                high_pass_filtered_roll
                low_pass_filtered_roll
                ping_interval/* seconds
/* last five are integers */
                mode/*  0=off, 1 =Wide, 2=UltraWide, 3=Narrow
                pulse_length/*  1 = 0.2, 2 = 0.6
                TVG/*  0 to 20 corresponding to  3dB steps
                attenuation/*  0 to 3 in 10 dB steps
                power/*  0 to 2 in 10 dB steps
```

Each listing of 26 parameters has a carriage return at the end.

SS	list	next	p-B-s	All/sel	bck	fwd	exit

Last
Port   Stbd

(1)
Plan View
Beam Locations
First

(4)
Rear View
Across Track Profiles
(unedited)

(5)
Side View
Along Beam Profiles
(unedited)

5m lines
(2)
Side View
Along Beam Profiles

First   Last

5m lines
(3)
Rear View
Across Track Profiles

Port   Stbd

First   Last

(6)
Along Track
Vessel Dynamics

Last

(7)
Beam Echo Strength
(by beam no.)
Beam 0   Beam 32
First

(8) Location of 80 swath subset, within file

Figure V.2   The swathed window (after Hughes Clarke, J. [1993]).

Print	Unassigned	Seabed	Fix	Image	Roll	Navi	Ship	Exit

Location of Subset Window within total file

File Info Box	Auto Select	Delay Widget	Colormap Widget
		Lag Widget	Echo Strength
		Scale Widget	Gain Options

Trace Window (1)

Trace Window (2)

Trace Window (3)

Trace Window (4)

Trace Window (5)

Figure V.3 The DelayEditor window (after Hughes Clarke, J. [1993]).

VITA

Name: André Godin

Place and date of birth: Verdun, Québec, Canada - August 2nd 1959

Permanent Address: 311, Paquet Sud, Pte-au-Père, Québec, Canada, G5L 1H4

Schools attended:

1980 - 1984	INSTITUT MARITIME du QUÉBEC, Rimouski College Diploma in Navigation (D.E.C.)
1986	CHAMPLAIN REGIONAL COLLEGE, Lennoxville Additional courses in Sciences

Universities attended:

1987 - 1989	UNIVERSITY OF SHERBROOKE One term in Computer Sciences Two terms in Physical Geography
1995 - 1997	UNIVERSITY OF NEW BRUNSWICK Master of Surveying Engineering Orientation: Hydrographic surveying specialized in multibeam echo-sounding systems and GPS positioning

Publications:

Godin, A. (1996). The Calibration of Shallow Water Multibeam Echo-Sounding Systems. Proceedings of the Canadian Hydrographic Conference, June 3-5 1996, Halifax, N.S., pp. 25-31.

Godin, A., B. Tessier, P. Hally and Denis Hains (1992). *Simrad EM1000 and SWATH vessel technology: The Perfect Match?*

Hare, R., A. Godin, and L. A. Mayer (1995). *Accuracy estimation of Canadian Swath (multibeam) and Sweep (multi-transducer) sounding systems.* Department of Fisheries and Oceans, Canadian Hydrographic Service internal report, Laurentian region.

Hughes Clarke, J. L.A. Mayer, N. Mitchell and A. Godin (1993). *Processing and Interpretation of 95 kHz Backscatter Data from Shallow-Water Multibeam Sonars.* Proceedings of OCEANS'93, October 18-21 1993, Victoria, B.C., pp. 437-442.

Hughes Clarke, J. and A. Godin (1993). *Investigation of the roll and heave errors present in Frederick G. Creed - EM1000 data when using a TSS 335B motion sensor.* Department of Fisheries and Oceans, Canada, DFO contract report FP707-3-5731.